8-2013

Optimal Control for Management in Gypsy Moth Models

Marco Vinisio Martinez
mmarti52@utk.edu

To the Graduate Council:

I am submitting herewith a dissertation written by Marco Vinisio Martinez entitled "Optimal Control for Management in Gypsy Moth Models." I have examined the final electronic copy of this dissertation for form and content and recommend that it be accepted in partial fulfillment of the requirements for the degree of Doctor of Philosophy, with a major in Mathematics.

Suzanne Lenhart, Major Professor

We have read this dissertation and recommend its acceptance:

Louis Gross, Charles Collins, Robert Mee

Accepted for the Council:

Carolyn R. Hodges

Vice Provost and Dean of the Graduate School

(Original signatures are on file with official student records.)

Optimal Control for Management in Gypsy Moth Models

A Dissertation

Presented for the

Doctor of Philosophy

Degree

The University of Tennessee, Knoxville

Marco Vinisio Martinez

August 2013

To my family

Acknowledgements

I would like to express my appreciation to those individuals who made this dissertation possible. First of all I want to express my deepest gratitude to my advisor Dr. Suzanne Lenhart, for guiding me through this process. I really appreciate all her support, advice, and encouragement. I would have not accomplished this dissertation without her. Also, I want to thank her for the many opportunities she provided during my graduate education to participate in workshops, conferences, working groups, and other endeavors that have made me a better researcher and educator.

I also want to thank my thesis committee members: Dr. Louis Gross, Dr. Charles Collins, and Dr. Robert Mee for their time and critical review of my work. They all contributed to my graduate studies. I would like to further thank Dr. Gross for his support and advice, in particular, during my first year of graduate school. I thank Dr. Collins for being a great mentor in teaching mathematics, and for always being available to discuss and provide advice about teaching.

The financial support of my graduate education came from a teaching assistantship funded through the Mathematics Department and a graduate research fellowship funded through the National Institute for Mathematical and Biological synthesis (NIMBioS). I am grateful to the Mathematics Department and the staff, in particular to Pam Armentrout who was a constant source of information about University policies.

I am grateful to all my friends in Knoxville and peers in the Mathematics Department, in particular: Ellie Abernethy, Erin Bodine, Steve Fassino, Ashley Rand, and Fei Xing. A special and profound gratitude to my family, especially to my parents, Ricardo and Nhora; my brothers, Paul and Santiago; my aunts, Vicky, Julia Emma, and Regina; and my cousins, Aleyda and Andrea.

Abstract

The gypsy moth, *Lymantria dispar (L.)*, is an invasive species and the most destructive forest defoliator in North America. Gypsy moth outbreaks are spatially synchronized over areas across hundreds of kilometers. Outbreaks can result in loss of timber and other forestry products. Greater losses tend to occur to the ecosystem services that forests provide, such as wildlife habitat, carbon sequestration, and nutrient cycling. The United States can be divided in three different areas: a generally infested area (populations established), an uninfested area (populations not established), and a transition zone between the two. There are different management programs matching these different areas: detection and eradication, the Slow-the-Spread program, and suppression of outbreaks in areas that are infested by the gypsy moth as a means to mitigate impacts. This dissertation focuses in optimal control techniques for models of areas where the population is established or in the invasion front.

We develop an optimal control formulation for models of an established population of the invasive pest gypsy moth. The models include interaction with a pathogen and a generalist predator. The population of gypsy moth is assumed to be controlled with the pesticide Bt. The assumed objective functional minimizes cost due to gypsy moth and cost for suppressing the population of gypsy moth. Optimization techniques in our numerical results, suggest the timing and intensity of control. Our results are consistent over different parameter values and initial conditions

To model the population in the invasion front, we develop the theory of optimal control for a system of integrodifference equations. Integrodifference equations incorporate continuous space into a system of discrete time equations. We design an objective

functional to minimize the cost generated by the defoliation caused by the gypsy moth and the cost of controlling the population. Existence and uniqueness results for the optimal control and corresponding states have been completed. We use a forward-backward sweep numerical method, and our numerical results suggest appropriate spatial and temporal location and intensity of optimal controls.

Table of Contents

1 Introduction **1**

1.1 The gypsy moth . . . 1

1.2 Mathematical models for gypsy moth . . . 4

1.3 Optimal control theory . . . 5

1.3.1 Discrete time state equations . . . 8

1.3.2 Integrodifference state equations . . . 11

1.4 Numerical methods . . . 12

1.4.1 Direct minimization of the objective functional . . . 12

1.4.2 Forward-Backward sweep method . . . 13

2 Discrete models **14**

2.1 Introduction . . . 14

2.2 Mathematical model . . . 16

2.3 Optimal control problem . . . 18

2.4 Methods . . . 19

2.4.1 Numerical Methods . . . 20

2.4.2 Parameter Selection . . . 24

2.5 Results . . . 29

2.6 Inclusion of a generalist predator . . . 41

2.6.1 Methods . . . 44

2.6.2 Results . . . 46

2.7 Conclusions . . . 50

3 Integrodifference model **52**

3.1 Introduction . . . 52
3.2 Mathematical model . . . 55
3.3 Existence of an optimal control . . . 57
3.4 Characterization of an optimal control . . . 60
3.5 Uniqueness of the Optimal Control . . . 68
3.6 Numerical Solutions . . . 79
3.7 Conclusions . . . 87

4 Conclusions and Future Extensions **88**
4.1 Non-Spatial model . . . 89
4.2 Spatial model . . . 90

Bibliography **91**

Appendices **101**

A **102**
A.1 Pontryagin's Maximum Principle approach . . . 102
A.2 Dynamics for the host-pathogen model . . . 106
A.3 Optimal control results for smaller times . . . 107
A.4 Variation of Parameters in the host-pathogen model . . . 109
A.5 Windows for the control . . . 114
A.6 Statistical results for the factorial experiment . . . 116
A.7 Box plots for the host-pathogen model at different starting conditions . . . 120
A.8 Statistical results for host-pathogen model . . . 122
A.9 Box plots for the model with predation at different starting conditions . . . 125
A.10 Statistical results for the model with predation . . . 126
A.11 Optimal control results for model with predation . . . 129

B **134**
B.1 Accuracy results for the trapezoidal rule . . . 134
B.2 Spatial initial conditions . . . 135

Vita **140**

List of Tables

2.1 Parameter values for the host-pathogen model 24

2.2 Parameter levels for the factorial experiment 35

2.3 Parameter values for the model with predation 46

3.1 Parameter values for the Integrodifference model 80

A.1 Effect of Variation of A on the optimal control. Empty space means a value of zero for the control, rows highlighted are in Figure 2.6(b). 109

A.2 Effect of Variation of δ on the optimal control. Empty space means a value of zero for the control, rows highlighted are in Figure 2.7(b). 109

A.3 Effect of Variation of γ on the optimal control.. Empty space means a value of zero for the control, rows highlighted are in Figure 2.9(b). 110

A.4 Effect of Variation of ϕ on the optimal control. Empty space means a value of zero for the control, rows highlighted are in Figure 2.10. 111

A.5 Effect of Variation of $\frac{1}{C^2}$ on the optimal control. Empty space means a value of zero for the control. 112

A.6 Effect of Variation of the Initial conditions on the optimal control. Empty space means a value of zero for the control. 113

List of Figures

1.1 U. S regions with presence of gypsy moth. Infested area (red), uninfested area (white) and transition zone (yellow). Taken from [77], using values from 2000. 3

2.1 Gypsy moth population from host-pathogen model. With long-period, large-amplitude cycles in gypsy moth densities. 17
2.2 Possibilities for order of events 17
2.3 Stopping criteria. Adapted from [34] 22
2.4 Gypsy moth population for varying initial conditions. a. $N_0 = 0.1$ and $Z_0 = 10$. b. $N_0 = 10$ and $Z_0 = 0.1$, with other parameters in Table 2.1 . . . 25
2.5 Time interval used for control. a. Starting point for the control. b. Interval of time to apply control, with parameters in Table 2.1 25
2.6 Control, gypsy moth, and virus densities resulting from variation in A, with other parameters in Table 2.1 27
2.7 Control, gypsy moth, and virus densities resulting from variation in δ, with other parameters in Table 2.1 28
2.8 Comparison of populations and objective functional values, without control(a) and with control(b), with parameters in Table 2.1 30
2.9 Variation in γ from 40, 75, to 110. a. Dynamics without control. b. Dynamics with control. With other parameters in Table 2.1 32
2.10 Variation in ϕ from 75, 110, to 140. a. Dynamics without control. b. Dynamics with control. With other parameters in Table 2.1 34
2.11 Different values for starting point for the control with respect the density of gypsy moth in the host-pathogen model, with parameters in Table 2.1 . 36

2.12 Variation for initial conditions for the optimal control, low, medium and high densities of gypsy moth in the host-pathogen model. a. Dynamics without control. b. Dynamics with control. With parameters in Table 2.1 . 37
2.13 Summary statistics for the optimal control for the host-pathogen model. Bar height represents the average value for the optimal control at each year, and the error bar is the standard deviation. a. With 100 different starting conditions. b. Starting conditions for the control at low densities. c. Medium densities. d. High densities. With parameters in Table 2.1 . . . 40
2.14 Fraction of gypsy moth density killed by predation, where a is the maximum fraction killed, and b is the gypsy moth density at which the fraction killed is maximized 42
2.15 Gypsy moth population in the model with predation and with no control, for varying initial conditions. a. $N_0 = 10$ and $Z_0 = 1$. b. $N_0 = 100$ and $Z_0 = 100$. c. $N_0 = 1000$ and $Z_0 = 1$, with other parameters in Table 2.3 . . 43
2.16 Time intervals to control in the model with predation. The lower graphic presents the windows to control. Initial conditions are $N_0 = 10$ and $Z_0 = 10$, with other parameters in Table 2.3 47
2.17 Results for the model with predation. The three windows correspond to the time interval selection in the long term dynamics in Figure 2.16. a. Dynamics without control. b. Dynamics with control. Initial conditions are $N_0 = 10$ and $Z_0 = 10$, with other parameters in Table 2.3 49
2.18 Summary statistics for the optimal control for the model with predation. Bar height represents the average value for the optimal control at each year, and the error bar is the standard deviation. Starting conditions for the control at: (a) low densities , and (b) high densities. With parameters in Table 2.3 50

3.1 Population dynamics of gypsy moth and the virus. a. Non-spatial model. b. Integrodifference model. With parameters in Table 3.1 81
3.2 a. No control. b. With Control. $A = B = C = 1$, with other parameters in Table 3.1 83
3.3 Aggregate spatial initial conditions 84

3.4 Shifted spatial initial conditions 84
3.5 Effect of the optimal control over a period of 15 years with aggregate spatial initial conditions in Figure 3.3(b). a. Dynamics without control. b. Dynamics with control. c. Different view of the control display in b 86

A.1 Gypsy moth and virus population from host-pathogen model. With long-period, large-amplitude cycles in the densities. 106
A.2 Comparison of populations and objective functional values for a shorter time period of 7 years, without control(a) and with control(b), with parameters in Table 2.1 107
A.3 Comparison of populations and objective functional values for a shorter time period of 13 years, without control(a) and with control(b), with parameters in Table 2.1 108
A.4 Impact in the gypsy moth densities by variation in γ. a. $\gamma = 40$. b. $\gamma = 75$. c. $\gamma = 110$ 114
A.5 Impact in the gypsy moth densities by variation in ϕ. a. $\phi = 70$. b. $\phi = 100$. c. $\phi = 140$ 115
A.6 Statistics for the factorial experiment with the objective functional as a response variable 116
A.7 Statistical analysis for the factorial experiment with the sum of controls over a period of 20 years as a response variable 117
A.8 Interaction plots for the five parameters of the host-pathogen model with sum of controls over a period of 20 years as a response variable 118
A.9 Interaction plots in the host-pathogen model with sum of controls over a period of 20 years as a response variable. a $A\phi$. b. $q\phi$ 119
A.10 Box plots for the optimal control for the host-pathogen model. a. Starting conditions for the control at low densities. b. Medium densities. c. High densities. With parameters in Table 2.1 121
A.11 Statistical analysis of the objective functional for different starting densities in the host-pathogen model 122
A.12 Statistical analysis of the sum of the controls for different starting densities in the host-pathogen model 123

A.13 Statistical analysis of the time of the maximum control for different starting densities in the host-pathogen model 124
A.14 Summary statistics for the optimal control for the model with predation. On each box, the central mark is the median, the edges of the box are the 25th and 75th percentiles, the whiskers extend to the most extreme data points not considered outliers, and outliers are plotted individually . a. With 100 different starting conditions. b. Starting conditions for the control at low densities. c. Medium densities. d. High densities. With parameters in Table 2.1 125
A.15 Statistical analysis of the objective functional for different starting densities in the model with predation 126
A.16 Statistical analysis of the sum of the controls for different starting densities in the model with predation 127
A.17 Statistical analysis of the time of the maximum control for different starting densities in the model with predation 128
A.18 Time intervals to control in the model with predation. The lower graphic presents the windows to control. Initial conditions are $N_0 = 10$ and $Z_0 = 1$, with other parameters in Table 2.3 129
A.19 Results for the model with predation. The three windows correspond to the time interval selection in the long term dynamics in Figure A.18. a. Dynamics without control. b. Dynamics with control. Initial conditions are $N_0 = 10$ and $Z_0 = 1$, with other parameters in Table 2.3 130
A.20 Time intervals to control in the model with predation. The lower graphic presents the windows to control. Initial conditions are $N_0 = 1000$ and $Z_0 = 1$, with other parameters in Table 2.3 131
A.21 Results for the model with predation. The three windows correspond to the time interval selection in the long term dynamics in Figure A.20. a. Dynamics without control. b. Dynamics with control. Initial conditions are $N_0 = 1000$ and $Z_0 = 1$, with other parameters in Table 2.3 132

A.22 Variation for starting point, low, medium and high densities of gypsy moth in the model with predation. a. Dynamics without control. b. Dynamics with control. With parameters in Table 2.3 133

B.1 Effect of the optimal control over a period of 15 years with aggregate spatial initial conditions in Figure 3.3(a). a. Dynamics without control. b. Dynamics with control. c. Different view of the control display in b 135

B.2 Effect of the optimal control over a period of 15 years with aggregate spatial initial conditions in Figure 3.3(c). a. Dynamics without control. b. Dynamics with control. c. Different view of the control display in b 136

B.3 Effect of the optimal control over a period of 15 years with shifted spatial initial conditions in Figure 3.4(a). a. Dynamics without control. b. Dynamics with control. c. Different view of the control display in b 137

B.4 Effect of the optimal control over a period of 15 years with shifted spatial initial conditions in Figure 3.4(b). a. Dynamics without control. b. Dynamics with control. c. Different view of the control display in b 138

B.5 Effect of the optimal control over a period of 15 years with shifted spatial initial conditions in Figure 3.4(c). a. Dynamics without control. b. Dynamics with control. c. Different view of the control display in b 139

Chapter 1

Introduction

1.1 The gypsy moth

Invasive species are one of the world's most critical immediate environmental threats [55, 79]. They can have a strong negative impact on ecosystem function and services, if they are not properly removed in a reasonable time frame [87].

The gypsy moth, *Lymantria dispar*, is perhaps the most destructive forest defoliator in North America. It was introduced into the United States near Boston in the late 1860s. In 1869, gypsy moth individuals were brought from France, by amateur entomologist Etienne Lopold Trouvelot. He was conducting experiments to use gypsy moths as an alternative for the production of silk. During this time, European silk production was severely affected by a protozoan disease [77, 78]. Since then gypsy moths have gradually spread, and now can be found in Virginia and North Carolina to the south, Indiana and Illinois to the west, and Wisconsin to the Midwest [68, 69]; see Figure 1.1. Larvae from gypsy moths are a highly polyphagous foliage feeder and can feed on over 300 species of trees. The gypsy moth original geographic range is temperate Eurasia and the Mediterranean coast of North Africa, where it sporadically presents damaging outbreaks [78].

There is one generation of gypsy moth per year. Eggs are dormant through the winter and larvae hatch in the spring. Individuals remain in the larval stage about four to six weeks, and the pupal phase lasts around two weeks. Adults come out in mid-summer and

typically stay alive a week or less; usually males emerge a little earlier than females. Adults do not feed. Females produce a sex pheromone that males use to locate mates. In some Asia populations, females' are able to fly. In European populations, the females ability to fly is totally absent. North American populations originate from Europe, therefore females are incapable of flight [78, 15].

Outbreaks, peaks of high density, have been environmentally and economically expensive in North America. Since 1924, over 81 million acres of U.S forests have been defoliated by the gypsy moth, including over 12 million acres just in 1981. Outbreaks in gypsy moths are likely to be spatially synchronized over regions across hundreds of kilometers. This can severely intensify the ecological and socioeconomic impacts of high density populations and overcome managing resources designated to alleviate impacts. Gypsy moth outbreaks defoliate several species of trees; repeated defoliation causes decreased growth and mortality. Outbreaks frequently occur in forested inhabited locations where, in addition to problems associated with defoliation, the presence of large amounts of caterpillars generate considerable irritation to homeowners. Gypsy moth outbreaks can result in loss of timber and other forestry products [69, 78].

Ecosystem services provided by forests, are also affected by outbreaks of gypsy moths, including impacts on: wildlife habitat, carbon sequestration, and nutrient cycling. Outbreaks are likely to change the composition of the community, creating indirect changes to herbivores and changing forest succession [69, 78]. Gypsy moth outbreaks can cause declines in populations of some avian species, since defoliation increases the visibility of nests to predators. Infestations can reduce the abundance of closed canopy species and increase the number of birds dependent on more open habitats. Outbreaks also elevate tree mortality, augment the amount of snags and so may favor cavity-nesting species [27, 75].

The United States can be separated in three different regions, shown in Figure 1.1, based on the status of the gypsy moth populations: An infested region (populations are established), an uninfested region (populations are not established), and a transition zone

between the two previous regions. There are different management programs matching these different regions [78, 77]:

- Detection/eradication, where the objective is to find and eliminate new colonies in areas uninfested by the gypsy moth, for example, the west coast of the U.S.
- The Slow the Spread program, that creates a barrier zone along the invasion front in the U.S.
- Suppression of outbreaks in regions that are infested by the gypsy moth with the objective to diminish the negative impacts.

This dissertation focuses on optimal control techniques for models of areas where the population is established (chapter 2) and in the invasion front (chapter 3). The control represents intervention actions to optimally manage populations of gypsy moth.

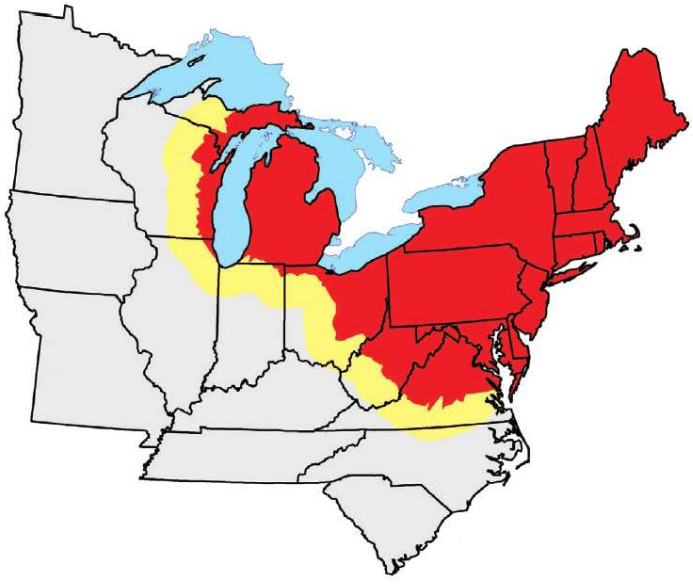

Figure 1.1: U. S regions with presence of gypsy moth. Infested area (red), uninfested area (white) and transition zone (yellow). Taken from [77], using values from 2000.

1.2 Mathematical models for gypsy moth

Almost all models of gypsy moth have been focused on the interaction between gypsy moth and the pathogen *Lymantria dispar* nucleopolyhedrosis virus (*Ld*MNPV). The first attempts to model the populations of gypsy moth, were based on Anderson and May's seminal work [1, 2, 3]. Foster and collaborators were one of the first to model the gypsy model population dynamics [24]. They modified the analytical model of invertebrate-pathogen dynamics from the work of Anderson and May to include vertical transmission. They also included host fecundity, infected host mortality and pathogen production as variables instead of constants. The next modeling efforts where made by Dwyer and Elkinton [18]. Rather than focusing on long term dynamics, as in [1, 2, 3], they adapted the model to focus on the within-season dynamics. In addition, they estimated parameters based in field and experimental work.

In 2000 Dwyer and collaborators developed a model that includes seasonality in host reproduction and heterogeneity among hosts in their susceptibility to the virus [16]. In order to simplify computations, the model was discretized; as a result they obtained an implicit equation to calculate the fraction of infected density of gypsy moth each year. Using this model as a base line, several additions were made. Dwyer and collaborators added a generalist predator using a type II functional response [17]. Others included gypsy moth evolving resistance to the virus [19]. The model of Bjørnstad *et al.*[53] allowed natural enemies of gypsy moth to operate in a sequential way, assuming the virus attacks the larva, and the predator attacks the pupae. They also introduced a type III functional response. Haynes *et al.*, using modifications from [53], included different forms of types II and III functional responses [32]. Finally, Fuller and collaborators developed a model that included heritable virus resistance [25]. In the first part of this dissertation we use the models developed by Dwyer and collaborators [16, 17], since they are the foundation for many other models.

To our knowledge, the first work that applied optimal control theory to the management of gypsy moths, was the paper by Whittle *et al.* [86]. Their model is a modification of the Nicholson-Bayley model [51], which incorporates the effect of tannins in the mortality of

gypsy moths. As the method of suppression they use a biocontrol. Their principal result is that the application of the biocontrol should take place when the virus populations are at their lowest levels. Also Whittle [85] generalized the work of [86] to optimal control of an integrodifference system.

1.3 Optimal control theory

Optimal control theory is an extension of the calculus of variations. It is the mathematical study of how to influence a dynamical system, with the aim to minimize or maximize the value of a function of the system, which we refer as the objective functional [5, 23]. There is a control function(s) that can modify the dynamical system. The behavior of the dynamical system is described by a state equation(s), and can have a variety of forms: ordinary differential equations, partial differential equations, discrete difference equations, stochastic differential equations or integrodifference equations [42]. In this dissertation we focus on optimal control problems for discrete difference equations (chapter 2) and integrodifference equations (chapter 3), we employ extensions of the ideas from Pontryagin's Maximum Principle (PMP)[59, 42].

Pontryagin and collaborators developed optimal control theory for ordinary differential equations (ODE) around 1950 in the Soviet Union. He had the idea of using the adjoint functions to connect the differential equation to the objective functional. The states satisfy ODEs containing control functions with initial conditions. They created necessary conditions for optimal control theory, which means that if the control and the corresponding states are optimal, then the conditions hold [59, 42].

Suppose we want to apply control to a single ordinary differential equation (ODE). Let $u(t)$ be the control and $x(t)$ be the state that satisfies the following ODE

$$\frac{dx}{dt} = x'(t) = g\big(t, x(t), u(t)\big). \tag{1.1}$$

We assume that both $u(t)$ and $x(t)$ affect the goal represented by the objective functional. The aim is to find an optimal control and corresponding state that achieve the maximum (or minimum) of the objective functional. Consider the optimal control problem in which the objective functional is defined as

$$J(u) = \int_0^T f\big(t, x(t), u(t)\big)dt. \tag{1.2}$$

subject to

$$x'(t) = g\big(t, x(t), u(t)\big) \tag{1.3}$$

where

$$x(0) = x_0 \text{ and } x(T) \text{ is free}, \tag{1.4}$$

where f and g are continuous and differentiable functions. We assume the control set U to be Lebesgue measurable functions. An optimal control, denoted by $u^*(t)$, achieves the maximum (or minimum) of the objective functional,

$$J(u^*) = \max_{u \in U} J(u) \tag{1.5}$$

When the state equation (1.3) with (1.4) is solved with an optimal control in g, we get the corresponding optimal state, $x^*(t)$. Assume we seek to maximize the objective functional, the first order necessary conditions using the simplest form of Pontryagin's Maximum Principle are below.

Theorem 1. *(Pontryagin's Maximum Principle (PMP)) If $u^*(t)$ and $x^*(t)$ are optimal for problem in (1.2) - (1.4), then there exists adjoint variable $\lambda(t)$ such that*

$$H\big(t, x^*(t), u(t), \lambda(t)\big) \leq H\big(t, x^*(t), u^*(t), \lambda(t)\big) \tag{1.6}$$

for all controls $u \in U$ at each time t, where the Hamiltonian H is

$$H\big(t, x(t), u(t), \lambda(t)\big) = f\big(t, x(t), u(t)\big) + \lambda(t) g\big(t, x(t), u(t)\big), \tag{1.7}$$

and the adjoint equation satisfies

$$\begin{aligned} \lambda'(t) &= -\frac{\partial H\big(t, x^*(t), u^*(t), \lambda(t)\big)}{\partial x} \\ \lambda(T) &= 0. \end{aligned} \tag{1.8}$$

The boundary condition, $\lambda(T) = 0$, is called the transversality condition.

We also need to check for concavity conditions to be able to determine which controls maximize the objective functional and which ones minimize it. We need

$$\frac{\partial^2 H}{\partial u^2} \leq 0 \text{ at } u^*(t) \tag{1.9}$$

for a maximization problem. Similarly

$$\frac{\partial^2 H}{\partial u^2} \geq 0 \text{ at } u^*(t) \tag{1.10}$$

holds for a minimization problem.

Pontryagin's Maximum Principle has an extension for several states and controls. Consider an optimal control with n state variables

$$\max_u \int_0^T f\big(t, x_1(t), x_2(t), \cdots, x_n(t), u(t)\big)dt \tag{1.11}$$

subject to

$$\begin{aligned} x_i'(t) &= g_i\big(t, x_1(t), x_2(t), \cdots, x_n(t), u(t)\big) \\ x_i(0) &= x_{i0} \text{ for } i = 1, 2, \cdots, n, \end{aligned} \tag{1.12}$$

where the functions f and g_i are continuously differentiable in all variables. Define the Hamiltonian as

$$\begin{aligned} H\Big(t, x_1(t), \cdots, x_n(t), u(t), \lambda(t)\Big) =& f\Big(t, x_1(t), \cdots, x_n(t), u(t)\Big) \\ &+\lambda_1(t) g_1\Big(t, x_1(t), \cdots, x_n(t), u(t)\Big) \\ &\vdots \\ &+\lambda_n(t) g_n\Big(t, x_1(t), \cdots, x_n(t), u(t)\Big), \end{aligned} \tag{1.13}$$

and the adjoint and transversality conditions satisfy

$$\lambda_i'(t) = -\frac{\partial H}{\partial x_i} \ , \ \lambda_i(T) = 0 \ , \text{ for } i = 1, 2, \cdots, n. \tag{1.14}$$

1.3.1 Discrete time state equations

For discrete states equations, the theory developed for ODE's has been extended. In our discrete time models, we use subscripts to indicate the time step. Define the control as

$$u = \big(u_0, u_1, \cdots, u_{T-1}\big), \tag{1.15}$$

and the difference state equation

$$x_{k+1} = g\big(k, x_k, u_k\big) \ , \text{ for } k = 0, 1, 2, \cdots, T-1. \tag{1.16}$$

Notice that the control vector has one less component that the state vector

$$\big(x_0, x_1, \cdots, x_T\big). \tag{1.17}$$

Consider the objective functional

$$J(u) = \sum_{k=0}^{T-1} f\big(k, x_k, u_k\big) \tag{1.18}$$

subject to

$$x_{k+1} = g\big(k, x_k, u_k\big), \tag{1.19}$$

where the initial state x_0 is given and x_T is free. Given a control set $U \subseteq \mathbb{R}^T$, an optimal control u^* satisfies

$$J(u^*) = \max_{u \in U} J(u). \tag{1.20}$$

Necessary conditions for an optimal control and corresponding states can be found using a generalization of Pontryagin's Maximum Principle.

Theorem 2. *(Pontryagin's Maximum Principle for discrete time) If u^* and x^* are optimal for the problem defined in equations (1.18) and (1.19), then there exists an adjoint vector $\lambda = \big(\lambda_0, \lambda_1, \cdots, \lambda_{T-1}\big)$ such that*

$$H_k\big(k, x_k^*, u_k, \lambda_k\big) \ \leq H\big(k, x_k^*, u_k^*, \lambda_k\big) \tag{1.21}$$

for all controls $u \in U$ at each time step k, where the Hamiltonian H at each time step k is defined as

$$H_k\big(k, x_k, u_k, \lambda_k\big) = f\big(k, x_k, u_k\big) + \lambda_{k+1} g\big(k, x_k, u_k\big), \tag{1.22}$$

and the adjoint vector satisfies

$$\lambda_k = \frac{\partial H_k}{\partial x_k} \ , \ \lambda_T = 0. \tag{1.23}$$

Similar to the continuous case, the final time condition of the adjoint is called the transversality condition. Notice in the Hamiltonian, the adjoint component is one index ahead of the state and control components forward in time. The concavity conditions are the same as the ones in the continuous case (1.9 and 1.10). Extension to several variables, is also possible using a similar procedure to the one used in the continuous

case, we introduce an adjoint equation for each state equation. Given n state equations,

$$\begin{aligned} x_{1,k+1} &= g_1\big(k, x_{1,k}, \cdots, x_{n,k}, u_k\big) \\ &\vdots \\ x_{n,k+1} &= g_n\big(k, x_{1,k}, \cdots, x_{n,k}, u_k\big) \end{aligned} \tag{1.24}$$

for $k = 0, 1, 2, \cdots, T-1$, we define the objective functional as

$$J(u) = \sum_{k=0}^{T-1} f\big(k, x_{1,k}, \cdots, x_{n,k}, u_k\big) \tag{1.25}$$

The Hamiltonian becomes

$$H_k = f\big(k, x_{1,k}, \cdots, x_{n,k}, u_k\big) + \sum_{i=1}^{n} \lambda_{i,k+1} g_i\big(k, x_{1,k}, \cdots, x_{n,k}, u_k\big) \tag{1.26}$$

where the adjoint equations and the transversality conditions are given by

$$\lambda_{i,k} = \frac{\partial H_k}{\partial x_{i,k}} \ , \ \lambda_{i,T} = 0, \tag{1.27}$$

for all $k = 0, 1, \cdots, T-1$ and $i = 1, \cdots, n$.

Since gypsy moths have a single generation each year it is appropriate to use discrete models for the state equation. In chapter 2, we use discrete models of gypsy moth that incorporate the interaction with a common pathogen and a generalist predator. First we focus in the interaction of gypsy moth and the virus. In our system, the gypsy moth individuals that survive the virus produce offspring. Dead infected gypsy moths become infectious cadavers that have virus particles. A fraction of particles survive the winter, to infect the next generation of gypsy moths. The fraction of infected individuals is an implicit function that depends in the densities of gypsy moth and the virus. We control the population of gypsy moth with aerial applications of a pesticide. We design an objective functional to minimize the cost generated by the defoliation caused by the population of gypsy moth and the cost of controlling the population with an aerial spray. Later we incorporate the effects of a generalist predator that make the model more realistic.

1.3.2 Integrodifference state equations

Spatial spread is a key element of the invasion processes. Movement of organisms has been incorporated in many mathematical models, starting with the work of Skellam, who used partial differential equations to describe movement in small mammals [71]. Since then partial differential equations (PDE) have been used to model biological movement [49, 10, 52, 48]. An alternative to the PDE approach is integrodifference equations in which a dispersal kernel is used to describe the redistribution of species [40, 81, 39, 31]. As a result integrodifference model have better predictions for the speed of invasion [70, 38]

Integrodifference equations are particularly useful for populations with distinct growth and dispersal stages. The dynamics of such population are better described by discrete time (for generations) and continuous space (for dispersal) . For a population $N_k(x)$ at location x in the spatial domain Ω at time k subject to local population demographic dynamics $f(N)$ and with spatial redistribution kernel $k(x, y)$, the model takes the form

$$N_{k+1}(x) = \int_{\Omega} k(x, y) f\big(N_t(y)\big) dy.$$

The kernel can be selected from a variety of probability density functions, that represent the dispersal patterns in a more realistic way. This provides more flexibility when compared with PDE models that just allow a normal distribution kernel [40, 81, 39, 31, 38].

Optimal control theory for integrodifference equations is a relatively new research area. The first work involved a harvesting model for a single population [36]. After that, several problems for models with single species have been solved using optimal control theory [26, 37, 89, 43, 41]. Nevertheless, there is little theory for optimal control for systems of integrodifference equations.

The purpose of chapter 3 is to address this gap by demonstrating the formulation and analysis of an optimal control problem in a system of two coupled integrodifference equations that represent the densities of gypsy moth and the virus. This extends the current literature which has focused on single population optimal control problems; such

development is a natural extension in the modeling of biological and ecological processes where interactions between populations are the norm. Following the analysis of the existence and the characterization of the optimal control, we apply our results to the control of gypsy moth populations that are in the invasion front. We design an objective functional that includes the cost of the damage produce by gypsy moth and the cost of using a biocontrol (we assume a quadratic cost). For the dynamics of the gypsy moth and the *Ld*MNPV virus we use a modification of the Nicholson-Bailey model.

1.4 Numerical methods

In chapters 2 and 3, after each problem formulation, analysis and parameter selection, we employ numerical algorithms to approximate solutions for the optimal control and state equations. In chapter 2 for our discrete time models, we have an example of an optimal control problem for which the concavity condition on the Hamiltonian is not fulfilled and we are not able to use Pontryagin's Maximum Principle. Therefore we use direct optimization techniques to minimize the objective functional. In chapter 3 for our integrodifference system, we use optimal control theory and an iterative scheme, called the forward-backwards sweep, to find the optimal control. We use the trapezoidal rule for integral approximations.

1.4.1 Direct minimization of the objective functional

For our discrete models in chapter 2, we were not able to guarantee the concavity condition for PMP, mostly because the derivatives of the Hamiltonian are very complex. Details are in Appendix A.1. To avoid this problem, we consider algorithms that do not require information on the derivative of the objective functional. We employ algorithms from the Global Optimization Toolbox from Matlab. These algorithms solve optimization problems in which the objective functional is discrete and there is not information on its derivatives with respect to the states and the control. We use three different algorithms, one that uses a local solver with several starting points, a direct search algorithm, and a genetic algorithm.

1.4.2 Forward-Backward sweep method

The Forward-Backward sweep method can be used to solve the optimality system, which is the state and adjoint equations, coupled with the optimal control characterization. This method can be used for discrete and continuous state equations. In general the iterative method follows these steps:

1. Create an initial guess for the control variable.

2. Using the initial conditions of the states, solve for the state equations forward in time using the integrodifference equation.

3. Given the transversality conditions and the values for the control and the state equations, solve the adjoint equations backwards in time using the integrodifference equation.

4. Calculate the new control value from the characterization, and then update the control using a convex combination of the new value and old value.

5. Repeat previous steps until the consecutive iterates of the control and state equations are close enough. If u is the control at current iteration and u_{old} is the control at previous iteration, then the values are close enough if

$$\frac{\|u - u_{old}\|}{\|u\|} \leq \epsilon, \tag{1.28}$$

where ϵ is the accepted tolerance.

Chapter 2

Discrete models

2.1 Introduction

In this chapter we will focus on models for gypsy moth populations that are already established. Dynamics of these populations are influenced by a diversity of trophic relations and generally oscillate among low and high densities [78, 20]. Many populations of gypsy moth show some periodicity with the dominant period between five to ten years . Low density populations are mainly influenced by small mammal predators like *Peromyscus* spp [77, 20]. In outbreaks, populations achieve very high levels but eventually decrease after one to three years, generally as a consequence of disease epizootics. In North America, of the pathogens affecting gypsy moth, *Lymantria dispar* nucleopolyhedrosis virus (*Ld*MNPV) is the most common, and it only infects gypsy moths [78, 15].

First we focus in the interaction between gypsy moth and the virus, *Ld*MNPV, which belongs to the family Baculoviridae. This family of double-stranded DNA viruses is exclusive to arthropods and frequent in Lepidoptera [8]. Infection happens when larva ingest a sufficient amount of viral particles with the foliage. The virus attacks internal tissues and organs of the larva, causing breakdown of internal tissues and death of the individual [14, 11, 82].

Gypsy moth larvae typically die hanging from branches by their first pair of prolegs in a reversed V pattern. Infection breaks down dermal cells, creating a host cadaver, which is

easily broken and then allows release of the virus back into the environment. When virus become assiciated with foliage after this release the virus is available to be consumed by other gypsy moth larvae, creating a new round of infection [61, 82]. If particles of virus are protected from ultraviolet rays, they can endure for at most one year, which can give enough time to infect the next generation of gypsy moths [58].

Virus infection possibly starts at low densities and when the host population increases the virus also multiplies [88] . *Ld*MNPV is believed to be a strongly host density dependent pathogen. It frequently generates high mortality rates in elevated density levels of gypsy moth populations [44, 45]. Reilly and Hajek (2008) found that resistance of gypsy moth larvae to the virus decreases at elevated densities of gypsy moth [63].

The United States can be divided in three areas, based on gypsy moth population status, Figure 1.1: a generally infested area, an uninfested areas, and a transition zone between the two [78]. There are different management programs matching these different areas: detection/eradication, the Slow-the-Spread program, and suppression of outbreaks [78]. One treatment method that is being employed in all three management programs is the biopesticide, *Bacillus thuringiensis* (*Bt*) [60].

Bacillus thuringiensis (*Bt*) is a gram positive, soil microbe that has been utilized in management programs to control several insects, including species of the orders Coleoptera, Diptera, Hymenoptera, and Lepidoptera [66]. The employment of *Bt* to control gypsy moth populations has been studied at length [30, 73]. Applications of *Bt* target early gypsy moth instars, which are the most vulnerable life stages [60].

Even though *Bt* is more host specific than chemical pesticides, its applications can have harmful effects on many species of Lepidoptera [54, 83], one of the major insect orders, with more than 11,000 species in the United States and Canada [9]. Since it is usually accepted as the insecticide with least harmful human impacts, *Bt* has been chosen for use in several eradication programs for gypsy moth [30].

2.2 Mathematical model

Since gypsy moths have a single generation each year, it is appropriate to use discrete models. We start with a model that includes gypsy moth and the virus. Dwyer and collaborators [16, 17] developed a model using data from studies of virus transmission in field and laboratory experiments ,

$$
\begin{aligned}
1 - I\big(N_k, Z_k\big) &= \left\{1 + \frac{\overline{v}C^2}{\mu}\Big[N_k I\big(N_k, Z_k\big) + \rho Z_k\Big]\right\}^{-\frac{1}{C^2}} \\
N_{k+1} &= \gamma N_k\Big[1 - I\big(N_k, Z_k\big)\Big] \\
Z_{k+1} &= f N_k I\big(N_k, Z_k\big).
\end{aligned}
\tag{2.1}
$$

Here N_k and Z_k are host(gypsy moth) and pathogen(LdMNPV) densities in generation k, where the density is the number of individuals(or particles) per hectare. The net host fecundity is denoted by γ and f is the pathogen over-winter survival times the average number of particles release by an infected cadaver of the host. The fraction of infected hosts, $I\big(N_k, Z_k\big)$, is a function of the densities of both both species, μ is the rate at which cadavers (gypsy moth individuals that die because of the pathogen) lose infectiousness, and ρ is the susceptibility of hatchlings relative to later-stage larvae. Finally, $\bar{v}$ is the average transmission rate, and C represents the coefficient of variation of the transmission rate [16, 17].

Using realistic values for the parameters (like the ones present in Table 2.1), this model generates long-period, large-amplitude cycles in gypsy moth densities, Figure 2.1. The amplitude and the period of these cycles are similar to the ones seen in gypsy moth populations. Nevertheless, the cycle period is much more regular in the model than in data [17].

Infection and control with Bt both occur at the larval stage. We need to decide which order to use for these 2 events. There are two possibilities, both shown in Figure 2.2.

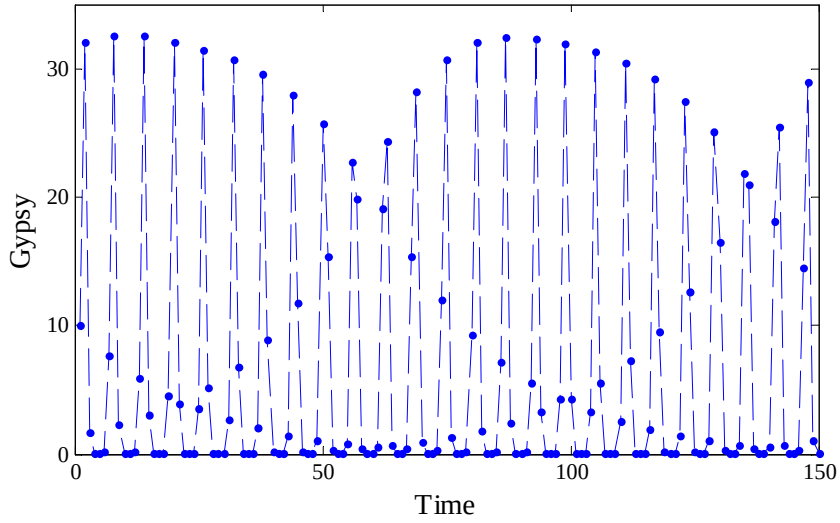

Figure 2.1: Gypsy moth population from host-pathogen model. With long-period, large-amplitude cycles in gypsy moth densities.

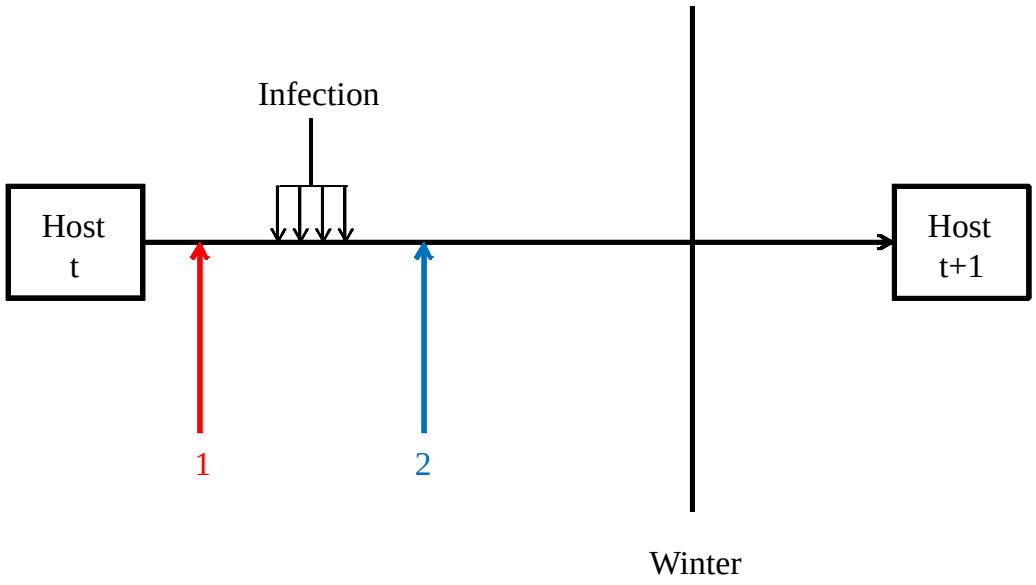

Figure 2.2: Possibilities for order of events

The first option is that the control occurs before the infection (red arrow with number 1), or after the infection (blue arrow with number 2).We use option one, since the majority of management programs spray Bt as early as possible due to higher mortality in earlier larval stages [60].

Using option one and host-pathogen model equation (2.1) we generate the following model:

$$1 - I\left(N_k\left(1-u_k\right), Z_k\right) = \left\{1 + \frac{\overline{v}C^2}{\mu}\left[N_k\left(1-u_k\right) I\left(N_k\left(1-u_k\right), Z_k\right) + \rho Z_k\right]\right\}^{-\frac{1}{C^2}} \tag{2.2}$$

$$N_{k+1} = \gamma N_k\left(1-u_k\right)\left[1 - I\left(N_k\left(1-u_k\right), Z_k\right)\right]$$

$$Z_{k+1} = f N_k\left(1-u_k\right) I\left(N_k\left(1-u_k\right), Z_k\right)$$

where

$$U = \Big\{u = (u_0, u_1, u_2, \cdots, u_{T-1}) | 0 \leq u_k \leq u_{max}, k = 0, 1, \cdots, T-1\Big\}. \tag{2.3}$$

The control, u_k, is the fraction of the density of gypsy moths that die because of the aerial spray of Bt at time k. We choose this control since most eradication programs use aerial applications of Bt [78].

2.3 Optimal control problem

We design an objective functional to minimize the cost arising from defoliation caused by the population of gypsy moth and the cost of controlling the population with an aerial spray of Bt.

$$\min_u \sum_{k=0}^{T-1} e^{-\delta k}\Big[EDN_k + C(u_k)\Big]. \tag{2.4}$$

We assume that the damage caused by gypsy moth is directly proportional to the density of gypsy moth. The constant D has units of dollars per density of gypsy moth. For the cost of applying Bt, we use a cost model specifically developed for gypsy moth . This cost function assumes that one full Bt application kills a u_{max} fraction of the target gypsy

moth. For operational aerial spray programs the cost for one application is 54.4 dollars per hectare [61, 76]. This cost function can be written as

$$\text{cost} = \frac{\log(1-u_k)}{\log(1-u_{max})/54.4} \ .$$

E is a weight constant balancing the importance of the two costs(damage and control). The term $e^{-\delta k}$ is a discounting factor, taking into account that money now is worth more that money in the future. Therefore we can rewrite our objective functional as:

$$\min_u \sum_{k=0}^{T-1} e^{-\delta k}\Big[EDN_k + \frac{\log(1-u_k)54.4}{\log(1-u_{max})}\Big] \tag{2.5}$$

Finally to simplify notation we define $A = ED$ and $B = \frac{54.4}{\log(1-u_{max})}$ obtaining:

$$\min_u \sum_{k=0}^{T-1} e^{-\delta k}\Big[AN_k + B\log(1-u_k)\Big]. \tag{2.6}$$

To solve this optimal control problem we first tried using the version of Pontryagin's Maximum Principle (PMP) for discrete time models [59]. The convexity of the Hamiltonian cannot be easily verified so we do not apply PMP. Complete calculation of the convexity of the Hamiltonian is presented in Appendix A.1.

2.4 Methods

To reduce the number of parameters, we use a non-dimensionalized version of the model in equation (2.1). To rescale the model, we divide the densities of both species by the epidemic threshold, $\overline{v}/mu$, which is the gypsy moth density needed for an epidemic to happen as the initial virus density approaches to zero [16, 17], the resulting system is:

$$\begin{aligned} 1 - I\big(\hat{N}_k, \hat{Z}_k\big) &= \left\{1 + C^2\Big[\hat{N}_k I\big(\hat{N}_k, \hat{Z}_k\big) + \hat{Z}_k\Big]\right\}^{-\frac{1}{C^2}} \\ \hat{N}_{k+1} &= \gamma \hat{N}_k\Big[1 - I\big(\hat{N}_k, \hat{Z}_k\big)\Big] \\ \hat{Z}_{k+1} &= \phi \hat{N}_k I\big(\hat{N}_k, \hat{Z}_k\big) \end{aligned} \tag{2.7}$$

where the new densities are $\hat{N}_k = \frac{\mu N_k}{\bar{v}}$ and $\hat{Z}_k = \rho\frac{\mu Z_k}{\bar{v}}$. Then $\phi = f\rho$ is defined, as the product of the probability f that a pathogen particle survives the winter, times the susceptibility of new emerging larvae ρ [16, 17].

The non-dimensionalized version has three parameters less than the original model. For our control problem, new state equations are:

$$1 - I\big(\hat{N}_k(1-u_k), \hat{Z}_k\big) = \left\{1 + C^2\left[\hat{N}_k(1-u_k)I\big(\hat{N}_k(1-u_k), \hat{Z}_k\big) + \hat{Z}_k\right]\right\}^{-\frac{1}{C^2}} \tag{2.8}$$

$$\hat{N}_{k+1} = \gamma\hat{N}_k(1-u_k)\Big[1 - I\big(\hat{N}_k(1-u_k), \hat{Z}_k\big)\Big]$$

$$\hat{Z}_{k+1} = \phi\hat{N}_k(1-u_k)I\big(\hat{N}_k(1-u_k), \hat{Z}_k\big).$$

2.4.1 Numerical Methods

Given that we cannot utilize Pontryagin's Maximum Principle(PMP), we must use alternative optimization methods that directly minimize the objective functional,

$$\min_u \sum_{k=0}^{T-1} e^{-\delta k}\Big[A\hat{N}_k + B\log(1-u_k)\Big]. \tag{2.9}$$

We can not guarantee the concavity condition for PMP basically because the fraction of infected individuals is an implicit function, which makes derivatives of the Hamiltonian fairly complex; see details in Appendix A.1. To avoid this problem, we consider algorithms that only use of objective functional and the state system but do not need derivative information for the objective functional. These algorithms are called derivative-free algorithms [64].

We use the Global Optimization Toolbox from MATLAB®. This toolbox offers multiple methods that search for global solutions to problems including: global search, multistart, pattern search, and genetic algorithms. This toolbox solves optimization problems for which the objective functional and corresponding state are discrete and derivatives are not needed [33].

Optimization solvers attempt find a local optimal value for the objective functional. These algorithms locate the optimal solution in the basin of attraction of the starting point of the search. Global Optimization Toolbox solvers are intended to search in several basins of attraction, to try to find a global solution. Nevertheless, none of the solvers has an algorithm that can assure a global solution [33]. We use two different methods. The MultiStart algorithm, that uses a local solver with a broad range of start points and the Patternsearch algorithm that searches in several basins at once, using direct search methods.

We chose the MultiStart algorithm because it generates uniformly distributed starting points, runs all starting points, allows a choice for the local solver, and can run several starting points in parallel. These characteristics allow this algorithm to search thoroughly for a global minimum [33].

The Multistart algorithm works as follows [33]:

1. Create starting points: Generate random points within the provided bounds. The points are uniformly distributed.

2. Run local solver: For each starting point we use the local solver fmincon.

3. Check stopping conditions: The algorithm stops when it has checked all starting points. It can also end when the total running time goes over a set limit.

4. Create output: Sort local solutions by objective functional value from lowest to highest and provides the best solution from all local results.

For local solver we use fmincon. The principal reason we chose fmincon as a local solver is that it does not need information on the derivative of the objective functional. When the gradient or Hessian are not provided the solver approximates the derivatives numerically. Also fmincon is one of the best options for a smooth nonlinear objective functional with bounds over the control, like our objective functional. Fmincon uses a trust region approach to minimize the objective functional [34].

To understand how fmincon works, suppose we want to find a minimum for the function f. We have a point x in an n-space with value $f(x)$ and we want to find a better value for our objective functional. The central idea is that we approximate f with a simpler function q (usually a quadratic function), that estimates the behavior of function f in a neighborhood around the point x. The neighborhood is called the trust region. If we find a better solution for the function f the current point is updated. If not, the region of trust is decreased and the computation is repeated [34].

The algorithm stopping criteria limits the number of iterations in the optimization. In the case of fmincon, the algorithm ends when the last step is smaller than TolFun or TolX, as illustrated in Figure 2.3 [34]. TolFun is a bound on the change in the value of the objective functional during each step. If

$$|f(x_i) - f(x_{i+1})| < \text{TolFun},$$

the iteration ends. The bound for the size of the step is TolX, therefore the solver stops if [34, 33],

$$|x_i - x_{i+1}| < \text{TolX}.$$

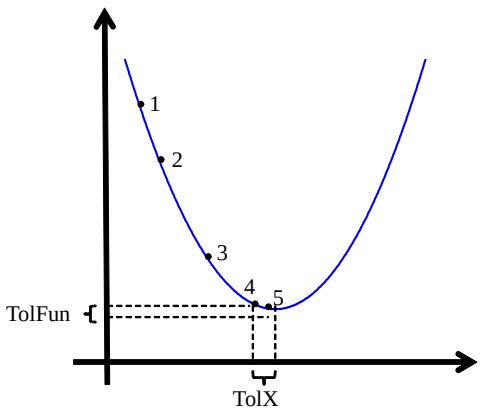

Figure 2.3: Stopping criteria. Adapted from [34]

Alternative to MultiStart, we used Patternsearch is a direct search scheme that does not involve any information on the derivatives of the objective functional. Direct search methods search using nearby points of the current point, looking for one that has a lower value of the objective functional. This method is commonly used when the objective functional is not differentiable or not continuous [33].

The algorithm searches a group of points around the current one, at each iteration. This set of points is called the mesh. The set of vectors v_j used by the algorithm to determine the points to search in each time step, is the pattern. This set is defined by the number of independent variables, N, in the objective functional. In our case we use the maximal basis, with $2N$ vectors as the pattern [33]. As an example, if we have 3 independent variables, the $2N$ basis will be:

$$v_1 = \begin{bmatrix} 1 & 0 & 0 \end{bmatrix} \qquad v_2 = \begin{bmatrix} 0 & 1 & 0 \end{bmatrix} \qquad v_3 = \begin{bmatrix} 0 & 0 & 1 \end{bmatrix}$$
$$v_4 = \begin{bmatrix} -1 & 0 & 0 \end{bmatrix} \qquad v_5 = \begin{bmatrix} 0 & -1 & 0 \end{bmatrix} \qquad v_6 = \begin{bmatrix} 0 & 0 & -1 \end{bmatrix}$$

In our case we have 20 independent variables, one for each year we want to apply the control. For the Patternsearch algorithm, there is an additional stopping criteria besides TolFun and TolX. The mesh tolerance generates a criteria, since if the current mesh size is below the value of mesh tolerance, the algorithm stops.

For our numerical approximations we use the MultiStart and the Patternsearch algorithms. For both we provide random starting points. For the Multistart approach we use 100 starting points. For both algorithms we use TolFun = TolX = 10^{-14}. Patternsearch uses a mesh tolerance of 10^{-6}. Both algorithms have a limit for the number of iterations and for the maximum number of objective functional evaluations used, and neither of those was achieved in any of our searches. For the host-pathogen model, in all cases both methods arrived to the same control solution.

2.4.2 Parameter Selection

For the numerical approximations we use the following values for the parameters:

Table 2.1: Parameter values for the host-pathogen model

Parameter	γ	ϕ	$\frac{1}{C^2}$	A	δ	u_{max}
Values	74.6	100	1.06	50	0.02	0.8

Parameters for the model (γ, ϕ, $\frac{1}{C^2}$) were taken from Dwyer's paper [17]. We assume that one full *Bt* application kills 80% of the target gypsy moths [61, 76]. Parameters for the objective functional, A and δ, are explained later in this section.

As we can see in Figure 2.4(a) and (b), initial conditions affect the initial behavior of the system but after some time there is a repetitive cycle. To neglect the transient dynamics due to initial conditions, we start all our analysis after 150 generations. For uniformity we start all our numerical approximations with a density of 10 for both species.

Given that our objective is to minimize the damage caused by defoliation, we want to include the time at which gypsy moth is at elevated densities(highest peaks). To allow comparison between different sets of parameters, we start all of our numerical approximations in the minimum density before the maximum peak of gypsy moth, as shown in Figure 2.5(a). We display a time series of 120 years and point out the section that we are going to use to find the optimal control, in Figure 2.5(b). Since planning and funding for control would be for a limited time frame, we restrict the time horizon for the optimal control to twenty years. Results for smaller time windows, seven and thirteen years, are presented in Appendix A.3.

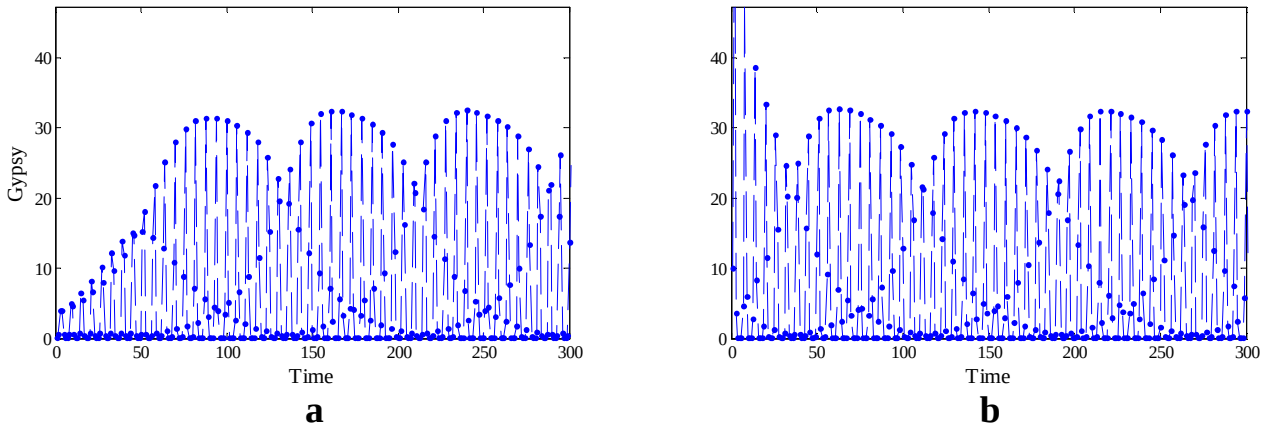

Figure 2.4: Gypsy moth population for varying initial conditions. a. $N_0 = 0.1$ and $Z_0 = 10$. b. $N_0 = 10$ and $Z_0 = 0.1$, with other parameters in Table 2.1

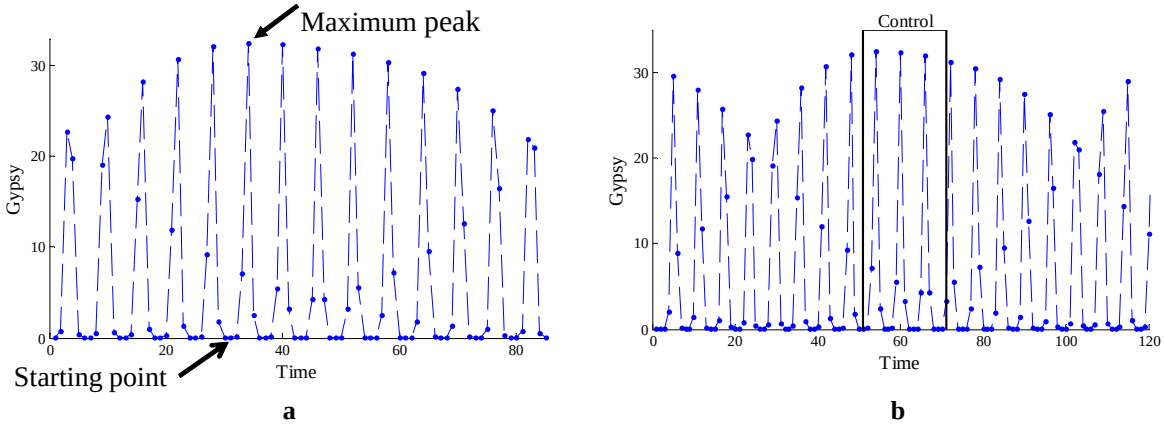

Figure 2.5: Time interval used for control. a. Starting point for the control. b. Interval of time to apply control, with parameters in Table 2.1

To find an appropriate value for the weight constant, A, several simulations were carried out, summarized in Table A.1 and in Figure 2.6. Each figure, has three graphs in each column, going from top to bottom: first is the control, second is the population of gypsy moth with control, and finally the population of the virus with control. Each column provides results for a value for the parameter being varied, in this case A. All the other parameters are constant at the values in Table 2.1. In the top right corner of the graph of the control we display the value of the objective functional for that set of controls.

In Figure 2.6, we see that as we increase A, the amount of control applied increases. For an A value of 1, small amounts of the control are applied. For $A = 1000$, control is applied at almost all times. In Figure 2.6, for A=50 and A=1000, the values of the densities of gypsy moth are almost the same, but the control values are much lower for $A = 50$. We classified the values in Table A.1 using the number of times control is applied, in four intervals of management: low or none (2 or less), medium (4 to 6), high (9 to 13), and very high (more than 13). Given that we are controlling populations that are already established we choose the level of management to be medium. High and very high will be for areas where there are not established populations of gypsy moth, like in the west coast. In the medium interval we choose 50, but our results will hold for values between 20 and 70.

Once a value for A is decided, choosing a value for δ is not complicated. Figure 2.7 and Table A.2, show that different values of δ have a very minor impact in the type of control selected. Even high values like 0.1 don't change the values of the control much. The only difference is in the final value of the objective functional, which decreases as expected when we increase the value of δ. Since $\delta = 0.02$ is a common value, for a 2% interest rate, in discount factors of exponential form, we use it for all our numerical approximations.

Using our base set of parameters in Table 2.1, we modified one at a time and found the numerical approximation of the optimal control for each new set of parameters. Most of the sensitivity results are presented in Appendix A.4.

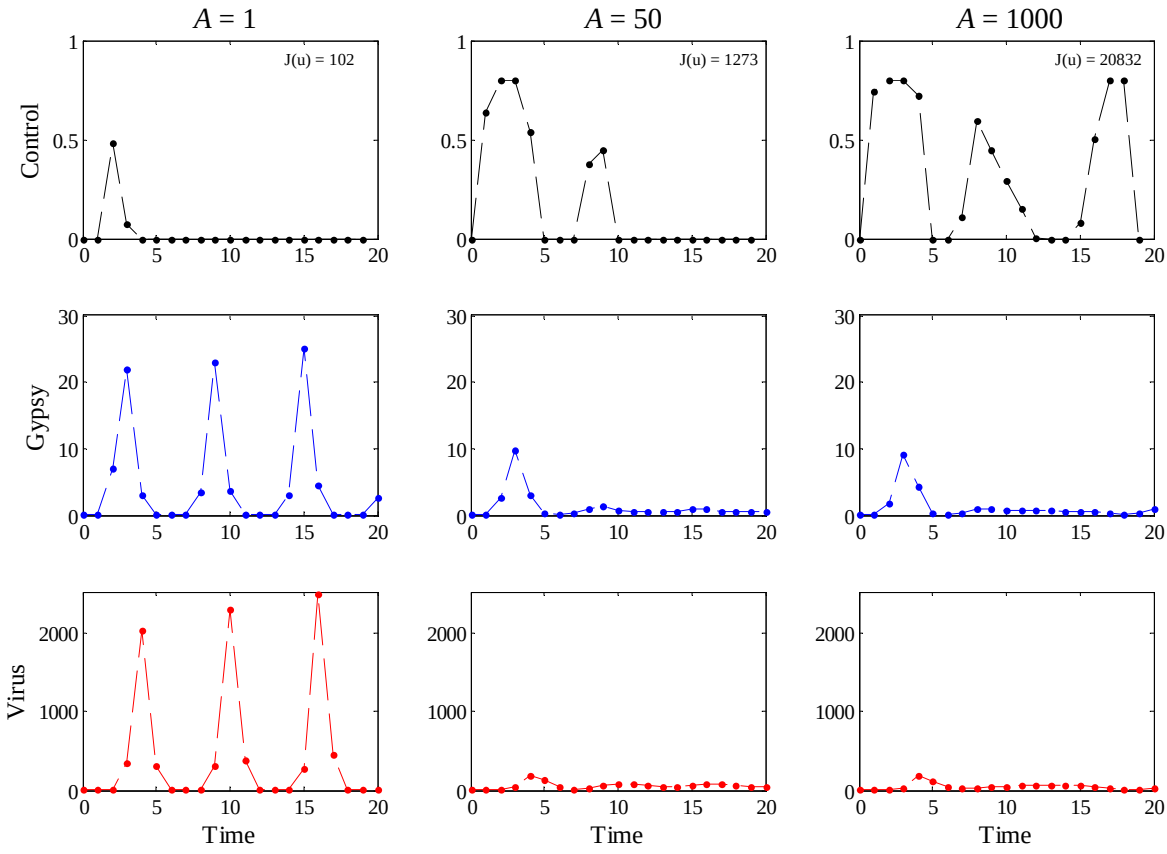

Figure 2.6: Control, gypsy moth, and virus densities resulting from variation in A, with other parameters in Table 2.1

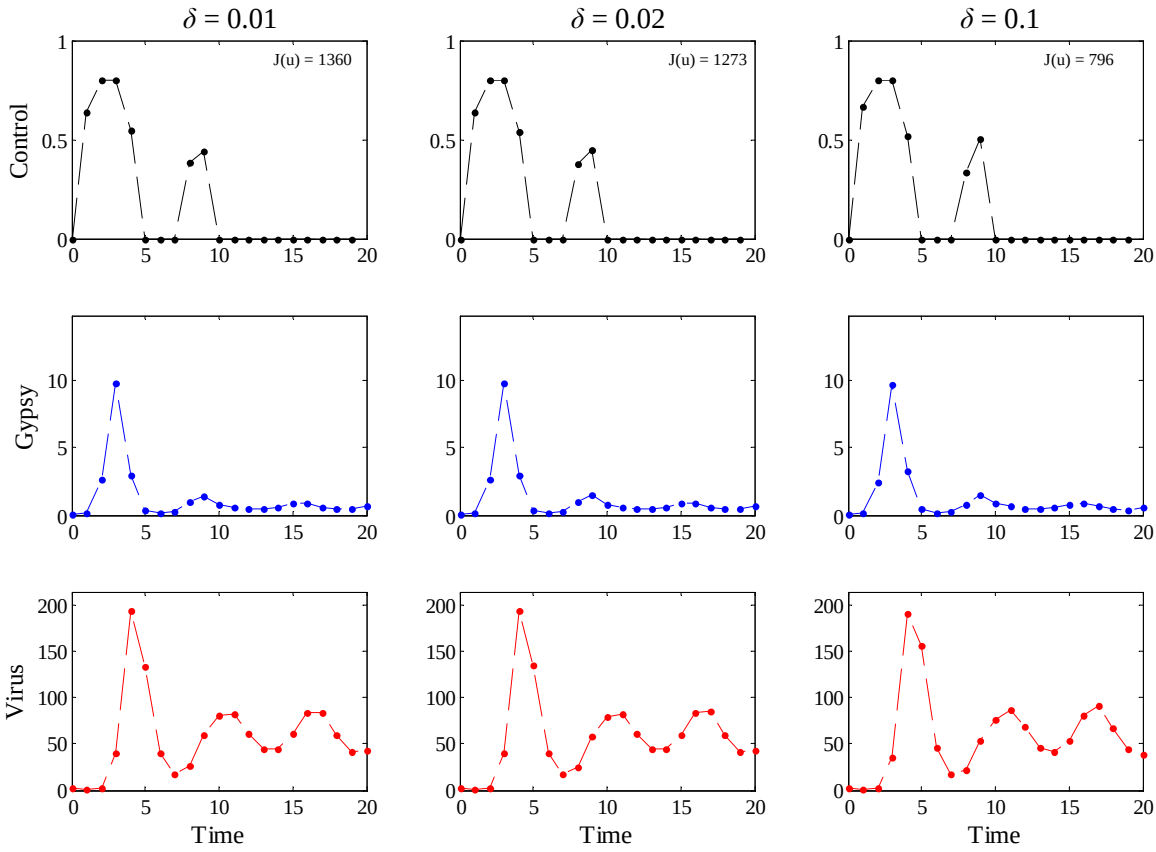

Figure 2.7: Control, gypsy moth, and virus densities resulting from variation in δ, with other parameters in Table 2.1

2.5 Results

Here we present results from the non-dimensionalized host-pathogen system [16, 17]. Unless otherwise noted the parameters used are in Table 2.1. In Figure 2.8(a), we present the population without control, and in part (b) with control. As usual, from top to bottom, the control, gypsy moth, and the virus densities are presented.

Our results, in Figure 2.8(b), show that with a limited number of spray applications (nonzero control values), in this case 6 over twenty years, we can reduce substantially the densities of gypsy moth and the objective functional. Of these applications just two are at the maximum value possible. This occurs in years three and four, during the maximum peak of gypsy moth. Values for the objective functional, present in the top-right corner of the control graphs, display a significance reduction when control is applied as compared to a nonmanagement scenario.

In general, our results for the control have a pattern of two peaks, as seen in Figure 2.8(b). The first peak is higher. The peaks of the control are one year before the peaks of the gypsy moth density in absence of control, years 3 and 9 in Figure 2.8(a). The number of times that we spray the virus (number of applications that control is non-zero) is lower in the second peak two times. We also investigate the cases where the time window for the control is smaller, see Appendix A.3. The optimal control over a period of 7 years (Figure A.2) has only one peak of control, very similar to the first peak found in the time period for 20 years. In the case of 13 years (Figure A.3), the results were almost identical to the ones in the window of 20 years. The only difference is that the second peak of the control is lower. The similarity between these 3 scenarios: 7, 13 and 20 years, may indicate that the optimal control does not depend much on the length of the period to apply control.

To investigate the robustness of our findings, we modified all parameters. Using our base set of parameters(Table 2.1), we varied one at a time and found the numerical approximation of the control for each new set of parameters.

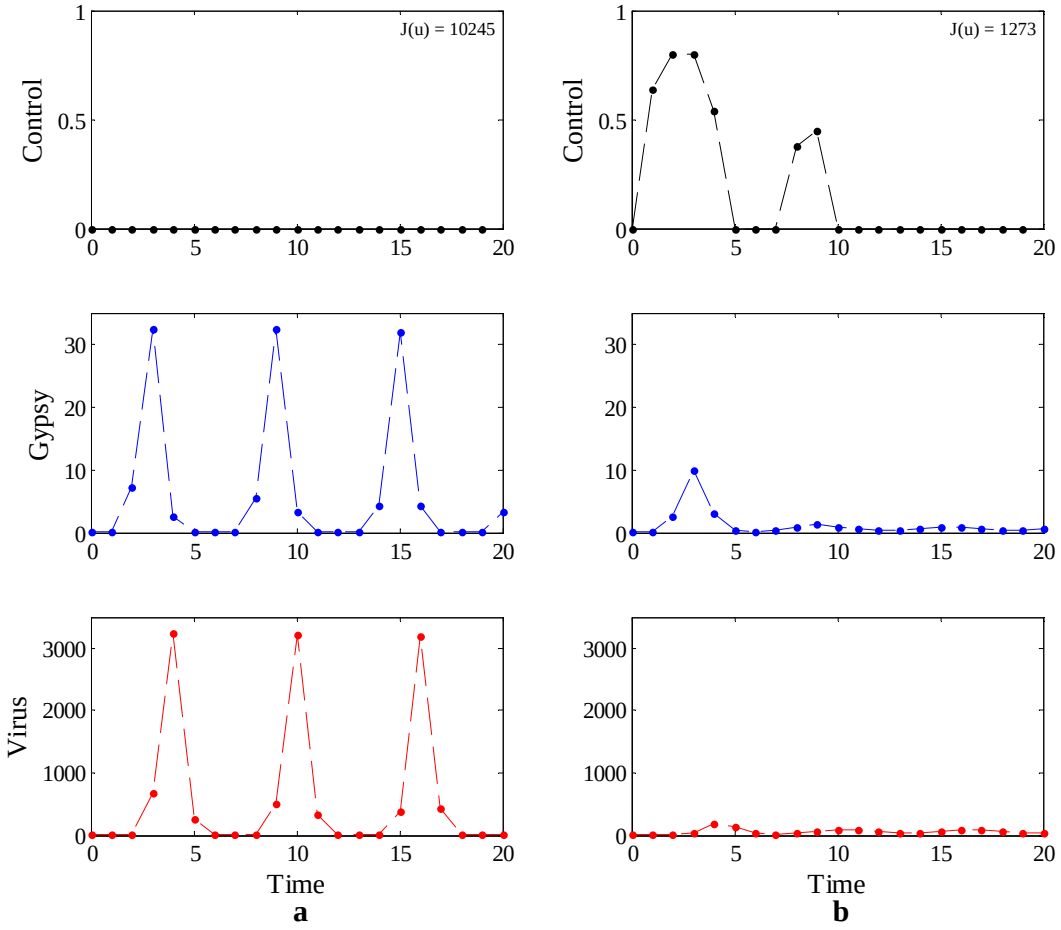

Figure 2.8: Comparison of populations and objective functional values, without control(a) and with control(b), with parameters in Table 2.1

We present our figures in two parts: in part a(top), we show the dynamics without control. In part b(bottom), results are with control. In part a, in each column, first the density of gypsy moth followed by the density of the virus. In part b, the control is first, then the gypsy moth and the virus densities. As in previous graphs each column represents a value for the parameter we are changing. In each figure we present three different values of the parameter. More results can be found at the Appendix A.4, in tables where we show several values of the parameter with the corresponding optimal control value for each year. In these tables an empty space means a value of zero for the control, and the rows that are highlighted are the values in the corresponding graph for the parameter.

The first parameter that we changed was the gypsy moth fecundity, γ. In the system without control, Figure 2.9(a), as we increase γ the density of gypsy moth and the virus increase. Dynamics with control are in Figure 2.9(b). The most important feature, is that when we apply the control the densities of gypsy moth are smaller in all three scenarios. The pattern of two peaks, with the first one being the highest, is present for the three values of the parameter. The number of times we apply control remains constant at six. The level of control increases at years two and nine, at the beginning of the peaks of the control. A small decrease occurs at years four and nine, at the end of the peaks of the control. The objective functional value, in the top right corner of the control of Figure 2.9(b), increases with γ since we apply more control and the densities of gypsy moth are higher. In Appendix A.5, we present the long term dynamics for the three values of γ and the window of 20 years for the control, Figure A.4. For these particular values, the system changes from complex dynamics to simpler ones when we increase γ.

Table A.3, provides results for values of γ from 5 to 150. The patterns observed in Figure 2.9 hold for most values of γ, close to our base value of $\gamma = 74.6$. When we increase γ, we observe an increment in the number of applications and in the level of control. For small values of γ, we have just one peak of control. At higher values we have three peaks of control. For extreme values of γ(small and large), we start the control a year later than usual.

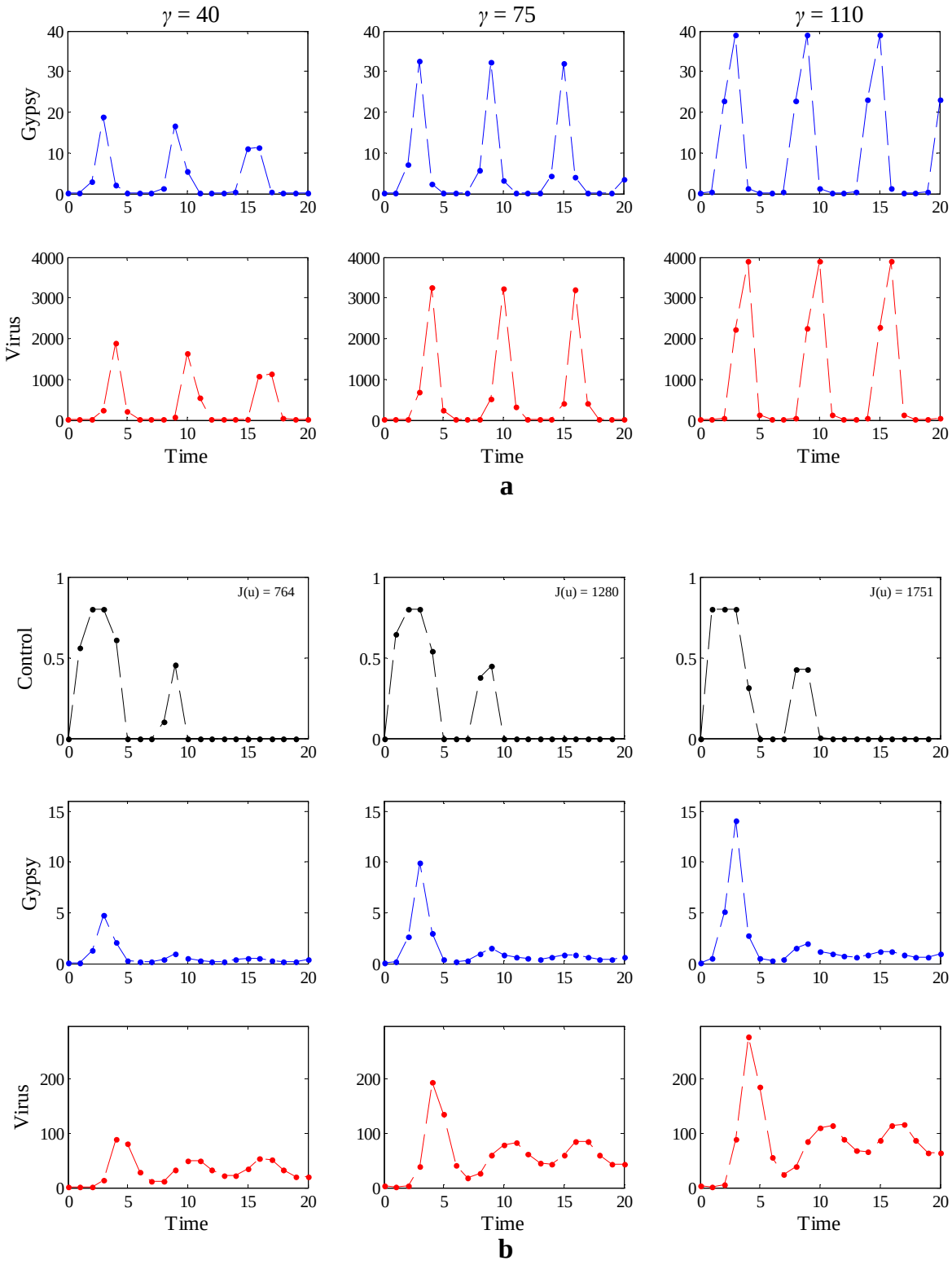

Figure 2.9: Variation in γ from 40, 75, to 110. a. Dynamics without control. b. Dynamics with control. With other parameters in Table 2.1

The next parameter that we modified was the between-season impact of the pathogen, ϕ. In absence of control, Figure 2.10(a), densities of both species increase, with gypsy moth at a slower rate than the virus. In Figure 2.10(b), we see that the control reduces the density of gypsy moth at the three values of the parameter. Again we have the two peaks scenario for the control. The number of applications of control is six, for the three values of ϕ. The amount of control increases at all times, except for the ones that are already at maximum value. There is not a clear pattern for the value of the objective functional. More results for the control at different values of ϕ are in Table A.4. For values below 70, we have two peaks but the second peak is at the end of the time period. The value of the objective functional, decreases with the rise of ϕ. For values over 70, we apply control at the same times, and the amount of control increases with ϕ. The objective functional, remains in the same range of values. Again to have a better idea of where the control portion is in the long term dynamics, see Figure A.5. In this case the system changes from simple dynamics to more complex when we increase ϕ.

We also made variations in $\frac{1}{C^2}$ and in initial conditions. Small variations in $\frac{1}{C^2}$ generate several changes; that is expected since $\frac{1}{C^2}$ is an exponent in the function that calculates the fraction of gypsy moth infected, $I\big(N_k(1-u_k), Z_k\big)$. In general, Table A.5, points out that more control is applied as $\frac{1}{C^2}$ increases. For small values, there is just one peak at the end. For higher values of $\frac{1}{C^2}$, there are four peaks of control, with several values at the maximum amount possible. Initial conditions have an impact only in the first few generations. Since we disregard those transient dynamics, the effect is minimum on the optimal control as we can observe in Table A.6.

In order to study the interactions between the parameters we perform a full factorial experiment. The value of the parameter are $\pm$ 50% of the values in Table 2.1, except for $\frac{1}{C^2}$, which was varied by $\pm$ 0.06 units. The difference in $\frac{1}{C^2}$ is due to its being an exponent in the function that calculates the fraction of gypsy moth infected. The parameter levels chosen are given below:

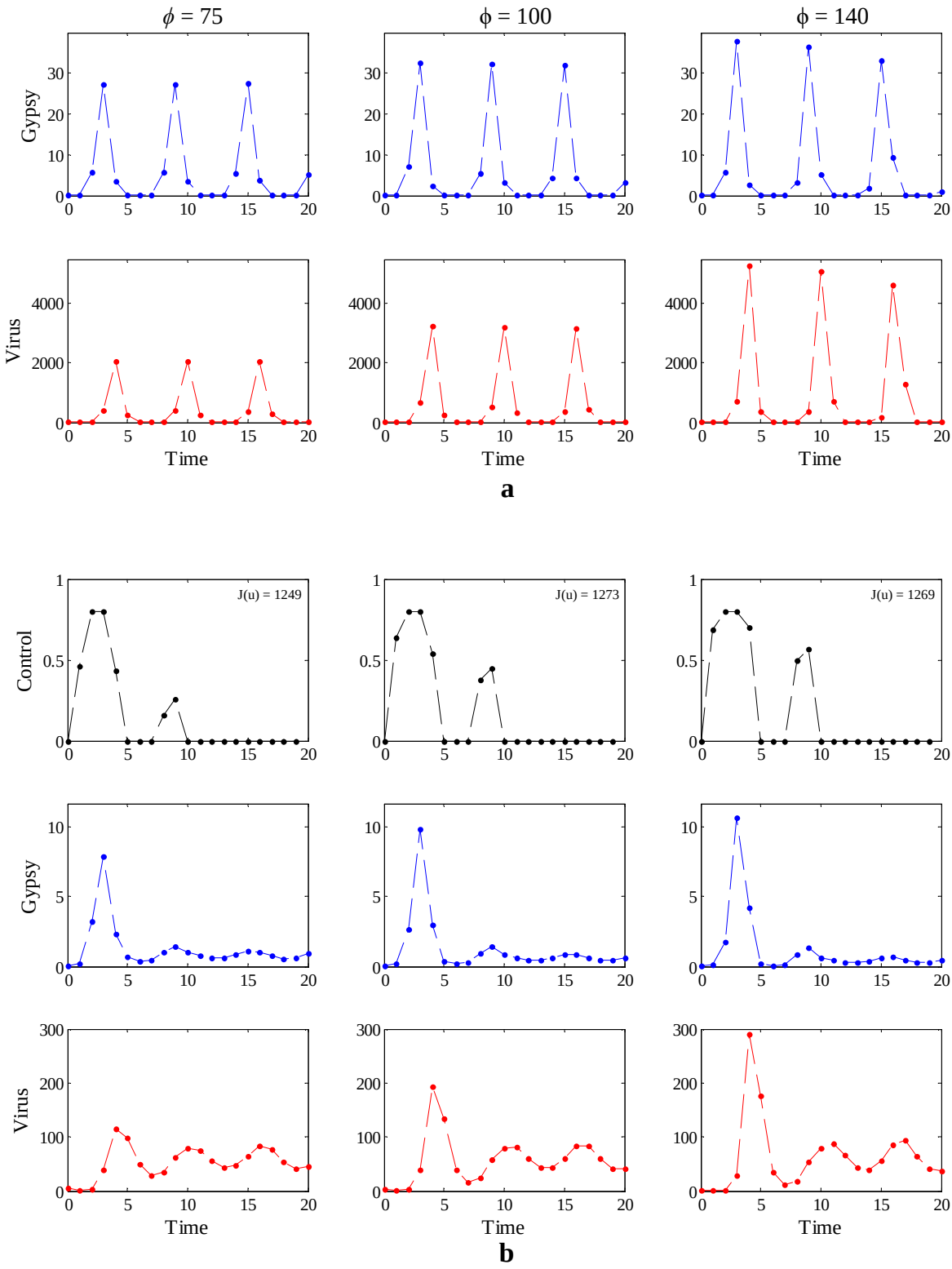

Figure 2.10: Variation in ϕ from 75, 110, to 140. a. Dynamics without control. b. Dynamics with control. With other parameters in Table 2.1

Table 2.2: Parameter levels for the factorial experiment

A	25	50	75
δ	0.01	0.02	0.03
γ	37.3	74.6	111.9
ϕ	50	100	150
$\frac{1}{C^2}$	1	1.06	1.12

Two response variables used for the experiment were the objective functional and the sum of the control over the period of 20 years. In the case of the objective functional all main effects were significant at the 1% level. All the two level interactions were also significant, except for $\delta, \frac{1}{C^2}$ and δ, ϕ. For the sum of the controls, all main effects where significant except for δ. All two level interactions were significant except for the ones involving δ. This is a consequence that δ only affects the values of the objective functional. However δ have a very small effect in the level and number of applications in the optimal control, as shown in Table A.2. We consider significant values of p below to 0.01. Details are in Appendix A.6.

To further investigate the interaction effects, we provide the interaction plots in Figure A.8 and Figure A.9, where we display the largest two interactions ($A\phi$ and $\frac{1}{C^2}\phi$). The largest interaction is between A and ϕ, and to explain this interaction we use Figure A.9(a). We can observe that for $A = 25$ the sum of the control rises as ϕ increases. For higher values of A the differences get smaller. When $A = 75$, the line is horizontal, which means the response variable is basically the same for the three values of ϕ. Recall A is a weight constant balancing the importance of the two costs (damage and control). High values of A mean that the management program gives a high importance to controlling the gypsy moth population. The interaction between A and ϕ implies that when we give a high importance to suppress the population of gypsy moth, the population parameter for the virus has little effect over the total amount of control applied. For the interaction between $\frac{1}{C^2}$ and ϕ, we use Figure A.9(b). We can observe that for high values of $\frac{1}{C^2}$ (for example, 1.06 (green line) and 1.12(blue line)), the response variable increases as we increase ϕ. On

the other hand for the smallest value of $\frac{1}{C^2} = 1$(red line), the response is almost invariant as we increase ϕ.

In most of the cases we explore for the host-pathogen model with starting point in the minimum density before the maximum peak of gypsy moth, we can say that six applications of the control can substantially reduce the densities of gypsy moth. These applications have two peaks, one in years 2 to 5 and another at years 9 and 10. In the first one we have higher levels of the control. The peaks of the control occur a year before the peaks of gypsy moth in the non-management scenario. Our results are consistent for a broad range of parameter values.

So far for the optimal control problem, we have been starting the initial conditions at low densities of gypsy moth. We want to evaluate how the optimal control will be affected by starting at different levels of density. We consider the density of gypsy moth to be at three possible different stages: low, medium, or high, and particular examples can be observed in Figure 2.11. Using the values pointed out in Figure 2.11, we find the optimal control for these three different cases, with parameter values in Table 2.1.

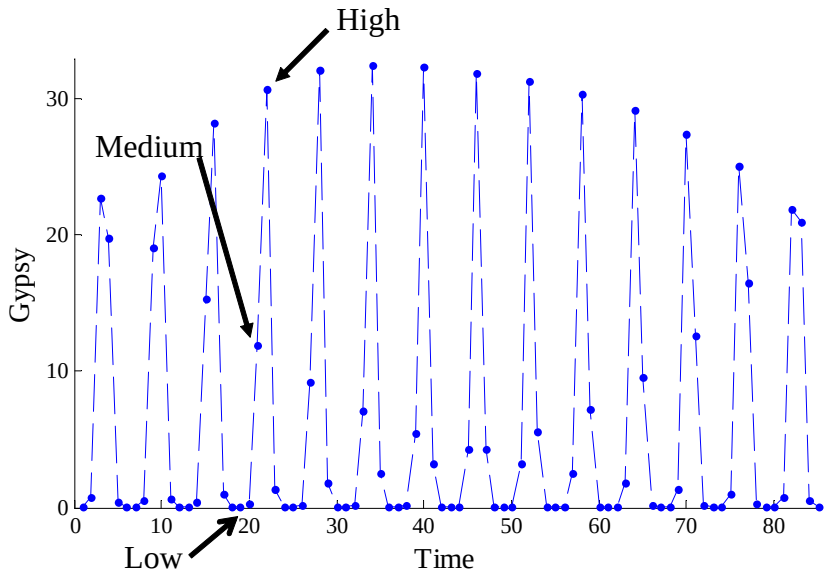

Figure 2.11: Different values for starting point for the control with respect the density of gypsy moth in the host-pathogen model, with parameters in Table 2.1

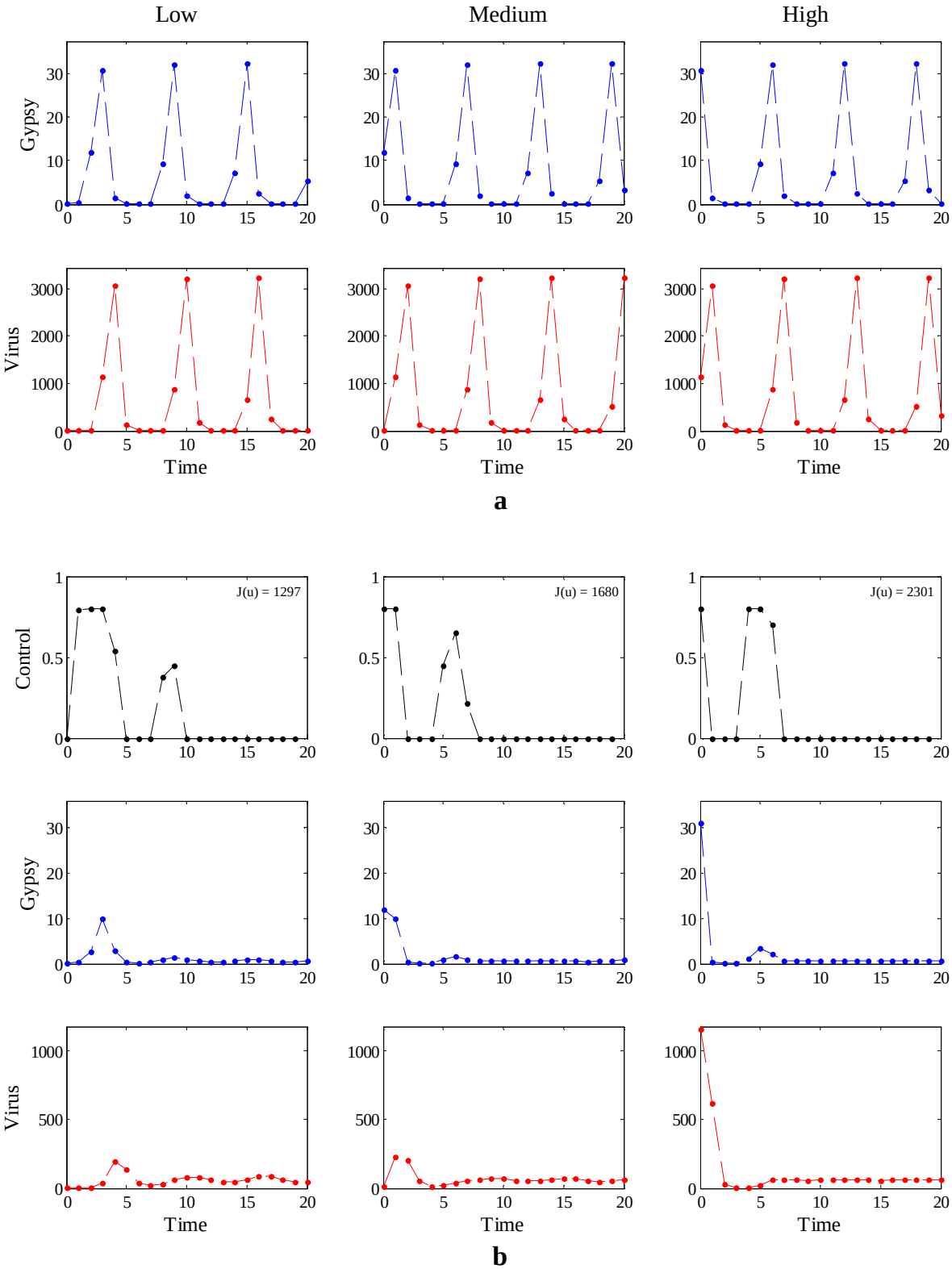

Figure 2.12: Variation for initial conditions for the optimal control, low, medium and high densities of gypsy moth in the host-pathogen model. a. Dynamics without control. b. Dynamics with control. With parameters in Table 2.1

Results are in Figure 2.12, using the same organization as in previous figures. As expected the non-control dynamics are dependent on the starting points. Results for the management option are in Figure 2.12(b), where the low density is in the left column, and the right column is the high density case. We can observe a two peak pattern for the optimal control in the three cases. The length of the first peak is shorter when the density of the starting gypsy moth populations increases. The second peak also changes when the density of the initial population increases; it is longer and the amount of control is higher. The number of times we need to apply control is smaller at higher starting densities. Most of these characteristics, could be a consequence of the fact that when we start the control at high densities, the population of gypsy moth will naturally decline because of the virus. On the other hand, when starting at low densities, the population is growing. The value of our objective functional increases with the starting density. In these three cases, the optimal control reduces the density of gypsy moth when compare to non-management option. It is important to note that the peaks of the control occur a year before the peaks of gypsy moth in the non-management option.

To understand better the effect of the starting point we ran 100 simulations with different starting points. We chose 100 simulations since in the long term the population of gypsy moth, after the transient dynamics of initial conditions, has behavior nearly cyclic with a period around 80 years, which can be observed in Figure 2.4. With 100 consecutive different starting points most of the behavior of the model will be taken into account. Results of these simulations are in Figure 2.13. The bars represent the average of the optimal control at each year, for the 20 years. The error bar represents the standard deviation at each year. In Figure 2.13(a) we have the results for all 100 simulations. To clarify this figure we divide our data into three categories based on the density of gypsy moth at the starting point of the control. Low densities for values below one, medium for values between one and fifteen, and high for values greater that fifteen.

Results are in Figure 2.13, with low densities in part (b) with 57 values, medium at (c) with 23 values, and high in (d) with 21 values. At low densities, Figure 2.13(b), we have two peaks with the first one being the highest and the longest. For medium densities,

Figure 2.13(c), we have three peaks, with the first two very similar in length and in amount of control and the third peak smaller than the first two. Finally, at high densities we have three completely separate peaks, the first one has a duration of two years with one application very high on average followed by a low application, second peak is the longest one and with the two middle applications the highest ones. Finally the third peak is the one with the lowest averages. One characteristic that all starting values share is that after year 13 no more control is necessary. Box plots are display in Figure A.10.

To confirm the qualitative differences in the optimal control observed in Figure 2.13, we performed and analysis of variance followed by a Tukey-Kramer HSD multiple comparison test. The density of gypsy moth was the independent variable, with levels: low, medium, and high. The objective functional, the sum of the controls, and the time of the maximum control, were used as response variables. The time of the maximum control, refers to the time (between 0 and 19) when the level of control is the maximum, if there are various times at maximum level of control, we pick always the one that occurs first. For the sum of the controls there were not significant differences, for the other two variables we find difference at the 1% level. This shows that the amount of control used is similar for different starting densities, but the corresponding objective functional is different. The significant difference found for the time of the maximum amount of control applied, confirms the distinct patterns observe in Figure 2.13. Details are in Appendix A.8.

In conclusion, the initial conditions and time in the cycle have an important influence on the optimal control solution. In Figure 2.13, we provide three different alternatives of optimal control base in initial populations of gypsy moth in the host-pathogen model. In general, populations at low densities need more applications of the control. Populations at high densities need fewer applications but at higher amounts of the control. Populations at medium densities have an average between the scenarios of low and high densities.

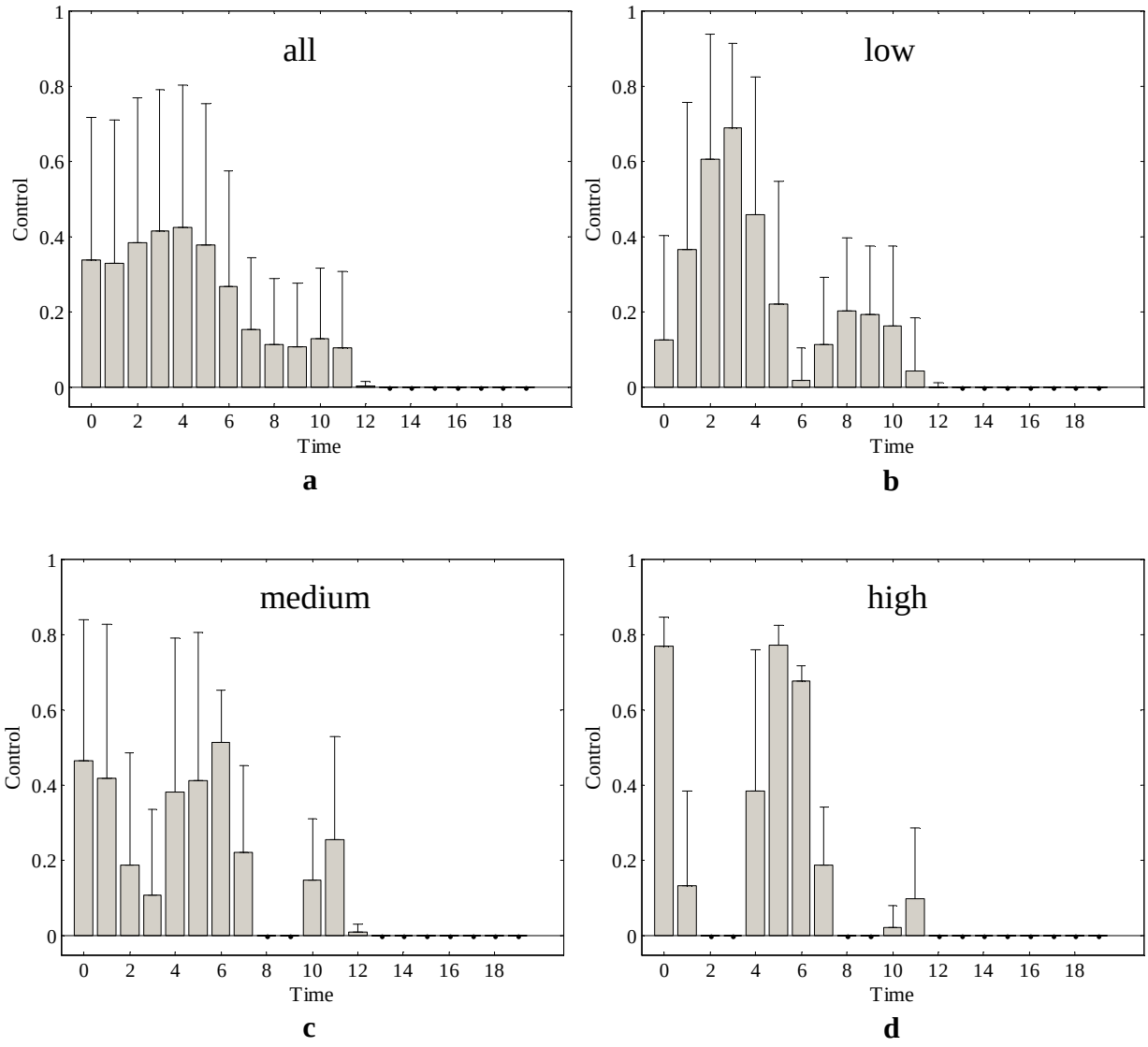

Figure 2.13: Summary statistics for the optimal control for the host-pathogen model. Bar height represents the average value for the optimal control at each year, and the error bar is the standard deviation. a. With 100 different starting conditions. b. Starting conditions for the control at low densities. c. Medium densities. d. High densities. With parameters in Table 2.1

2.6 Inclusion of a generalist predator

The model that includes just the interaction between gypsy moth and the virus, has cycle periods much more regular that the ones occurring in nature [17]. Generalist rodent predators are recognized as the major cause of mortality on late stages of larva, and on pupae, in low-density gypsy moth populations [7, 12, 72]. These generalist predators feed on a range of fruits, seeds, and insects. As a result, their populations are not directly affected by gypsy moth cycles [21, 35]. Therefore, we use a modified model that includes a generalist small mouse predator, *Peromyscus* spp [17],

$$
\begin{aligned}
1 - I\left(N_k, Z_k\right) &= \left\{1 + \frac{\overline{v}C^2}{\mu}\left[N_k I\big(N_k, Z_k\big) + \rho Z_k\right]\right\}^{-\frac{1}{C^2}} \\
N_{k+1} &= \gamma N_k\Big[1 - I(N_k, Z_k)\Big]\left[1 - \frac{2abN_k}{b^2 + N_k^2}\right] \\
Z_{k+1} &= f N_k I(N_k, Z_k)
\end{aligned}
\tag{2.10}
$$

The fraction of gypsy moths killed by the predator is

$$\frac{2abN_k}{b^2 + N_k^2}$$

where a is the maximum fraction killed, and b is the gypsy moth density at which the fraction killed is maximized [17].

The fraction consumed by the predator increases quickly when the prey density rises, as the predator specializes on the new abundant prey, this is shown in Figure 2.14 [17]. However, at high densities, the predator is overwhelmed inducing a reduction in the attack rate. As a result, the decrease in the gypsy moth population is maximized at low to intermediate densities [17]. At high densities of gypsy moth, a generalist predator has a small impact, but usually generates density dependent regulation at low densities [46, 20, 21, 29]. The function used for predation in the model is consistent with these ecological characteristics [17].

Inclusion of the interaction with the generalist predator generates much more complex dynamics in comparison with the host-pathogen model, as seen in Figure 2.15. The presence of multiple equilibria explains in part this dynamics [17]. For realistic parameter values, the model (2.10) with predation has a high-density equilibrium where the predator is relatively unimportant and gypsy moth is controlled by the virus *Ld*MNPV. There is also a low-density equilibrium where the virus is less important, and the population of gypsy moth is controlled by the predator. This low-density equilibrium is not present in the host-pathogen model (2.1).

Comparison of the model with data is complicated. Since the model is very sensitive to initial conditions, as displayed in Figure 2.15, and there are not estimates of the starting densities of gypsy moth [17]. Even though, the authors contrast the statistical moments of the model with the ones of the data, they compare the average and the coefficient of variation of the time between outbreaks. The model with predation, creates high variability in the time between outbreaks, and, long average times between outbreaks, characteristics that are consistent with most of the data [17].

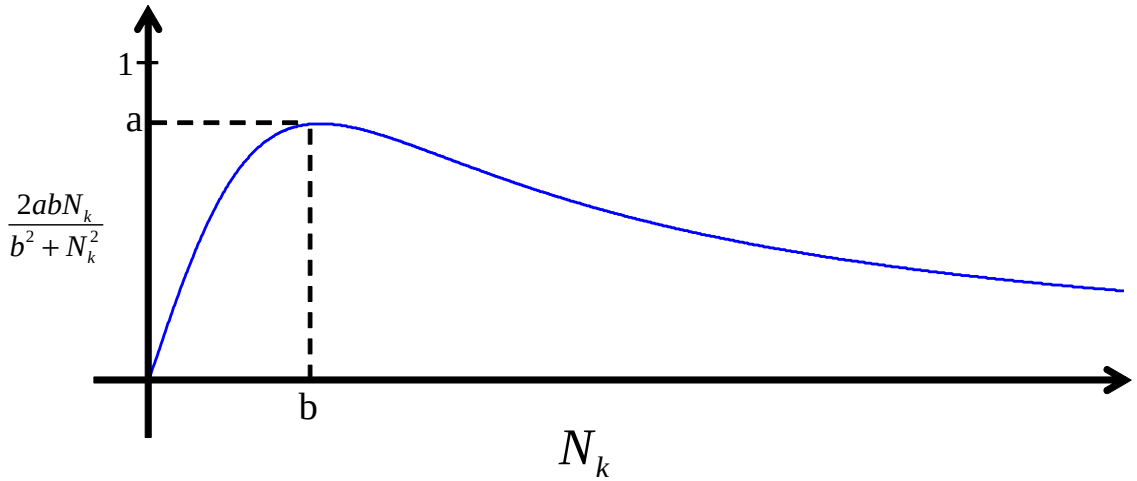

Figure 2.14: Fraction of gypsy moth density killed by predation, where a is the maximum fraction killed, and b is the gypsy moth density at which the fraction killed is maximized

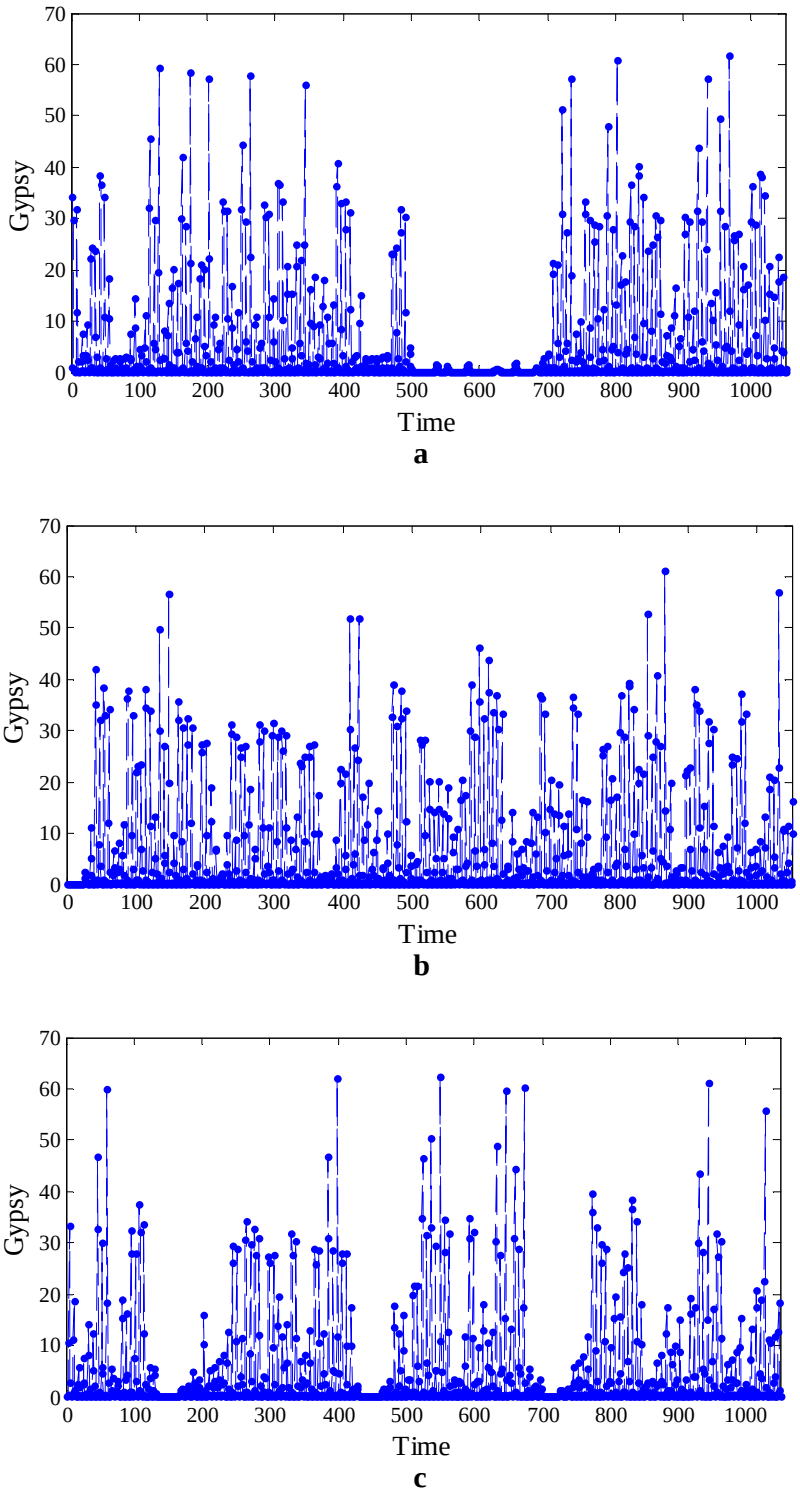

Figure 2.15: Gypsy moth population in the model with predation and with no control, for varying initial conditions. a. $N_0 = 10$ and $Z_0 = 1$. b. $N_0 = 100$ and $Z_0 = 100$. c. $N_0 = 1000$ and $Z_0 = 1$, with other parameters in Table 2.3

2.6.1 Methods

We use again a non-dimensionalized version of the model:

$$
\begin{aligned}
1 - I\big(\hat{N}_k, \hat{Z}_k\big) &= \left\{1 + C^2\left[\hat{N}_k I\big(\hat{N}_k, \hat{Z}_k\big) + \hat{Z}_k\right]\right\}^{-\frac{1}{C^2}} \\
\hat{N}_{k+1} &= \gamma \hat{N}_k\left[1 - I\big(\hat{N}_k, Z_k\big)\right]\left[1 - \frac{2a\hat{b}\hat{N}_k}{\hat{b}^2 + \hat{N}_k{}^2}\right] \\
\hat{Z}_{k+1} &= \phi \hat{N}_k I\big(\hat{N}_k, \hat{Z}_k\big).
\end{aligned}
\tag{2.11}
$$

The new densities are $\hat{N}_k = \frac{\mu N_k}{\bar{v}}$ and $\hat{Z}_k = \rho\frac{\mu Z_k}{\bar{v}}$. While $\phi = f\rho$ is defined, as the product of the probability f that a pathogen particle survives the winter, times the susceptibility of new emerge larvae ρ. Also $\hat{b} = b/\frac{u}{\bar{v}}$ is the ratio of the density at maximum predation to the epidemic threshold [16, 17].

Therefore our new state equations are:

$$
\begin{aligned}
1 - I\big(\hat{N}_k\,(1-u_k)\,, \hat{Z}_k\big) &= \left\{1 + C^2\left[\hat{N}_k\,(1-u_k)\,I\big(\hat{N}_k\,(1-u_k)\,, \hat{Z}_k\big) + \hat{Z}_k\right]\right\}^{-\frac{1}{C^2}} \\
\hat{N}_{k+1} &= \gamma \hat{N}_k\,(1-u_k)\left[1 - I\big(\hat{N}_k\,(1-u_k)\,, Z_k\big)\right]\left[1 - \frac{2a\hat{b}\hat{N}_k\,(1-u_k)}{b^2 + \big(\hat{N}_k\,(1-u_k)\big)^2}\right] \\
\hat{Z}_{k+1} &= \phi \hat{N}_k I\big(\hat{N}_k, \hat{Z}_k\big).
\end{aligned}
\tag{2.12}
$$

with objective functional:

$$
\min_u \sum_{k=0}^{T-1} e^{-\delta k}\Big[A\hat{N}_k + B\log(1-u_k)\Big]. \tag{2.13}
$$

The numerical approximation for the model with predation we start using the same approaches employed in the host-pathogen model, but none of those algorithms converged. We tried different modifications, like increasing the number of iterations or change the values for TolFun, TolX, and the size of the mesh, but none of these changes were helpful. Therefore we limit the possibilities for the values of the control. We discretize the control

space U, in the interval $[0, u_{max}]$. Define n as the number of values in the interval and let

$$h = \frac{u_{max} - 0}{n - 1} = \frac{u_{max}}{n - 1}.$$

Therefore, given a value of n, the discrete values for the control are given by:

$$U_{new} = \{0, h, 2h, 3h, \cdots, (n-2)h, u_{max}\}$$

For our searches we choose a value of $h = 0.01$, therefore we use $n = 81$ and $u_{max} = 0.8$, to obtain

$$U_{new} = \{0, 0.01, 0.02, 0.03, \cdots, 0.79, 0.8\}.$$

Evaluating the objective functional for all possible combination of the new set of controls will be inefficient and will take a considerable amount of time. In the Global Optimization Toolbox of MATLAB®, the only algorithm that allows specific discrete values for the control, is the genetic algorithm [33].

The GA is an optimization method based on natural selection. The GA repeatedly changes a population of individual solutions. At each iteration, individuals from the current population are, randomly selected to be the parents of the next generation. Over iterations, the population may evolve to an optimal solution. Genetic algorithms are useful when the objective functional is not continuous or not differentiable. The GA can handle problems where the components are restricted to be integer-valued or discrete spaced values [33].

To design the next generation, genetic algorithms employ three main types of rules [33]:

- Selection rules: Select the parents, that create the individuals for the next generation.
- Crossover rules: Cross two parents to produce offspring for the next generation
- Mutation rules: Random changes are introduce to individual parent to form new individuals

Classical optimization approaches and genetics algorithms, have two main differences. At each time step, classical algorithms create a single point, the sequence of these points converge to an optimal value. In contrast, GA builds a population of points at each step. The best individuals of the population approaches an optimal result. In classical schemes, the selection of the next point is made by deterministic calculations. In GA, the selection of the next individual follows a stochastic approach [33].

We use the following approach. First we use the genetic algorithm to do a preliminary search of possible control, with at least 30 searches for each window of controls. Then we use the output of the GA as the starting points for the Patternsearch algorithm. From these results we pick the value that minimizes our objective functional. Since this approach is more computational intensive, we use the Apps@UT cloud computing application. We run our code in parallel, with four workers, using the command parfor from MATLAB®. For this model we use the following values for the parameters:

Table 2.3: Parameter values for the model with predation

Parameter	γ	ϕ	$\frac{1}{C^2}$	a	$\hat{b}$	A	δ	u_{max}
Values	74.6	60	1.06	0.967	0.14	50	0.02	0.8

Parameters for the model (γ, ϕ, $\frac{1}{C^2}$, a, b) were taken from Dwyer's work [17]. Other parameters were the same used before.

2.6.2 Results

In this model, deciding in what interval to apply the control was more complicated. In Figure 2.16, in top we present output of the model. We selected a particular section of the top graph, and then we selected three sections of 20 years, and we perform numerical approximations to find the control. These selections were made without any particular criteria.

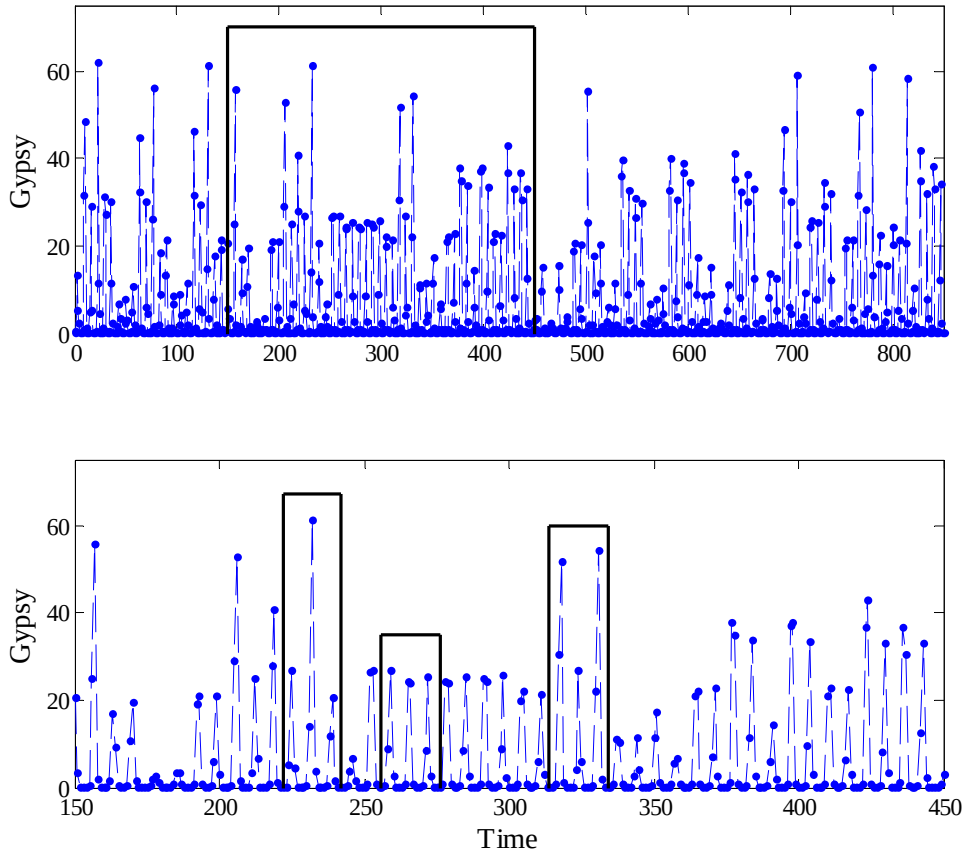

Figure 2.16: Time intervals to control in the model with predation. The lower graphic presents the windows to control. Initial conditions are $N_0 = 10$ and $Z_0 = 10$, with other parameters in Table 2.3

In Figure 2.17, we present the results of those approximations. Each column represents the dynamics for the sections selected in Figure 2.16. In the three cases, the density of gypsy moth is reduced from the case without management. The optimal control just has one peak and more control is applied when densities of gypsy moth are higher (last column); more results can be see in Appendix A.11.

We also explored the effect of different densities for starting conditions for applying the control. In Figure A.22, low density is in the left column and high density is in the right column. As expected, the initial density also affects the optimal control in the model with predation. As we increase the starting density, we apply the control in the first year and we have a second peak of control around year 5, that is not present when the we start at low densities. To understand better the effect of the starting point we ran 200 simulations with different starting points. Results of these simulations are in Figure 2.18. The error bar represents the standard deviation at each year. For better interpretation we divide our data into two categories based on the density of gypsy moth at the starting point of the control. Low densities for values below two, and high for values greater that two. In Figure 2.13, at low densities in part (a) with 100 values, and high in (b) with 100 values. At low densities, Figure 2.13(b), we have one peak of control around years 2 and 3. At high densities we have two separate peaks of control; the first one at the beginning is the highest one, the second around years 5 and 6. One characteristic that all starting values share is that after year 7 no more control is necessary. Box plots are display in Figure A.14.

We also carry out an analysis of variance, using as the independent variable the density of gypsy moth (low and high). The objective functional, the sum of the controls, and the time of the maximum control were used as response variables. As in the host-pathogen model we find significant differences at the 1% level for the objective functional, and the time of the maximum control. The sum of the control did not present significant differences. These results confirm the distinct patterns observed in Figure 2.18. Details are in Appendix A.10.

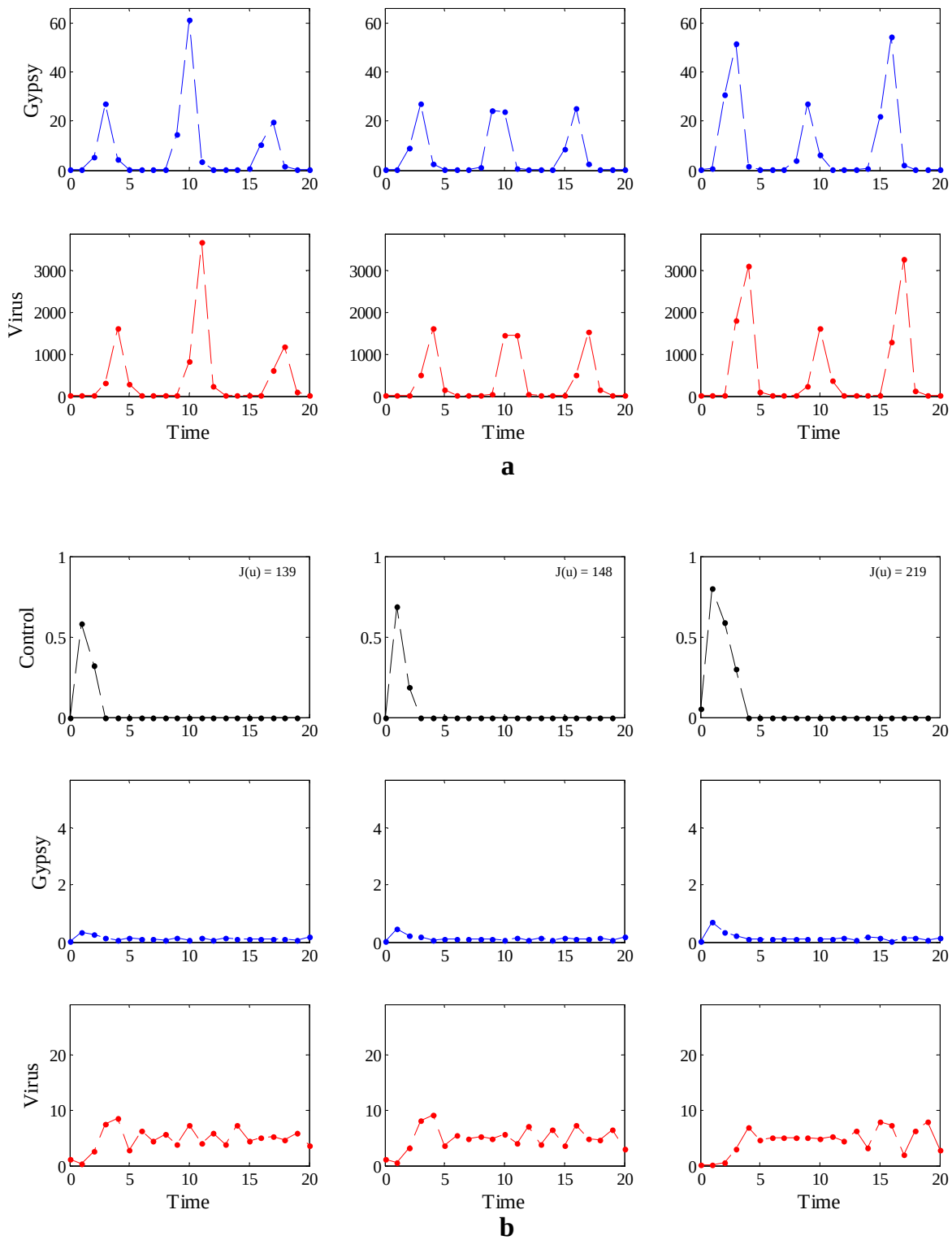

Figure 2.17: Results for the model with predation. The three windows correspond to the time interval selection in the long term dynamics in Figure 2.16. a. Dynamics without control. b. Dynamics with control. Initial conditions are $N_0 = 10$ and $Z_0 = 10$, with other parameters in Table 2.3

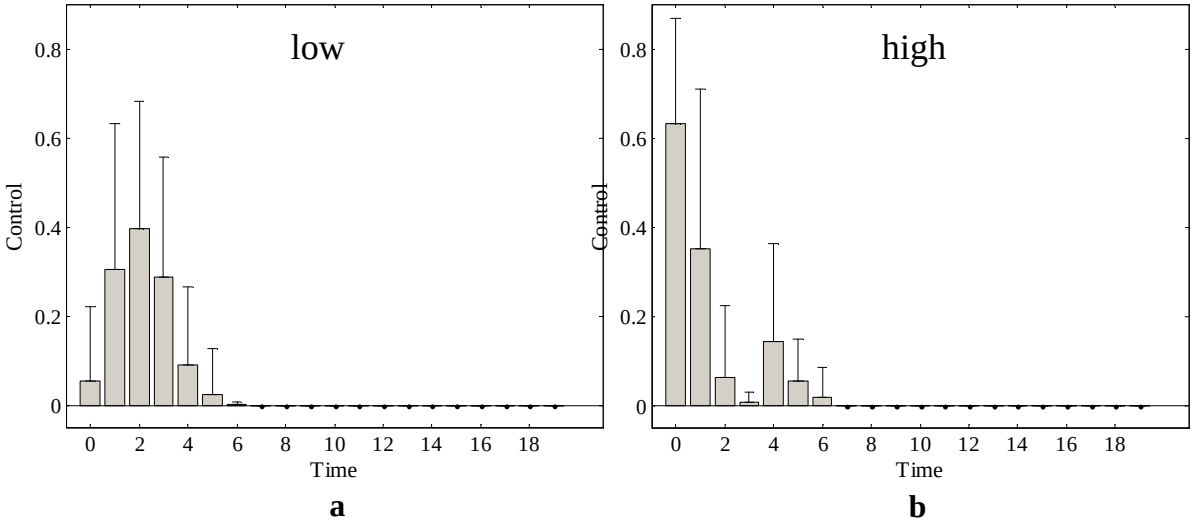

Figure 2.18: Summary statistics for the optimal control for the model with predation. Bar height represents the average value for the optimal control at each year, and the error bar is the standard deviation. Starting conditions for the control at: (a) low densities , and (b) high densities. With parameters in Table 2.3

In conclusion, the starting conditions at the moment we start to implement the control has an important influence on the optimal control solution. In Figure 2.18, we provide two different alternatives of optimal control base in initial populations of gypsy moth for the model that includes predation. In general, populations at low densities need to be controlled after 1 or 2 years. Populations at high densities need more applications, with one application at a high level of control immediately and subsequent applications around years 5 and 6 at lower levels of the control.

2.7 Conclusions

In this chapter we developed an optimal control formulation for the invasive pest gypsy moth. First we explored a model that includes the interaction of gypsy moths with the virus *Ld*MNPV, we refer to this model as the host-pathogen model. When we start the control at low densities of gypsy moth, the optimal control has a pattern of two peaks, with the first being higher and longer. The two peaks of control occur a year before

the peaks of gypsy moth in the non-management scenario. These results hold for a wide range of parameter values. We also investigated how the density at the starting time to implement control can affect the optimal control solution in the host-pathogen model. We divided the initial density in three cases: low (values below 1), medium (between 1 and 15), and high (more than 15). Using simulations at several different starting points, we can conclude, that the optimal control is highly affected by the starting conditions. Low densities need more control applications than high densities. This is mainly a consequence that at high densities the population of gypsy moth is decreasing as a result of the virus epidemic. We provided three general possible optimal control management options based on the starting densities of gypsy moth.

In the host-pathogen model the gypsy moth is cycling regularly and with a short period length. In the model with predation there is some greater lag time between outbreaks because of predation effects. The optimal control for the model that includes predation, as expected, is at a lower level as compared with the host-pathogen model. We also found the optimal control is very sensitive to initial conditions, and we provided two general options based in the starting densities of gypsy moth. Higher densities require action intermediately. In general the peaks of the control occur a year or two before the peaks of gypsy moth in the non-management scenario.

In the two models that we used the optimal control is highly dependent to the initial conditions. These results highlight the importance of knowing the status of the populations before starting any management program. This suggests the necessity to have programs that monitor the densities of gypsy moth populations and have different management programs that incorporate the initial densities as a parameter.

Acknowledgments

This work was done in collaboration with Suzanne Lenhart, Andrew (Sandy) Liebhold (USDA Forest Service), Greg Dwyer (The University of Chicago), and Kyle Haynes (University of Virginia).

Chapter 3

Integrodifference model

3.1 Introduction

In this chapter we will focus on models for gypsy moth populations that are in the invasion front. In North America, gypsy moth females are incapable of flying and typically oviposit within 2m of where they come out as adults [78, 20]. Dispersal happens during early instar ballooning, promoted by atmospheric transport, and is relatively short ranged, at most a few hundred meters. The typical behavior of late instars looking for hidden resting sites often results in larvae pupating and consequently emerging females ovipositing on human-made objects like motor vehicles [78, 46]. Unintentional transportation, in particular for egg masses that overwinter, is a method of dispersal that plays a significant role in the invasion spread [78, 77].

The spread of the gypsy moth is a process known as stratified dispersal, in which local growth and dispersal is joined with the long range dispersal of early life stages by human objects [78, 77]. Long distance dispersal allows the establishment of populations, beyond the invasion front, which can eventually merge with the expanding population front. The effect is a much quicker speed of expansion than the one estimated under local population growth and diffusive spread [78, 47].

Spatial spread is a key element of invasion processes. There is a long history of modeling movement of biological organisms, starting with Skellam [71] who explored the role of

random motion to describe biological movement using a linear diffusion partial differential equation. Many extensions to this structure have been proposed; see [48] for a recent review and [49, 10, 52] for an overview of partial differential equation (PDE) approaches to modelling biological movement and dynamics.

An alternative to the PDE approach to modeling invasive spatial spread uses integrodifference equations in which a dispersal kernel is used to describe the redistribution of species [40, 81, 39, 31]. Some classical approaches to the study of PDEs have been applied to integrodifference systems within the ecological literature including calculation of traveling wave speeds [84] and determination of the conditions required for spatial pattern formation [39, 50]. In the case where the underlying dynamics are generational or best described in discrete time, and the dispersal stage is separate from the growth stage, the population dynamics can be represented by an integrodifference equation. For a population $N_k(x)$ at location x in the spatial domain Ω at time k subject to local population demographic dynamics $f(N)$ and with spatial redistribution kernel $k(x, y)$, the model system takes the form:

$$N_{k+1}(x) = \int_{\Omega} k(x, y) f\big(N_k(y)\big) dy. \tag{3.1}$$

The redistribution kernel can be chosen from a wide range of probability density functions to best represent observed dispersal patterns. This increases model flexibility when compared with a PDE approach, itself structured around a normal distribution, and integrodifference equations have resulted in more accurate model predictions of spread [70, 39, 38]. In chapter 3, we focus on integrodifference equations given the nature of the dynamics for populations that are in the invasion front.

The management of invasive species leads to investigation of optimal control of intervention actions in appropriate models. The first application of optimal control theory to integrodifference equations was presented by Joshi and collaborators [36] for a harvesting model of a single population. Since then, the mathematical framework proposed in that work has been applied to a range of problems for single species [26, 37, 89, 43, 41]. However, to date, very little work (only [85])has been carried out to extend that theory

to optimal control in a system of integrodifference equations.

In the previous chapter, we use control aerial sprays of *Bacillus thuringiensis* (*Bt*), because it is the most popular management treatment for the gypsy moth; though there are possible harmful effects on other species of Lepidoptera [54, 83]. In chapter 3, we assume control by Gypchek. The theory developed in this chapter can be easily modified to allow control with *Bt* instead of Gypchek.

In the 1950's, the USDA Forest Service started to investigate the possibility of developing the naturally occurring nucleopolyhedrosis virus (*Ld*MNPV) as an alternative for the management of the gypsy moth [57, 62]. The main reasons is that the *Ld*MNPV virus has an extremely narrow host range [4], does not have deleterious effects on beneficial insects or vertebrates, [28, 61, 62], and is not known to be related to any human pathogen [80]. In 1978 the *Ld*MNPV virus product, Gypchek, was registered by the U.S. Environmental Protection Agency as an insecticide for the gypsy moth [57].

The majority of toxicological tests of Gypchek using laboratory animals, wild mammals, birds and fish, revealed no deleterious effects [61]. In 1994, a seven year long research project was started to assess the effects of the two insecticides, *Bt* and Gypchek, on non-target arthropods and selected vertebrate [74]. This work concluded that Gypchek had less impact on non-target organisms. The researchers state that "Gypchek is the preferred option in gypsy moth control because it is environmentally benign and its toxicity is specific to gypsy moth."

Gypchek is produced using an *in-vivo* process that is very labor intensive, so applications of Gypchek are more expensive than other control products [6, 56]. Research is currently underway to develop *in-vitro* production; this could eventually provide a less expensive product[62].

Next we formulate our model with control and the corresponding objective functional. In section 3.3 we prove the existence of the optimal control. The characterization of an

optimal control, in terms of the state and the adjoint variables is given in section 3.4. In section 3.5 we show uniqueness of the optimal control. Finally in the last section, we apply the optimal control theory developed to numerical simulations for the gypsy moth problem.

3.2 Mathematical model

We form a bioeconomic model by creating an objective functional for the control of gypsy moths which is constrained by the underlying spatio-temporal dynamics of the moth with the nucleopolyhedrosis virus (NPV) control agent. To do this, we define the state variables for the problem as

$$\begin{aligned} N_k(x) &= \text{Density of gypsy moths at generation } k \text{ and spatial location } x \\ Z_k(x) &= \text{Density of } Ld\text{MNPV virus at generation } k \text{ and spatial location } x \end{aligned}$$

where $k = 0, 1, ...T$ is the time index determined by the gypsy moth annual population generations and x is the spatial variable in a one-dimensional bounded domain Ω.

The control, $u = \big(u_0(x), ..., u_{T-1}(x)\big)$, is the amount of spray of the biocontrol agent Gypchek used at location x for each generation. We assume that there is a cost A_k associated with the gypsy moth density N_k which includes the direct economic costs for the forestry industry and the indirect costs resulting in a reduction of tourism in regions where gypsy moth outbreaks are occurring. The cost of using Gypchek is a function of the amount of spraying that is undertaken, and we assume a quadratic cost of the form, $B_k u_k + C_k u_k^2$. The objective functional is defined as

$$J(u) = \int_\Omega A_T N_T(x)dx + \sum_{k=0}^{T-1} \int_\Omega \Big[A_k N_k(x) + B_k u_k(x) + C_k u_k^2(x)\Big]dx, \tag{3.2}$$

subject to the constraints of the population dynamics:

$$N_{k+1}(x) = \int_\Omega k_1(x,y)F\Big(N_k(y), Z_k(y)\Big)dy \tag{3.3}$$
$$Z_{k+1}(x) = \int_\Omega k_2(x,y)G\Big(N_k(y), Z_k(y)\Big)dy + \int_\Omega k_3(x,y)u_k(y)dy$$

where $k = 0, 1, 2, ...T-1$, $x \in \Omega$, and

$$F(N_k, Z_k) = \gamma N_k e^{-rN_k - bZ_k} \tag{3.4}$$
$$G(N_k, Z_k) = fZ_k + \rho N_k\big(1 - e^{-bZ_k}\big)$$

with initial conditions specified as

$$0 \leq N_0(x) = N_{initial}(x)$$
$$0 \leq Z_0(x) = Z_{initial}(x),$$

and $A_k \geq 0$, $B_k \geq 0$, and $C_k > 0$ for $k = 0, 1, \cdots, T$. The kernels are bounded and Lebesgue measurable such that

$$0 < \int_\Omega k_i(x,y)dy \leq 1 \text{ for all } x \in \Omega, \text{ where } i = 1, 2, 3 \tag{3.5}$$
$$0 \leq k_i(x,y) \leq K \text{ for } (x,y) \in \Omega.$$

We use a simple modification of the Nicholson-Bailey model [51]. In the absence of the virus, gypsy moth dynamics are density dependent and can be represented by the Ricker equation, where γ denotes the average per capita number of moths produced and e^{-rN_k} is the density dependent probability that each new moth will survive until the next generation. Addition of virus adds to the constraints on between generation survival for the gypsy moths; we assume that in the presence of virus the probability that a moth does not become infected at generation k is e^{-bZ_k}. Thus $e^{-rN_k - bZ_k}$ is the probability of survival combining effects of the density dependence and the infection.

For the virus, we assume a probability f that virus in the environment can survive between moth generations (over winter survival). The probability that a gypsy moth individual at time k will get the virus infection is $1 - e^{-bZ_k}$. After gypsy moths die the cadaver will provide ρ viral spores, on average, into the environment.

Given the set of bounded controls,

$$U = \Big\{ u = \big(u_0(x), ..., u_{T-1}(x)\big) \in \left(L^\infty(\Omega)\right)^T | 0 \leq u_k(x) \leq u_{max}, k = 0, 1, ..., T-1 \Big\}, \quad (3.6)$$

we seek to find an optimal control, $u^* \in U$, such that

$$J(u^*) = \min_{u \in U} J(u).$$

We denote the states corresponding to the control $u \in U$ as $N = N(u), Z = Z(u)$. The redistributing kernels have the properties,

$$0 < \int_\Omega k_i(x, y)dy \leq 1 \text{ where } i = 1, 2, 3 \quad (3.7)$$
$$0 \leq k_i(x) \leq K \text{ for } x \in \Omega$$

3.3 Existence of an optimal control

We begin by verifying that there exists a solution to the optimal control problem for the gypsy moth model. We first show that the states are bounded over a finite interval.

Lemma 1. *There exists a constant D such that $0 \leq N_k(x) \leq D$, $0 \leq Z_k(x) \leq D$ for all $x \in \Omega$, $k = 0, 1, ..., T$.*

Proof. The state equations are positive invariant, given fixed initial conditions N_0, Z_0 are non-negative then N_k, Z_k, are non-negative for all k. Therefore the states are bounded below by zero. So it remains to show the states are bounded above. From the structure

of F and G, there exists a constant D_1 such that

$$\begin{aligned} F\big(N_0(x), Z_0(x)\big) &\leq D_1 \\ G\big(N_0(x), Z_0(x)\big) &\leq D_1 \text{ for all } x \in \Omega. \end{aligned} \tag{3.8}$$

Then substituting the bounds above into system (3.3), we have

$$\begin{aligned} N_1(x) &\leq D_1 \int_\Omega k_1(x,y)dy \\ Z_1(x) &\leq D_1 \int_\Omega k_2(x,y)dy + \int_\Omega k_3(x,y)u_0(y)dy. \end{aligned} \tag{3.9}$$

Then from (3.6) and (3.7) we obtain

$$\begin{aligned} N_1(x) &\leq D_1 \\ Z_1(x) &\leq D_1 + u_{max}. \end{aligned} \tag{3.10}$$

Therefore $N_1(x)$, $Z_1(x)$ are bounded above for all $x \in \Omega$. Following the same idea we can find bounds for $N_2(x)$, $Z_2(x)$. There exists a constant D_2 such that:

$$\begin{aligned} F(N_1, Z_1) &\leq D_2 \\ G(N_1, Z_1) &\leq D_2. \end{aligned} \tag{3.11}$$

Substituting the bounds yields

$$\begin{aligned} N_2(x) &\leq D_2 \int_\Omega k_1(x,y)dy \\ Z_2(x) &\leq D_2 \int_\Omega k_2(x,y)dy + \int_\Omega k_3(x,y)u_1(y)dy \end{aligned} \tag{3.12}$$

and then

$$\begin{aligned} N_2(x) &\leq D_2 \\ Z_2(x) &\leq D_2 + u_{max}. \end{aligned} \tag{3.13}$$

Subsequently it follows iteratively that N_k, Z_k are bounded for all $x \in \Omega$ and all $k = 0, 1, 2, ..., T$. □

Now we can use Lemma 1 to establish the existence of an optimal control.

Theorem 3. *An optimal control $u^* \in U$ exists that minimizes the objective functional $J(u)$.*

Proof. The objective functional is bounded below by zero. Thus let $\{u^i\}$ be a minimizing sequence for the objective functional J and $\{N^i\}$ and $\{Z^i\}$ be the corresponding state sequences. As the sequences are bounded (Lemma 1) there exists $u^* \in U$ and $N^*, Z^* \in \left(L^\infty(\Omega)\right)^{T+1}$ such that on a subsequence

$$\begin{aligned} u_k^i(x) &\rightharpoonup u_k^*(x) \\ N_k^i(x) &\rightharpoonup N_k^*(x) \\ Z_k^i(x) &\rightharpoonup Z_k^*(x) \end{aligned} \tag{3.14}$$

as $i \to \infty$, weakly in $L^2(\Omega)$ for each k.

We now show that the states N^* and Z^* correspond to the control u^*. Using the structure of the model, we show that the state sequences converge pointwise. Due to the fixed initial conditions, we have from (3.3)

$$\begin{aligned} N_1^i(x) &= \int_\Omega k_1(x,y) F(N_0(y), Z_0(y)) dy \\ Z_1^i(x) &= \int_\Omega k_2(x,y) G(N_0(y), Z_0(y)) dy + \int_\Omega k_3(x,y) u_0^i(y) dy. \end{aligned} \tag{3.15}$$

Hence the sequence $\{N_1^i\}$ is constant with value N_1 from (3.10). The weak convergence of the sequence $\{u_0^i\}$ gives $Z_1^i(x) \to Z_1^*(x)$ pointwise for each x as $i \to \infty$. Thus this pointwise convergence of the sequences $\{N_1^i\}$ and Z_1^i and the continuity of F, G gives convergence pointwise of $\{F(N_1^i, Z_1^i)\}, \{G(N_1^i, Z_1^i)\}$ and then gives convergence of the integral terms by Lebesque's Dominated Convergence Theorem. Thus we obtain pointwise convergence of N_2^i, Z_2^i and by iteration, the pointwise convergence of N_k^i, Z_k^i as $i \to \infty$, $k = 0, 1, ..., T$.

Hence $N^* = N(u^*)$ and $Z^* = Z(u^*)$.

Now we verify that u^* is an optimal control. For the quadratic term of the control in the objective functional, the lower semi-continuity of the L^2 norm with respect to weak convergence of control sequences gives:

$$\begin{aligned}
\min_{u\in U} J(u) &= \lim_{i\to\infty} \int_\Omega \sum_{k=0}^{T-1} \left[A_k N_k^i(x) + B_k u_k^i(x) + C_k (u_k^i(x))^2\right] dx + \int_\Omega A_T N_T^i(x) dx \qquad (3.16)\\
&\geq \lim_{i\to\infty} \int_\Omega \sum_{k=0}^{T-1} \left[A_k N_k^i(x) + B_k u_k^i(x)\right] dx + \liminf_{k\to\infty} \int_\Omega \sum_{k=0}^{T-1} C_k (u_k^i(x))^2 dx \\
&\quad + \lim_{i\to\infty} \int_\Omega A_T N_T^i(x) dx \\
&\geq \int_\Omega \sum_{k=0}^{T-1} \left[A_k N_k^*(x) + B_k u_k^*(x) + C_k (u_k^*(x))^2\right] dx + \int_\Omega A_T N_T^*(x) dx.
\end{aligned}$$

Consequently an optimal control u^* exists with corresponding states N^* and Z^*. □

3.4 Characterization of an optimal control

We characterize an optimal control for our system of integrodifference equations. In order to find this characterization we need to differentiate the objective functional with respect to the control, in the sense

$$\lim_{\varepsilon\to 0^+} \left(\frac{J(u^* + \varepsilon l) - J(u^*)}{\varepsilon}\right) \geq 0 \qquad (3.17)$$

where l is a directional vector. We will refer to expression (3.17) as the directional derivative. Since the states are involved in J, we must first be able to differentiate the states with respect to the control, and the derivatives of the control $\to$ states map are called "sensitivities".

Notation 1. *For simplicity we define*

$$\begin{aligned}
N^\varepsilon(x) &:= N(u + \varepsilon l) & Z^\varepsilon(x) &:= Z(u + \varepsilon l) \qquad (3.18)\\
N(x) &:= N(u) & Z(x) &:= Z(u)
\end{aligned}$$

Theorem 4. *The mapping $u \to N, Z$ is differentiable in the following sense: For any $u \in U$ and $l \in (L^\infty(\Omega))^T$, such that $(u + \varepsilon l) \in U$ for ε small, there exists sensitivities $\psi_k^N(x), \psi_k^Z(x) \in (L^\infty(\Omega))^{T+1}$ such that for $k = 0, 1, ..., T$:*

$$\begin{aligned} \frac{N_k^\varepsilon(x) - N_k(x)}{\varepsilon} &\rightharpoonup \psi_k^N(x) \\ \frac{Z_k^\varepsilon(x) - Z_k(x)}{\varepsilon} &\rightharpoonup \psi_k^Z(x) \end{aligned} \tag{3.19}$$

pointwise on Ω as $\varepsilon \to 0^+$, for $0 < \varepsilon << 1$ such that $(u + \varepsilon l) \in U$. Furthermore the sensitivities satisfy the following system for $k = 0, 1, ..., T-1$

$$\begin{aligned} \psi_{k+1}^N(x) &= \int_\Omega k_1(x,y) \left(\frac{\partial F\big(N_k(y), Z_k(y)\big)}{\partial N} \psi_k^N(y) + \frac{\partial F\big(N_k(y), Z_k(y)\big)}{\partial Z} \psi_k^Z(y) \right) dy \\ \psi_{k+1}^Z(x) &= \int_\Omega k_2(x,y) \left(\frac{\partial G\big(N_k(y), Z_k(y)\big)}{\partial N} \psi_k^N(y) + \frac{\partial G\big(N_k(y), Z_k(y)\big)}{\partial Z} \psi_k^Z(y) \right) dy \\ &\quad + \int_\Omega k_3(x,y) l_k(y) dy \end{aligned} \tag{3.20}$$

with initial conditions $\psi_0^N(x) = \psi_0^Z(x) = 0$.

Proof. We vary the control from u to $u + \varepsilon l$, where l is an arbitrary variation. Then from the state equations (3.3) and notation (3.18) we have

$$\begin{aligned} N_{k+1}^\varepsilon(x) - N_{k+1}(x) &= \int_\Omega k_1(x,y) \Big[F\big(N_k^\varepsilon(y), Z_k^\varepsilon(y)\big) - F\big(N_k(y), Z_k(y)\big) \Big] dy \\ Z_{k+1}^\varepsilon(x) - Z_{k+1}(x) &= \int_\Omega k_2(x,y) \Big[G\big(N_k^\varepsilon(y), Z_k^\varepsilon(y)\big) - G\big(N_k(y), Z_k(y)\big) \Big] dy \\ &\quad + \int_\Omega k_3(x,y) \left(u_k + \varepsilon l_k - u_k\right)(y) dy \end{aligned} \tag{3.21}$$

Substituting the initial conditions into equations above and assuming $N_0^\varepsilon = N_0$ and $Z_0^\varepsilon = Z_0$ we find

$$\begin{aligned} N_1^\varepsilon(x) - N_1(x) = 0 &\Rightarrow \psi_1^N(x) = 0 \\ Z_1^\varepsilon(x) - Z_1(x) = 0 + \int_\Omega k_3(x,y) \varepsilon l_1(y) dy &\Rightarrow \psi_1^Z(x) = \int_\Omega k_3(x,y) \varepsilon l_1(y) dy \end{aligned} \tag{3.22}$$

Thus the quotients $\left\{\frac{N_1^\varepsilon(x)-N_1(x)}{\varepsilon}\right\}, \left\{\frac{Z_1^\varepsilon(x)-Z_1(x)}{\varepsilon}\right\}$, are independent of ε, and thus give directly the desired sensitivities $\psi_1^N(x), \psi_1^Z(x)$, and the convergences in (3.19).

For the second components of the sensitivities, consider

$$N_2^\varepsilon(x) - N_2(x) = \int_\Omega k_1(x,y)\Big[F\big(N_1^\varepsilon(y), Z_1^\varepsilon(y)\big) - F\big(N_1(y), Z_1(y)\big)\Big]dy \tag{3.23}$$
$$Z_2^\varepsilon(x) - Z_2(x) = \int_\Omega k_2(x,y)\Big[G\big(N_1^\varepsilon(y), Z_1^\varepsilon(y)\big) - G\big(N_1(y), Z_1(y)\big)\Big]dy + \int_\Omega k_3(x,y)(\varepsilon l_1)(y)dy.$$

Concentrating on the first equation, (3.24), we will use the simplified notation:

$$F(N_1^\varepsilon(y), Z_1^\varepsilon(y)) - F(N_1(y), Z_1(y)) = F(N_1^\varepsilon, Z_1^\varepsilon) - F(N_1, Z_1).$$

We have the following quotients:

$$\begin{aligned}
N_2^\varepsilon(x) - N_2(x) &= \int_\Omega k_1(x,y)\big[F(N_1^\varepsilon, Z_1^\varepsilon) - F(N_1, Z_1)\big]dy \qquad (3.24)\\
\frac{N_2^\varepsilon(x) - N_2(x)}{\varepsilon} &= \int_\Omega k_1(x,y)\left[\frac{F(N_1^\varepsilon, Z_1^\varepsilon) - F(N_1, Z_1)}{\varepsilon}\right]dy\\
&= \int_\Omega k_1(x,y)\left[\frac{F(N_1^\varepsilon, Z_1^\varepsilon) - F(N_1, Z_1^\varepsilon)}{\varepsilon} + \frac{F(N_1, Z_1^\varepsilon) - F(N_1, Z_1)}{\varepsilon}\right]dy\\
&= \int_\Omega k_1(x,y)\left[\left(\frac{F(N_1^\varepsilon, Z_1^\varepsilon) - F(N_1, Z_1^\varepsilon)}{N_1^\varepsilon - N_1}\right)\left(\frac{N_1^\varepsilon - N_1}{\varepsilon}\right)\right.\\
&\quad \left. + \left(\frac{F(N_1, Z_1^\varepsilon) - F(N_1, Z_1)}{Z_1^\varepsilon - Z_1}\right)\left(\frac{Z_1^\varepsilon - Z_1}{\varepsilon}\right)\right]dy.
\end{aligned}$$

From the uniform convergence of $Z_1^\varepsilon(x)$ to $Z_1(x)$ and the differentiability of F and G, we can pass the limit in the right hand side of (3.24) and get the pointwise convergence of the quotient $\left\{\frac{N_2^\varepsilon(x)-N_2(x)}{\varepsilon}\right\}$. Doing a similar process for $Z_2^\varepsilon - Z_2$, we obtain the existence

of $\psi_2^N(x), \psi_2^Z(x)$ solving

$$\psi_2^N(x) = \int_\Omega k_1(x,y) \left[\frac{\partial F\big(N_1(y), Z_1(y)\big)}{\partial N} \psi_1^N(y) + \frac{\partial F\big(N_1(y), Z_1(y)\big)}{\partial Z} \psi_1^Z(y) \right] dy \tag{3.25}$$

$$\psi_2^Z(x) = \int_\Omega k_2(x,y) \left(\frac{\partial G\big(N_1(y), Z_1(y)\big)}{\partial N} \psi_1^N(y) + \frac{\partial G\big(N_1(y), Z_1(y)\big)}{\partial Z} \psi_1^Z(y) \right) dy + \int_\Omega k_3(x,y) l_1(y) dy.$$

In the next step, $N_2^\varepsilon(x) \to N_2(x)$ and $Z_2^\varepsilon(x) \to Z_2(x)$ uniformly, and we obtain the pointwise convergence of $\frac{N_3^\varepsilon(x) - N_3(x)}{\varepsilon}$, $\frac{Z_3^\varepsilon(x) - Z_3(x)}{\varepsilon}$ to $\psi_3^N(x), \psi_3^Z(x)$. Continuing iteratively it follows that $\left\{ \frac{N_k^\varepsilon(x) - N_k(x)}{\varepsilon} \right\}, \left\{ \frac{Z_k^\varepsilon(x) - Z_k(x)}{\varepsilon} \right\}$, converge pointwise to the desired sensitivities $\psi_k^N(x), \psi_k^Z(x)$, which satisfy system (3.20).

□

To obtain the adjoint system, we will rewrite the system (3.20), leaving all the sensitivity terms on the left hand side and all other terms on the right hand side,

$$\psi_{k+1}^N(x) - \int_\Omega k_1 \left(\frac{\partial F\big(N_k(y), Z_k(y)\big)}{\partial N} \psi_k^N(y) + \frac{\partial F\big(N_k(y), Z_k(y)\big)}{\partial Z} \psi_k^Z(y) \right) dy = 0 \tag{3.26}$$

$$\psi_{k+1}^Z(x) - \int_\Omega k_2 \left(\frac{\partial G\big(N_k(y), Z_k(y)\big)}{\partial N} \psi_k^N(y) + \frac{\partial G\big(N_k(y), Z_k(y)\big)}{\partial Z} \psi_k^Z(y) \right) dy = \int_\Omega k_3 l_k(y) dy.$$

By differentiating $J(u)$ with respect to u and introducing the adjoint system, we can characterize an optimal control.

Theorem 5. *Given an optimal control u^* with corresponding solutions N^*, Z^*, then there exists adjoint variables λ^N, λ^Z, satisfying this system for $k = 0, 1, ..., T-1$*

$$\lambda_k^N(x) = \frac{\partial F\big(N_k^*(x), Z_k^*(x)\big)}{\partial N} \int_\Omega k_1(y,x) \lambda_{k+1}^N(y) dy + \frac{\partial G\big(N_k^*(x), Z_k^*(x)\big)}{\partial N} \int_\Omega k_2(y,x) \lambda_{k+1}^Z(y) dy + A_k \tag{3.27}$$

$$\lambda_k^Z(x) = \frac{\partial F\big(N_k^*(x), Z_k^*(x)\big)}{\partial Z} \int_\Omega k_1(y,x) \lambda_{k+1}^N(y) dy + \frac{\partial G\big(N_k^*(x), Z_k^*(x)\big)}{\partial Z} \int_\Omega k_2(y,x) \lambda_{k+1}^Z(y) dy$$

with the transversality conditions

$$\lambda_T^N(x) = A_T,\ \lambda_T^Z(x) = 0,\ \forall x \in \Omega. \tag{3.28}$$

Furthermore $u_k^*(x)$ *is given by*

$$u_k^*(x) = \max\left(0, \min\left(-\frac{\int_\Omega k_3(x,y)\lambda_{k+1}^Z(y)dy + B_k}{2C_k}, u_{max}\right)\right) \tag{3.29}$$

for $k = 0, 1, ..., T-1$.

Proof. We start by taking the directional derivative of the objective functional. Since $J(u^*)$ is the minimum value, for $0 < \varepsilon$ and directional vector l, for $u^* + \varepsilon l \in U$, we have

$$\begin{aligned}
0 &\leq \lim_{\varepsilon\to 0^+}\left(\frac{J(u^*+\varepsilon l) - J(u^*)}{\varepsilon}\right) \\
&= \lim_{\varepsilon\to 0^+}\frac{1}{\varepsilon}\Bigg[\sum_{k=0}^{T-1}\int_\Omega \left(A_k N_k^\varepsilon(x) + B_k(u_k^*+\varepsilon l_k)(x) + C_k(u_k^*+\varepsilon l_k)^2(x)\right)dx \\
&\quad + \int_\Omega A_T N_T^\varepsilon(x)dx \\
&\quad - \sum_{k=0}^{T-1}\int_\Omega \left(A_k N_k^*(x) + B_k u_k^*(x) + C_k(u_k^*)^2(x)\right)dx + \int_\Omega A_T N_T^*(x)dx\Bigg] \\
&= \lim_{\varepsilon\to 0^+}\sum_{k=0}^{T-1}\int_\Omega\Bigg[A_k\left(\frac{N_k^\varepsilon(x) - N_k^*(x)}{\varepsilon}\right) + B_k\left(\frac{(u_k^*+\varepsilon l_k)(x) - (u_k^*)(x)}{\varepsilon}\right) \\
&\quad + C_k\left(\frac{(u_k^*+\varepsilon l_k)^2(x) - (u_k^*)^2(x)}{\varepsilon}\right)\Bigg]dx + \lim_{\varepsilon\to 0^+}\int_\Omega A_T\frac{N_T^\varepsilon(x) - N_T^*(x)}{\varepsilon}dx \\
&= \sum_{k=0}^{T-1}\int_\Omega \left[A_k\psi_k^N(x) + B_k l_k(x) + C_k 2u_k^* l_k(x)\right]dx + \int_\Omega A_T\psi_T^N(x)dx.
\end{aligned} \tag{3.30}$$

We will focus just on the terms: $\sum_{k=0}^{T-1}\int_\Omega A_k\psi_k^N(x)dx + \int_\Omega A_T\psi_T^N(x)$, and later we will come back to the complete expression in (3.30). First we will add the term $0\psi_k^Z(x)$ and then substituting from the adjoint system (3.27), we obtain

$$
\begin{aligned}
&\sum_{k=0}^{T-1}\int_\Omega A_k\psi_k^N(x)dx+\int_\Omega A_T\psi_T^N(x)dx \qquad (3.31)\\
=&\sum_{k=0}^{T-1}\int_\Omega \left[A_k\psi_k^N(x)+0\psi_k^Z(x)\right]dx+\int_\Omega A_T\psi_T^N(x)dx\\
=&\sum_{k=0}^{T-1}\int_\Omega\Bigg[\Bigg(\lambda_k^N(x)-\frac{\partial F\big(N_k^*(x),Z_k^*(x)\big)}{\partial N}\int_\Omega k_1(y,x)\lambda_{k+1}^N(y)dy\\
&-\frac{\partial G\big(N_k^*(x),Z_k^*(x)\big)}{\partial N}\int_\Omega k_2(y,x)\lambda_{k+1}^Z(y)dy\Bigg)\psi_k^N(x)\\
&+\Bigg(\lambda_k^Z(x)-\frac{\partial F\big(N_k^*(x),Z_k^*(x)\big)}{\partial Z}\int_\Omega k_1(y,x)\lambda_{k+1}^N(y)dy\\
&-\frac{\partial G\big(N_k^*(x),Z_k^*(x)\big)}{\partial Z}\int_\Omega k_2(y,x)\lambda_{k+1}^Z(y)dy\Bigg)\psi_k^Z(x)\Bigg]dx+\int_\Omega A_T\psi_T^N(x)dx\\
=&\sum_{k=0}^{T-1}\int_\Omega\left[\lambda_k^N(x)\psi_k^N(x)+\lambda_k^Z(x)\psi_k^Z(x)\right]dx\\
&+\sum_{k=0}^{T-1}\int_\Omega\left[\int_\Omega k_1(y,x)\lambda_{k+1}^N(y)dy\left(-\frac{\partial F\big(N_k^*(x),Z_k^*(x)\big)}{\partial N}\psi_k^N(x)-\frac{\partial F\big(N_k^*(x),Z_k^*(x)\big)}{\partial Z}\psi_k^Z(x)\right)\right]dx\\
&+\sum_{k=0}^{T-1}\int_\Omega\left[\int_\Omega k_2(y,x)\lambda_{k+1}^Z(y)dy\left(-\frac{\partial G\big(N_k^*(x),Z_k^*(x)\big)}{\partial N}\psi_k^N(x)-\frac{\partial G\big(N_k^*(x),Z_k^*(x)\big)}{\partial Z}\psi_k^Z(x)\right)\right]dx\\
&+\int_\Omega A_T\psi_T^N(x)dx.
\end{aligned}
$$

We work first with the first sum and the last term. We introduce the term $\int_\Omega 0\psi_T^Z(x)dx$, use the transversality conditions (3.28) and include these new terms in the first sum:

$$
\begin{aligned}
&\sum_{k=0}^{T-1}\int_\Omega\left[\lambda_k^N(x)\psi_k^N(x)+\lambda_k^Z(x)\psi_k^Z(x)\right]dx+\int_\Omega A_T\psi_T^N(x)dx+\int_\Omega 0\psi_T^Z(x)dx \qquad (3.32)\\
=&\sum_{k=0}^{T-1}\int_\Omega\left[\lambda_k^N(x)\psi_k^N(x)+\lambda_k^Z(x)\psi_k^Z(x)\right]dx+\int_\Omega\lambda_T^N(x)\psi_T^N(x)dx+\int_\Omega\lambda_T^Z(x)\psi_T^Z(x)dx\\
=&\sum_{k=0}^{T}\int_\Omega\left[\lambda_k^N(x)\psi_k^N(x)+\lambda_k^Z(x)\psi_k^Z(x)\right]dx.
\end{aligned}
$$

Since the initial conditions for the sensitivities are all zero, we can exclude those two terms from this sum. We also reindexed the first sum to match the other two sums

$$\sum_{k=1}^{T}\int_{\Omega}\left[\lambda_k^N(x)\psi_k^N(x)+\lambda_k^Z(x)\psi_k^Z(x)\right]dx \tag{3.33}$$
$$=\sum_{k=0}^{T-1}\int_{\Omega}\left[\lambda_{k+1}^N(x)\psi_{k+1}^N(x)+\lambda_{k+1}^Z(x)\psi_{k+1}^Z(x)\right]dx.$$

Coming back to expression (3.31) and working just in the second and third sums, we first change the order of integration and then interchange variables x and y:

$$\begin{aligned}
&\sum_{k=0}^{T-1}\int_{\Omega}\left[\lambda_{k+1}^N(y)\int_{\Omega}k_1(y,x)\left(-\frac{\partial F\left(N_k^*(x),Z_k^*(x)\right)}{\partial N}\psi_k^N(x)-\frac{\partial F\left(N_k^*(x),Z_k^*(x)\right)}{\partial Z}\psi_k^Z(x)\right)dx\right]dy \qquad (3.34)\\
&+\sum_{k=0}^{T-1}\int_{\Omega}\left[\lambda_{k+1}^Z(y)\int_{\Omega}k_2(y,x)\left(-\frac{\partial G\left(N_k^*(x),Z_k^*(x)\right)}{\partial N}\psi_k^N(x)-\frac{\partial G\left(N_k^*(x),Z_k^*(x)\right)}{\partial Z}\psi_k^Z(x)\right)dx\right]dy\\
=&\sum_{k=0}^{T-1}\int_{\Omega}\left[\lambda_{k+1}^N(x)\int_{\Omega}k_1(x,y)\left(-\frac{\partial F\left(N_k^*(y),Z_k^*(y)\right)}{\partial N}\psi_k^N(y)-\frac{\partial F\left(N_k^*(y),Z_k^*(y)\right)}{\partial Z}\psi_k^Z(y)\right)dy\right]dx\\
&+\sum_{k=0}^{T-1}\int_{\Omega}\left[\lambda_{k+1}^Z(x)\int_{\Omega}k_2(x,y)\left(-\frac{\partial G\left(N_k^*(y),Z_k^*(y)\right)}{\partial N}\psi_k^N(y)-\frac{\partial G\left(N_k^*(y),Z_k^*(y)\right)}{\partial Z}\psi_k^Z(y)\right)dy\right]dx.
\end{aligned}$$

Using the results from (3.33) and (3.34) we put the sums together and use sensitivities (3.20):

$$\begin{aligned}
&\sum_{k=0}^{T-1}\int_{\Omega}\left[\lambda_{k+1}^N(x)\psi_{k+1}^N(x)+\lambda_{k+1}^Z(x)\psi_{k+1}^Z(x)\right]dx \qquad (3.35)\\
&+\sum_{k=0}^{T-1}\int_{\Omega}\left[\lambda_{k+1}^N(x)\int_{\Omega}k_1(x,y)\left(-\frac{\partial F\left(N_k^*(y),Z_k^*(y)\right)}{\partial N}\psi_k^N(y)-\frac{\partial F\left(N_k^*(y),Z_k^*(y)\right)}{\partial Z}\psi_k^Z(y)\right)dy\right]dx\\
&+\sum_{k=0}^{T-1}\int_{\Omega}\left[\lambda_{k+1}^Z(x)\int_{\Omega}k_2(x,y)\left(-\frac{\partial G\left(N_k^*(y),Z_k^*(y)\right)}{\partial N}\psi_k^N(y)-\frac{\partial G\left(N_k^*(y),Z_k^*(y)\right)}{\partial Z}\psi_k^Z(y)\right)dy\right]dx\\
=&\sum_{k=0}^{T-1}\int_{\Omega}\lambda_{k+1}^N(x)\left[\psi_{k+1}^N(x)-\int_{\Omega}k_1(x,y)\left(\frac{\partial F\left(N_k^*(y),Z_k^*(y)\right)}{\partial N}\psi_k^N(y)+\frac{\partial F\left(N_k^*(y),Z_k^*(y)\right)}{\partial Z}\psi_k^Z(y)\right)dy\right]dx\\
&+\sum_{k=0}^{T-1}\int_{\Omega}\lambda_{k+1}^Z(x)\left[\psi_{k+1}^Z(x)-\int_{\Omega}k_2(x,y)\left(\frac{\partial G\left(N_k^*(y),Z_k^*(y)\right)}{\partial N}\psi_k^N(y)+\frac{\partial G\left(N_k^*(y),Z_k^*(y)\right)}{\partial Z}\psi_k^Z(y)\right)dy\right]dx\\
=&\sum_{k=0}^{T-1}\int_{\Omega}\lambda_{k+1}^N(x)[0]dx+\sum_{k=0}^{T-1}\int_{\Omega}\lambda_{k+1}^Z(x)\left[\int_{\Omega}k_3(x,y)l_k(y)dy\right]dx.
\end{aligned}$$

Therefore we can say

$$\sum_{k=0}^{T-1}\int_\Omega A_k\psi_k^N(x)dx+\int_\Omega A_T\psi_T^N(x)dx=\sum_{k=0}^{T-1}\int_\Omega\lambda_{k+1}^Z(x)\left[\int_\Omega k_3(x,y)l_k(y)dy\right]dx. \tag{3.36}$$

Using the last expression in inequality (3.30) gives

$$\begin{aligned}
0\leq&\sum_{k=0}^{T-1}\int_\Omega\left[A_k\psi_k^N(x)+B_kl_k(x)+C_k2u_k^*l_k(x)\right]dx+\int_\Omega A_T\psi_T^N(x)dx \qquad (3.37)\\
=&\sum_{k=0}^{T}\int_\Omega\left[\lambda_{k+1}^Z(x)\int_\Omega k_3(x,y)l_k(y)dy+B_kl_k(x)+C_k2u_k^*l_k(x)\right]dx\\
=&\sum_{k=0}^{T-1}\int_\Omega\left[\lambda_{k+1}^Z(x)\int_\Omega k_3(x,y)l_k(y)dy\right]dx+\int_\Omega\left[B_kl_k(x)+C_k2u_k^*l_k(x)\right]dx\\
=&\sum_{k=0}^{T-1}\int_\Omega\left[l_k(y)\int_\Omega k_3(x,y)\lambda_{k+1}^Z(x)dx\right]dy+\int_\Omega\left[B_kl_k(x)+C_k2u_k^*l_k(x)\right]dx\\
=&\sum_{k=0}^{T-1}\int_\Omega\left[l_k(y)\int_\Omega k_3(x,y)\lambda_{k+1}^Z(x)dx\right]dy+\int_\Omega\left[B_kl_k(y)+C_k2u_k^*l_k(y)\right]dy\\
=&\sum_{k=0}^{T-1}\int_\Omega l_k(y)\left[\int_\Omega k_3(x,y)\lambda_{k+1}^Z(x)dx+B_k+C_k2u_k^*\right]dy.
\end{aligned}$$

Recall we are calculating the directional derivative when $0<\varepsilon$ and directional vector l, for $u^*+\varepsilon l$. On the set $0<u_k^*(x)<u_{max}$, then $l_k(x)$ can have any sign, because the optimal control can be modified in a small amount up or down and still be within bounds. Thus on this set the integrand of (3.37) must be zero; therefore we obtain

$$u_k^*(x)=-\frac{\int_\Omega k_3(y,x)\lambda_{k+1}^Z(y)dy+B_k}{2C_k}.$$

If on the set of $x\in\Omega$ with $u_k^*(x)=0$, then $l_k(x)$ must be non-negative. Then the integrand of (3.37) must be non-negative and rearranges to

$$u_k^*(x)\geq-\frac{\int_\Omega k_3(y,x)\lambda_{k+1}^Z(y)dy+B_k}{2C_k}.$$

Finally on the set of $x \in \Omega$ with $u_k^*(x) = u_{max}$, then $l_k(x)$ must be negative. The integrand of (3.37) must be non-positive, giving

$$u_k^*(x) \leq -\frac{\int_\Omega k_3(y,x)\lambda_{k+1}^Z(y)dy + B_k}{2C_k}.$$

Taking into account the previous three options, we obtain

$$u_k^*(x) = \begin{cases} 0 & if \quad -\frac{\int_\Omega k_3(y,x)\lambda_{k+1}^Z(y)dy+B_k}{2C_k} \leq 0 \\ -\frac{\int_\Omega k_3(y,x)\lambda_{k+1}^Z(y)dy+B_k}{2C_k} & if \quad 0 \leq -\frac{\int_\Omega k_3(y,x)\lambda_{k+1}^Z(y)dy+B_k}{2C_k} \leq u_{max} \\ u_{max} & if \quad u_{max} \leq -\frac{\int_\Omega k_3(y,x)\lambda_{k+1}^Z(y)dy+B_k}{2C_k}. \end{cases} \tag{3.38}$$

Therefore

$$u_k^*(x) = \max\left(0, \min\left(-\frac{\int_\Omega k_3(y,x)\lambda_{k+1}^Z(y)dy + B_k}{2C_k}, u_{max}\right)\right) \tag{3.39}$$

and we get the adjoint system and control characterization as originally stated. □

3.5 Uniqueness of the Optimal Control

We show uniqueness of the optimal control under a largeness assumption on the coefficients of the quadratic cost term.

Notation 2. *For simplicity we use the notation*

$$\begin{aligned} &N^\varepsilon(x) := N\big(u + \varepsilon(l-u)\big) && Z^\varepsilon(x) := Z\big(u + \varepsilon(l-u)\big) \\ &N^{\varepsilon+\tau}(x) := N\big(u + (\varepsilon+\tau)(l-u)\big) && Z^{\varepsilon+\tau}(x) := Z\big(u + (\varepsilon+\tau)(l-u)\big) \\ &\frac{N_k^{\varepsilon+\tau}(x) - N_k^\varepsilon(x)}{\tau} \rightharpoonup \psi_k^{N^\varepsilon}(x) \ as \ \tau \to 0 && \frac{Z_k^{\varepsilon+\tau}(x) - Z_k^\varepsilon(x)}{\tau} \rightharpoonup \psi_k^{Z^\varepsilon}(x) \ as \ \tau \to 0 \end{aligned} \tag{3.40}$$

Theorem 6. *If C_k, $k = 0, 1, ..., T-1$ are sufficiently large, then the optimal control is unique.*

Proof. We show uniqueness by showing strict concavity of the map:

$$u \in U \to J(u).$$

The concavity follows from showing for all $u, l \in U$, $0 < \varepsilon < 1$,

$$g''(\varepsilon) > 0,$$

where $g(\varepsilon) = J\big(\varepsilon l + (1-\varepsilon)u\big) = J\big(u + \varepsilon(l-u)\big)$.

First we calculate $g'(\varepsilon)$:

$$\begin{aligned}
g'(\varepsilon) &= \lim_{\tau\to 0}\left(\frac{J\big(u_k + (\varepsilon+\tau)(l_k-u_k)\big) - J\big(u_k+\varepsilon(l_k-u_k)\big)}{\tau}\right) \qquad (3.41)\\
&= \lim_{\tau\to 0}\sum_{k=0}^{T-1}\frac{1}{\tau}\int_\Omega \Big\{\Big[A_k N_k^{\varepsilon+\tau}(x) + B_k\big(u_k+(\varepsilon+\tau)(l_k-u_k)\big)(x)\\
&\quad + C_k\big(u_k+(\varepsilon+\tau)(l_k-u_k)\big)^2(x)\Big]\\
&\quad - \Big[A_k N_k^{\varepsilon}(x) + B_k\big(u_k+\varepsilon(l_k-u_k)\big)(x) + C_k\big(u_k+\varepsilon(l_k-u_k)\big)^2(x)\Big]\Big\}dx\\
&\quad + \lim_{\tau\to 0}\frac{1}{\tau}\int_\Omega \left[A_T N_T^{\varepsilon+\tau}(x) - A_T N_T^{\varepsilon}(x)\right]dx\\
&= \lim_{\tau\to 0}\sum_{k=0}^{T-1}\frac{1}{\tau}\int_\Omega \Big\{A_k\left[N_k^{\varepsilon+\tau}(x) - N_k^{\varepsilon}(x)\right] + B_k\left[\tau(l_k-u_k)\right](x)\\
&\quad + C_k\left[2\big(u_k+\varepsilon(l_k-u_k)\big)\tau(l_k-u_k) + \tau^2(l_k-u_k)^2\right](x)\Big\}dx\\
&\quad + \lim_{\tau\to 0}\frac{1}{\tau}\int_\Omega A_T\left[N_T^{\varepsilon+\tau}(x) - N_T^{\varepsilon}(x)\right]dx\\
&= \lim_{\tau\to 0}\sum_{k=0}^{T-1}\int_\Omega \Big\{A_k\left[\frac{N_k^{\varepsilon+\tau}(x) - N_k^{\varepsilon}(x)}{\tau}\right] + B_k(l_k-u_k)(x)\\
&\quad + C_k\left[2\big(u_k+\varepsilon(l_k-u_k)\big)(l_k-u_k) + \tau(l_k-u_k)^2\right](x)\Big\}dx\\
&\quad + \lim_{\tau\to 0}\int_\Omega A_T\left[\frac{N_T^{\varepsilon+\tau}(x) - N_T^{\varepsilon}(x)}{\tau}\right]dx\\
&= \sum_{k=0}^{T-1}\int_\Omega \Big\{A_k\psi_k^{N^\varepsilon}(x) + B_k(l_k-u_k)(x) + C_k 2\left[u_k+\varepsilon(l_k-u_k)\right](l_k-u_k)(x)\Big\}dx\\
&\quad + \int_\Omega A_T\psi_T^{N^\varepsilon}(x)dx.
\end{aligned}$$

The results in Theorem 2 were used in the limits of these quotients in $g'(\varepsilon)$:

$$\begin{aligned}
&\frac{N_k^{\varepsilon+\tau}(x) - N_k^{\varepsilon}(x)}{\tau} \rightharpoonup \psi_k^{N^\varepsilon}(x) \qquad (3.42)\\
&\frac{Z_k^{\varepsilon+\tau}(x) - Z_k^{\varepsilon}(x)}{\tau} \rightharpoonup \psi_k^{Z^\varepsilon}(x) \text{ as } \tau\to 0
\end{aligned}$$

with

$$\begin{aligned}
\psi_{k+1}^{N^\varepsilon}(x) =& \int_\Omega k_1(x,y)\left(\frac{\partial F\big(N_k^\varepsilon(y), Z_k^\varepsilon(y)\big)}{\partial N}\psi_k^{N^\varepsilon}(y) + \frac{\partial F\big(N_k^\varepsilon(y), Z_k^\varepsilon(y)\big)}{\partial Z}\psi_k^{Z^\varepsilon}(y)\right)dy \\
\psi_{k+1}^{Z^\varepsilon}(x) =& \int_\Omega k_2(x,y)\left(\frac{\partial G\big(N_k^\varepsilon(y), Z_k^\varepsilon(y)\big)}{\partial N}\psi_k^{N^\varepsilon}(y) + \frac{\partial G\big(N_k^\varepsilon(y), Z_k^\varepsilon(y)\big)}{\partial Z}\psi_k^{Z^\varepsilon}(y)\right)dy \\
&+ \int_\Omega k_3(x,y)(l_k - u_k)(y)dy \\
\psi_0^{N^\varepsilon}(x) =& \psi_0^{Z^\varepsilon}(x) = 0
\end{aligned} \tag{3.43}$$

and

$$\begin{aligned}
\psi_{k+1}^{N^{\varepsilon+\tau}}(x) =& \int_\Omega k_1(x,y)\bigg(\frac{\partial F\big(N_k^{\varepsilon+\tau}(y), Z_k^{\varepsilon+\tau}(y)\big)}{\partial N}\psi_k^{N^{\varepsilon+\tau}}(y) \\
&+ \frac{\partial F\big(N_k^{\varepsilon+\tau}(y), Z_k^{\varepsilon+\tau}(y)\big)}{\partial Z}\psi_k^{Z^{\varepsilon+\tau}}(y)\bigg)dy \\
\psi_{k+1}^{Z^{\varepsilon+\tau}}(x) =& \int_\Omega k_2(x,y)\bigg(\frac{\partial G\big(N_k^{\varepsilon+\tau}(y), Z_k^{\varepsilon+\tau}(y)\big)}{\partial N}\psi_k^{N^{\varepsilon+\tau}}(y) \\
&+ \frac{\partial G\big(N_k^{\varepsilon+\tau}(y), Z_k^{\varepsilon+\tau}(y)\big)}{\partial Z}\psi_k^{Z^{\varepsilon+\tau}}(y)\bigg)dy \\
&+ \int_\Omega k_3(x,y)(l_k - u_k)(y)dy \\
\psi_0^{N^{\varepsilon+\tau}}(x) =& \psi_0^{Z^{\varepsilon+\tau}}(x) = 0.
\end{aligned} \tag{3.44}$$

We want to estimate $\psi_k^{N^\varepsilon}(x)$ in terms of the components $l - u$:

$$\begin{aligned}
\big|\psi_1^{N^\varepsilon}(x)\big| =& \bigg|\int_\Omega k_1(x,y)\bigg(\frac{\partial F\big(N_0^\varepsilon(y), Z_0^\varepsilon(y)\big)}{\partial N}\psi_0^{N^\varepsilon}(y) \\
&+ \frac{\partial F\big(N_0^\varepsilon(y), Z_0^\varepsilon(y)\big)}{\partial Z}\psi_0^{Z^\varepsilon}(x)\bigg)dy\bigg| \\
=& 0 \\
\big|\psi_1^{Z^\varepsilon}(x)\big| =& \left|\int_\Omega k_2(x,y)\left(\frac{\partial G\big(N_0^\varepsilon(y), Z_0^\varepsilon(y)\big)}{\partial N}\psi_0^{N^\varepsilon}(y) + \frac{\partial G\big(N_0^\varepsilon(y), Z_0^\varepsilon(y)\big)}{\partial Z}\psi_0^{Z^\varepsilon}(y)\right)dy\right| \\
&+ \left|\int_\Omega k_3(x,y)(l_0 - u_0)(y)dy\right| \\
\leq& E_1\int_\Omega |(l_0 - u_0)(y)|\,dy.
\end{aligned} \tag{3.45}$$

Using these results we can obtain

$$
\begin{aligned}
\left|\psi_2^{N^\varepsilon}(x)\right| =& \left| \int_\Omega k_1(x,y) \Bigg(\frac{\partial F\left(N_1^\varepsilon(y), Z_1^\varepsilon(y)\right)}{\partial N} \psi_1^{N^\varepsilon}(y) \right. \\
&\left. + \frac{\partial F\left(N_1^\varepsilon(y), Z_1^\varepsilon(y)\right)}{\partial Z} \psi_1^{Z^\varepsilon}(x) \Bigg) dy \right| \\
=& \left| \int_\Omega k_1(x,y) \frac{\partial F\left(N_1^\varepsilon(y), Z_1^\varepsilon(y)\right)}{\partial Z} \psi_1^{Z^\varepsilon}(x) dy \right| \\
\leq& D_2 \int_\Omega \left| (l_0 - u_0)(y) \right| dy \\
\left|\psi_2^{Z^\varepsilon}(x)\right| \leq& \left| \int_\Omega k_2(x,y) \left(\frac{\partial G\left(N_1^\varepsilon(y), Z_1^\varepsilon(y)\right)}{\partial N} \psi_1^{N^\varepsilon}(y) + \frac{\partial G\left(N_1^\varepsilon(y), Z_1^\varepsilon(y)\right)}{\partial Z} \psi_1^{Z^\varepsilon}(y) \right) dy \right| \\
&+ \left| \int_\Omega k_3(x,y)(l_1 - u_1)(y) dy \right| \\
\leq& \left| \int_\Omega k_2(x,y) \frac{\partial G\left(N_1^\varepsilon(y), Z_1^\varepsilon(y)\right)}{\partial Z} \psi_1^{Z^\varepsilon}(y) dy \right| + \left| \int_\Omega k_3(x,y)(l_1 - u_1)(y) dy \right| \\
\leq& E_2 \left[\int_\Omega \left| (l_0 - u_0)(y) \right| dy + \int_\Omega \left| (l_1 - u_1)(y) \right| dy \right].
\end{aligned} \tag{3.46}
$$

If we continue this iterative process, we find

$$
\begin{aligned}
|\psi_{k+1}^{N^\varepsilon}(x)| \leq& D_{k+1} \sum_{j=0}^{k} \int_\Omega |l_j - u_j|(y) dy \\
|\psi_{k+1}^{Z^\varepsilon}(x)| \leq& E_{k+1} \sum_{j=0}^{k} \int_\Omega |l_j - u_j|(y) dy \text{ with } k = 0, 1, ..., T-1
\end{aligned} \tag{3.47}
$$

where the constants D_k and E_k do not depend on ε.

To find $g''(\varepsilon)$, using (3.43) and (3.44), we calculate the difference quotient for directional derivative of $\psi_k^{N^\varepsilon}$ and $\psi_k^{Z^\varepsilon}$ with respect $\big(u_k+\varepsilon(l_k-u_k)\big)$ in the direction l_k-u_k:

$$
\begin{aligned}
&\frac{\psi_{k+1}^{N^{\varepsilon+\tau}}(x)-\psi_{k+1}^{N^\varepsilon}(x)}{\tau} \qquad (3.48)\\
=&\frac{1}{\tau}\Bigg[\int_\Omega k_1(x,y)\left(\frac{\partial F\big(N_k^{\varepsilon+\tau}(y),Z_k^{\varepsilon+\tau}(y)\big)}{\partial N}\psi_k^{N^{\varepsilon+\tau}}(y)+\frac{\partial F\big(N_k^{\varepsilon+\tau}(y),Z_k^{\varepsilon+\tau}(y)\big)}{\partial Z}\psi_k^{Z^{\varepsilon+\tau}}(y)\right)dy\\
&-\int_\Omega k_1(x,y)\left(\frac{\partial F\big(N_k^{\varepsilon}(y),Z_k^{\varepsilon}(y)\big)}{\partial N}\psi_k^{N^{\varepsilon}}(y)+\frac{\partial F\big(N_k^{\varepsilon}(y),Z_k^{\varepsilon}(y)\big)}{\partial Z}\psi_k^{Z^{\varepsilon}}(y)\right)dy\Bigg]\\
=&\frac{1}{\tau}\int_\Omega k_1(x,y)\Bigg[\left(\frac{\partial F\big(N_k^{\varepsilon+\tau}(y),Z_k^{\varepsilon+\tau}(y)\big)}{\partial N}\psi_k^{N^{\varepsilon+\tau}}(y)-\frac{\partial F\big(N_k^{\varepsilon}(y),Z_k^{\varepsilon}(y)\big)}{\partial N}\psi_k^{N^{\varepsilon}}(y)\right)\\
&+\left(\frac{\partial F\big(N_k^{\varepsilon+\tau}(y),Z_k^{\varepsilon+\tau}(y)\big)}{\partial Z}\psi_k^{Z^{\varepsilon+\tau}}(y)-\frac{\partial F\big(N_k^{\varepsilon}(y),Z_k^{\varepsilon}(y)\big)}{\partial Z}\psi_k^{Z^{\varepsilon}}(y)\right)\Bigg]dy\\
=&\frac{1}{\tau}\int_\Omega k_1(x,y)\Bigg\{\Bigg[\frac{\partial F\big(N_k^{\varepsilon+\tau}(y),Z_k^{\varepsilon+\tau}(y)\big)}{\partial N}\psi_k^{N^{\varepsilon+\tau}}(y)-\frac{\partial F\big(N_k^{\varepsilon}(y),Z_k^{\varepsilon}(y)\big)}{\partial N}\psi_k^{N^{\varepsilon+\tau}}(y)\\
&+\frac{\partial F\big(N_k^{\varepsilon}(y),Z_k^{\varepsilon}(y)\big)}{\partial N}\psi_k^{N^{\varepsilon+\tau}}(y)-\frac{\partial F\big(N_k^{\varepsilon}(y),Z_k^{\varepsilon}(y)\big)}{\partial N}\psi_k^{N^{\varepsilon}}(y)\Bigg]\\
&+\Bigg[\frac{\partial F\big(N_k^{\varepsilon+\tau}(y),Z_k^{\varepsilon+\tau}(y)\big)}{\partial Z}\psi_k^{Z^{\varepsilon+\tau}}(y)-\frac{\partial F\big(N_k^{\varepsilon}(y),Z_k^{\varepsilon}(y)\big)}{\partial Z}\psi_k^{Z^{\varepsilon+\tau}}(y)\\
&+\frac{\partial F\big(N_k^{\varepsilon}(y),Z_k^{\varepsilon}(y)\big)}{\partial Z}\psi_k^{Z^{\varepsilon+\tau}}(y)-\frac{\partial F\big(N_k^{\varepsilon}(y),Z_k^{\varepsilon}(y)\big)}{\partial Z}\psi_k^{Z^{\varepsilon}}(y)\Bigg]\Bigg\}dy\\
=&\frac{1}{\tau}\int_\Omega k_1(x,y)\Bigg\{\Bigg[\left(\frac{\partial F\big(N_k^{\varepsilon+\tau}(y),Z_k^{\varepsilon+\tau}(y)\big)}{\partial N}-\frac{\partial F\big(N_k^{\varepsilon}(y),Z_k^{\varepsilon}(y)\big)}{\partial N}\right)\psi_k^{N^{\varepsilon+\tau}}(y)\\
&+\frac{\partial F\big(N_k^{\varepsilon}(y),Z_k^{\varepsilon}(y)\big)}{\partial N}\left(\psi_k^{N^{\varepsilon+\tau}}(y)-\psi_k^{N^{\varepsilon}}(y)\right)\Bigg]\\
&+\Bigg[\left(\frac{\partial F\big(N_k^{\varepsilon+\tau}(y),Z_k^{\varepsilon+\tau}(y)\big)}{\partial Z}-\frac{\partial F\big(N_k^{\varepsilon}(y),Z_k^{\varepsilon}(y)\big)}{\partial Z}\right)\psi_k^{Z^{\varepsilon+\tau}}(y)\\
&+\frac{\partial F\big(N_k^{\varepsilon}(y),Z_k^{\varepsilon}(y)\big)}{\partial Z}\left(\psi_k^{Z^{\varepsilon+\tau}}(y)-\psi_k^{Z^{\varepsilon}}(y)\right)\Bigg]\Bigg\}dy.
\end{aligned}
$$

We will use $\sigma_k^{N^\varepsilon}$ and $\sigma_k^{Z^\varepsilon}$ to represent the limit of the difference quotients for directional derivative of $\psi_k^{N^\varepsilon}$ and $\psi_k^{Z^\varepsilon}$ with respect $\big(u_k+\varepsilon(l_k-u_k)\big)$ in the direction l_k-u_k. From estimates on these difference quotients and using the similar ideas as used in Theorem 2,

we have the existence of $\sigma^{N^\varepsilon}, \sigma^{Z^\varepsilon} \in (L^\infty(\Omega))^{T+1}$ such that for $k = 0, 1, ..., T$:

$$\begin{aligned} \frac{\psi_k^{N^{\varepsilon+\tau}}(x) - \psi_k^{N^\varepsilon}(x)}{\tau} &\rightharpoonup \sigma_k^{N^\varepsilon} \\ \frac{\psi_k^{Z^{\varepsilon+\tau}}(x) - \psi_k^{Z^\varepsilon}(x)}{\tau} &\rightharpoonup \sigma_k^{Z^\varepsilon} \end{aligned} \tag{3.49}$$

weakly in $L^2(\Omega)$ as $\tau \to 0^+$, for $0 < \tau << 1$ such that $\big(u + (\varepsilon + \tau)(l - u)\big) \in U$.
If we take the limit in both sides of (3.48) as $\tau \to 0$, we obtain

$$\begin{aligned} &\lim_{\tau\to 0} \frac{\psi_{k+1}^{N^{\varepsilon+\tau}}(x) - \psi_{k+1}^{N^\varepsilon}(x)}{\tau} \\ &= \int_\Omega k_1(x,y) \Bigg\{ \Bigg[\left(\frac{\partial^2 F\big(N_k^\varepsilon(y), Z_k^\varepsilon(y)\big)}{\partial N^2} \psi_k^{N^\varepsilon}(y) + \frac{\partial^2 F\big(N_k^\varepsilon(y), Z_k^\varepsilon(y)\big)}{\partial N \partial Z} \psi_k^{Z^\varepsilon}(y) \right) \psi_k^{N^\varepsilon}(y) \\ &\quad + \frac{\partial F\big(N_k^\varepsilon(y), Z_k^\varepsilon(y)\big)}{\partial N} \sigma_k^{N^\varepsilon}(y) \Bigg] \\ &\quad + \Bigg[\left(\frac{\partial^2 F\big(N_k^\varepsilon(y), Z_k^\varepsilon(y)\big)}{\partial Z^2} \psi_k^{Z^\varepsilon}(y) + \frac{\partial^2 F\big(N_k^\varepsilon(y), Z_k^\varepsilon(y)\big)}{\partial N \partial Z} \psi_k^{N^\varepsilon}(y) \right) \psi_k^{Z^\varepsilon}(y) \\ &\quad + \frac{\partial F\big(N_k^\varepsilon(y), Z_k^\varepsilon(y)\big)}{\partial Z} \sigma_k^{Z^\varepsilon}(y) \Bigg] \Bigg\} dy \\ &= \int_\Omega k_1(x,y) \Bigg[\frac{\partial^2 F\big(N_k^\varepsilon(y), Z_k^\varepsilon(y)\big)}{\partial N^2} \left(\psi_k^{N^\varepsilon}(y)\right)^2 + 2 \frac{\partial^2 F\big(N_k^\varepsilon(y), Z_k^\varepsilon(y)\big)}{\partial N \partial Z} \psi_k^{Z^\varepsilon}(y) \psi_k^{N^\varepsilon}(y) \\ &\quad + \frac{\partial F\big(N_k^\varepsilon(y), Z_k^\varepsilon(y)\big)}{\partial N} \sigma_k^{N^\varepsilon}(y) + \frac{\partial^2 F\big(N_k^\varepsilon(y), Z_k^\varepsilon(y)\big)}{\partial Z^2} \left(\psi_k^{Z^\varepsilon}(y)\right)^2 \\ &\quad + \frac{\partial F\big(N_k^\varepsilon(y), Z_k^\varepsilon(y)\big)}{\partial Z} \sigma_k^{Z^\varepsilon}(y) \Bigg] dy. \end{aligned} \tag{3.50}$$

Following the same ideas we can obtain

$$\begin{aligned} &\lim_{\tau\to 0} \frac{\psi_{k+1}^{Z^{\varepsilon+\tau}}(x) - \psi_{k+1}^{Z^\varepsilon}(x)}{\tau} \\ &= \int_\Omega k_2(x,y) \Bigg[\frac{\partial^2 G\big(N_k^\varepsilon(y), Z_k^\varepsilon(y)\big)}{\partial N^2} \left(\psi_k^{N^\varepsilon}(y)\right)^2 + 2 \frac{\partial^2 G\big(N_k^\varepsilon(y), Z_k^\varepsilon(y)\big)}{\partial N \partial Z} \psi_k^{Z^\varepsilon}(y) \psi_k^{N^\varepsilon}(y) \\ &\quad + \frac{\partial G\big(N_k^\varepsilon(y), Z_k^\varepsilon(y)\big)}{\partial N} \sigma_k^{N^\varepsilon}(y) + \frac{\partial^2 G\big(N_k^\varepsilon(y), Z_k^\varepsilon(y)\big)}{\partial Z^2} \left(\psi_k^{Z^\varepsilon}(y)\right)^2 \\ &\quad + \frac{\partial G\big(N_k^\varepsilon(y), Z_k^\varepsilon(y)\big)}{\partial Z} \sigma_k^{Z^\varepsilon}(y) \Bigg] dy. \end{aligned} \tag{3.51}$$

Note that the term $\int_\Omega k_3(x,y)(l_k-u_k)(y)dy$ is the same in the $\psi_{k+1}^{Z^{\varepsilon+\tau}}$ equation (3.43) and in the $\psi_{k+1}^{Z^\varepsilon}$ equation (3.44); therefore it cancels.

Using the results of (3.49), (3.50) and (3.51) we obtain:

$$\begin{aligned}
\sigma_k^{N^\varepsilon}(x) := \int_\Omega k_1(x,y)\Bigg[&\frac{\partial^2 F\big(N_k^\varepsilon(y),Z_k^\varepsilon(y)\big)}{\partial N^2}\left(\psi_k^{N^\varepsilon}(y)\right)^2 \\
&+2\frac{\partial^2 F\big(N_k^\varepsilon(y),Z_k^\varepsilon(y)\big)}{\partial N\partial Z}\psi_k^{Z^\varepsilon}(y)\psi_k^{N^\varepsilon}(y)+\frac{\partial F\big(N_k^\varepsilon(y),Z_k^\varepsilon(y)\big)}{\partial N}\sigma_k^{N^\varepsilon}(y) \\
&+\frac{\partial^2 F\big(N_k^\varepsilon(y),Z_k^\varepsilon(y)\big)}{\partial Z^2}\left(\psi_k^{Z^\varepsilon}(y)\right)^2+\frac{\partial F\big(N_k^\varepsilon(y),Z_k^\varepsilon(y)\big)}{\partial Z}\sigma_k^{Z^\varepsilon}(y)\Bigg]dy \\
\sigma_k^{Z^\varepsilon}(x) := \int_\Omega k_2(x,y)\Bigg[&\frac{\partial^2 G\big(N_k^\varepsilon(y),Z_k^\varepsilon(y)\big)}{\partial N^2}\left(\psi_k^{N^\varepsilon}(y)\right)^2+2\frac{\partial^2 G\big(N_k^\varepsilon(y),Z_k^\varepsilon(y)\big)}{\partial N\partial Z}\psi_k^{Z^\varepsilon}(y)\psi_k^{N^\varepsilon}(y) \\
&+\frac{\partial G\big(N_k^\varepsilon(y),Z_k^\varepsilon(y)\big)}{\partial N}\sigma_k^{N^\varepsilon}(y)+\frac{\partial^2 G\big(N_k^\varepsilon(y),Z_k^\varepsilon(y)\big)}{\partial Z^2}\left(\psi_k^{Z^\varepsilon}(y)\right)^2 \\
&+\frac{\partial G\big(N_k^\varepsilon(y),Z_k^\varepsilon(y)\big)}{\partial Z}\sigma_k^{Z^\varepsilon}(y)\Bigg]dy.
\end{aligned} \tag{3.52}$$

with $\sigma_0^{N^\varepsilon}=\sigma_0^{Z^\varepsilon}=0$.

We now use an iterative method to estimate $\sigma_k^{N^\varepsilon}$ and $\sigma_k^{Z^\varepsilon}$ in terms of the components of $(l-u)^2$. Using $\psi_0^{N^\varepsilon} = \psi_0^{Z^\varepsilon} = \sigma_0^{N^\varepsilon} = \sigma_0^{Z^\varepsilon} = 0$, we obtain

$$\begin{aligned}
\sigma_1^{N^\varepsilon}(x) = \int_\Omega k_1(x,y) \Bigg[& \frac{\partial^2 F\big(N_0^\varepsilon(y), Z_0^\varepsilon(y)\big)}{\partial N^2} \left(\psi_0^{N^\varepsilon}(y)\right)^2 \\
& + 2\frac{\partial^2 F\big(N_0^\varepsilon(y), Z_0^\varepsilon(y)\big)}{\partial N \partial Z} \psi_0^{Z^\varepsilon}(y)\psi_0^{N^\varepsilon}(y) + \frac{\partial F\big(N_0^\varepsilon(y), Z_0^\varepsilon(y)\big)}{\partial N} \sigma_0^{N^\varepsilon}(y) \\
& + \frac{\partial^2 F\big(N_0^\varepsilon(y), Z_0^\varepsilon(y)\big)}{\partial Z^2} \left(\psi_0^{Z^\varepsilon}(y)\right)^2 + \frac{\partial F\big(N_0^\varepsilon(y), Z_0^\varepsilon(y)\big)}{\partial Z} \sigma_0^{Z^\varepsilon}(y) \Bigg] dy \\
=& 0 \\
\sigma_1^{Z^\varepsilon}(x) = \int_\Omega k_2(x,y) \Bigg[& \frac{\partial^2 G\big(N_0^\varepsilon(y), Z_0^\varepsilon(y)\big)}{\partial N^2} \left(\psi_0^{N^\varepsilon}(y)\right)^2 + 2\frac{\partial^2 G\big(N_0^\varepsilon(y), Z_0^\varepsilon(y)\big)}{\partial N \partial Z} \psi_0^{Z^\varepsilon}(y)\psi_0^{N^\varepsilon}(y) \\
& + \frac{\partial G\big(N_0^\varepsilon(y), Z_0^\varepsilon(y)\big)}{\partial N} \sigma_0^{N^\varepsilon}(y) + \frac{\partial^2 G\big(N_0^\varepsilon(y), Z_0^\varepsilon(y)\big)}{\partial Z^2} \left(\psi_0^{Z^\varepsilon}(y)\right)^2 \\
& + \frac{\partial G\big(N_0^\varepsilon(y), Z_0^\varepsilon(y)\big)}{\partial Z} \sigma_0^{Z^\varepsilon}(y) \Bigg] dy \\
=& 0.
\end{aligned} \tag{3.53}$$

These results and inequalities (3.47) give

$$
\begin{aligned}
\left|\sigma_2^{N^\varepsilon}(x)\right| \leq & \left| \int_\Omega k_1(x,y) \left[\frac{\partial^2 F\left(N_1^\varepsilon(y), Z_1^\varepsilon(y)\right)}{\partial N^2} \left(\psi_1^{N^\varepsilon}(y)\right)^2 \right.\right. \\
& + 2\frac{\partial^2 F\left(N_1^\varepsilon(y), Z_1^\varepsilon(y)\right)}{\partial N \partial Z} \psi_1^{Z^\varepsilon}(y)\psi_1^{N^\varepsilon}(y) + \frac{\partial F\left(N_1^\varepsilon(y), Z_1^\varepsilon(y)\right)}{\partial N}\sigma_1^{N^\varepsilon}(y) \\
& \left.\left. + \frac{\partial^2 F\left(N_1^\varepsilon(y), Z_1^\varepsilon(y)\right)}{\partial Z^2} \left(\psi_1^{Z^\varepsilon}(y)\right)^2 + \frac{\partial F\left(N_1^\varepsilon(y), Z_1^\varepsilon(y)\right)}{\partial Z}\sigma_1^{Z^\varepsilon}(y) \right] dy \right| \\
\leq & \left| \int_\Omega k_1(x,y) \left(\frac{\partial^2 F\left(N_1^\varepsilon(y), Z_1^\varepsilon(y)\right)}{\partial Z^2} \left(\psi_1^{Z^\varepsilon}(y)\right)^2 \right) dy \right| \\
\leq & L_1 \int_\Omega (l_0 - u_0)^2(y) dy \\
\left|\sigma_2^{Z^\varepsilon}(x)\right| = & \left| \int_\Omega k_2(x,y) \left[\frac{\partial^2 G\left(N_1^\varepsilon(y), Z_1^\varepsilon(y)\right)}{\partial N^2} \left(\psi_1^{N^\varepsilon}(y)\right)^2 + 2\frac{\partial^2 G\left(N_1^\varepsilon(y), Z_1^\varepsilon(y)\right)}{\partial N \partial Z} \psi_1^{Z^\varepsilon}(y)\psi_1^{N^\varepsilon}(y) \right.\right. \\
& + \frac{\partial G\left(N_1^\varepsilon(y), Z_1^\varepsilon(y)\right)}{\partial N}\sigma_1^{N^\varepsilon}(y) + \frac{\partial^2 G\left(N_1^\varepsilon(y), Z_1^\varepsilon(y)\right)}{\partial Z^2} \left(\psi_1^{Z^\varepsilon}(y)\right)^2 \\
& \left.\left. + \frac{\partial G\left(N_1^\varepsilon(y), Z_1^\varepsilon(y)\right)}{\partial Z}\sigma_1^{Z^\varepsilon}(y) \right] dy \right| \\
\leq & \left| \int_\Omega k_2(x,y) \left(\frac{\partial^2 G\left(N_1^\varepsilon(y), Z_1^\varepsilon(y)\right)}{\partial Z^2} \left(\psi_1^{Z^\varepsilon}(y)\right)^2 \right) dy \right| \\
\leq & M_1 \int_\Omega (l_0 - u_0)^2(y) dy,
\end{aligned}
\tag{3.54}
$$

using $\psi_1^{N^\varepsilon} = 0$, $\sigma_1^{N^\varepsilon} = 0$, and $\sigma_1^{Z^\varepsilon} = 0$.

Next, we focus on $\sigma_3^{N^\varepsilon}(x)$:

$$
\begin{aligned}
\left|\sigma_3^{N^\varepsilon}(x)\right| \leq & \left| \int_\Omega k_1(x,y) \frac{\partial^2 F\left(N_2^\varepsilon(y), Z_2^\varepsilon(y)\right)}{\partial N^2} \left(\psi_2^{N^\varepsilon}(y)\right)^2 dy \right| \\
& + 2\left| \int_\Omega k_1(x,y) \frac{\partial^2 F\left(N_2^\varepsilon(y), Z_2^\varepsilon(y)\right)}{\partial N \partial Z} \psi_2^{Z^\varepsilon}(y)\psi_2^{N^\varepsilon}(y) dy \right| \\
& + \left| \int_\Omega k_1(x,y) \frac{\partial F\left(N_2^\varepsilon(y), Z_2^\varepsilon(y)\right)}{\partial N} \sigma_2^{N^\varepsilon}(y) dy \right| \\
& + \left| \int_\Omega k_1(x,y) \frac{\partial^2 F\left(N_2^\varepsilon(y), Z_2^\varepsilon(y)\right)}{\partial Z^2} \left(\psi_2^{Z^\varepsilon}(y)\right)^2 dy \right| \\
& + \left| \int_\Omega k_1(x,y) \frac{\partial F\left(N_2^\varepsilon(y), Z_2^\varepsilon(y)\right)}{\partial Z} \sigma_2^{Z^\varepsilon}(y) dy \right| \\
\leq & L_{21} \Bigg\{ \int_\Omega (l_0 - u_0)^2(y) dy \\
& + \left[\int_\Omega \left|(l_0 - u_0)(y)\right| dy + \int_\Omega \left|(l_1 - u_1)(y)\right| dy \right] \int_\Omega \left|(l_0 - u_0)(y)\right| dy \\
& + \left[\int_\Omega \left|(l_0 - u_0)(y)\right| dy + \int_\Omega \left|(l_1 - u_1)(y)\right| dy \right]^2 \\
& + \int_\Omega (l_1 - u_1)^2(y) dy \Bigg\} \\
\leq & L_{22} \Bigg[\int_\Omega (l_0 - u_0)^2(y) dy + \int_\Omega (l_1 - u_1)^2(y) dy \\
& + \int_\Omega (l_0 - u_0)(y)(l_1 - u_1)(y) dy \Bigg] \\
\left|\sigma_3^{N^\varepsilon}(x)\right| \leq & L_{22} \Bigg[\int_\Omega (l_0 - u_0)^2(y) dy + \int_\Omega (l_1 - u_1)^2(y) dy \\
& + 2\int_\Omega (l_0 - u_0)^2(y) dy + 2\int_\Omega (l_1 - u_1)^2(y) dy \Bigg] \\
\leq & L_2 \left[\int_\Omega (l_0 - u_0)^2(y) dy + \int_\Omega (l_1 - u_1)^2(y) dy \right],
\end{aligned}
\tag{3.55}
$$

where the last step is justified by the inequality $ab \leq \frac{1}{2}a^2 + \frac{1}{2}b^2$. Using the same ideas for $\sigma_3^{Z^\varepsilon}$, we have:

$$
\left|\sigma_3^{Z^\varepsilon}(x)\right| \leq M_2 \left[\int_\Omega (l_0 - u_0)^2(y) dy + \int_\Omega (l_1 - u_1)^2(y) dy \right] \tag{3.56}
$$

Then by iteration, we obtain

$$\begin{aligned}\left|\sigma_{k+1}^{N^\varepsilon}(x)\right| \leq & L_k \sum_{j=0}^{k} \int_\Omega (l_j - u_j)^2(y)dy \\ \left|\sigma_{k+1}^{Z^\varepsilon}(x)\right| \leq & M_k \sum_{j=0}^{k} \int_\Omega (l_j - u_j)^2(y)dy \text{ with } k = 1, ..., T-1,\end{aligned} \tag{3.57}$$

where the constants, L_k and M_k, do not depend on ε or τ.

From (3.57) and using the fact that

$$|a| \leq b \Rightarrow -b \leq a \leq b,$$

we obtain

$$\begin{aligned}\sigma_{k+1}^{N^\varepsilon}(x) \geq & - L_k \sum_{j=0}^{k} \int_\Omega (l_j - u_j)^2(y)dy \\ \sigma_{k+1}^{Z^\varepsilon}(x) \geq & - M_k \sum_{j=0}^{k} \int_\Omega (l_j - u_j)^2(y)dy.\end{aligned} \tag{3.58}$$

We can now take the second derivative of the function g:

$$
\begin{aligned}
g''(\varepsilon) &= \lim_{\tau\to 0}\frac{g'(\varepsilon+\tau)-g'(\varepsilon)}{\tau} \qquad (3.59)\\
&= \lim_{\tau\to 0}\frac{1}{\tau}\sum_{k=0}^{T-1}\int_\Omega \Bigg\{\Bigg[A_k\psi_k^{N^{\varepsilon+\tau}}(x)+B_k(l_k-u_k)(x)\\
&\quad + C_k 2\left[u_k+(\varepsilon+\tau)(l_k-u_k)\right](l_k-u_k)(x)\Bigg]\\
&\quad -\left[A_k\psi_k^{N^{\varepsilon}}(x)+B_k(l_k-u_k)(x)+C_k 2\left[u_k+\varepsilon(l_k-u_k)\right](l_k-u_k)(x)\right]\Bigg\}dx\\
&\quad + \lim_{\tau\to 0}\frac{1}{\tau}\int_\Omega A_T\left[\psi_T^{N^{\varepsilon+\tau}}(x)-\psi_T^{N^{\varepsilon}}(x)\right]dx\\
&= \lim_{\tau\to 0}\sum_{k=0}^{T-1}\int_\Omega\left[A_k\frac{\psi_k^{N^{\varepsilon+\tau}}(x)-\psi_k^{N^{\varepsilon}}(x)}{\tau}+C_k 2(l_k-u_k)^2(x)\right]dx\\
&\quad + \lim_{\tau\to 0}\int_\Omega A_T\frac{\psi_T^{N^{\varepsilon+\tau}}(x)-\psi_T^{N^{\varepsilon}}(x)}{\tau}dx\\
&= \sum_{k=0}^{T-1}\int_\Omega\left[A_k\sigma_k^{N^{\varepsilon}}(x)+C_k 2(l_k-u_k)^2(x)\right]dx+\int_\Omega A_T\sigma_T^{N^{\varepsilon}}(x)dx\\
&\geq \sum_{k=0}^{T-1}\left[A_k(-L_k)+2C_k\right]\int_\Omega(l_k-u_k)^2dx+\int_\Omega A_T(-L_{T-1})(l_{T-1}-u_{T-1})^2dx\\
&\geq \sum_{k=0}^{T-1}(-H_k+2C_k)\int_\Omega(l_k-u_k)^2dx+\int_\Omega(-H_{T-1})(l_{T-1}-u_{T-1})^2dx\\
&\geq \sum_{k=0}^{T-1}(2C_k-H_k)\int_\Omega(l_k-u_k)^2dx
\end{aligned}
$$

which gives the desire concavity for C_k's sufficiently large. Thus the uniqueness of the optimal control has been shown. □

3.6 Numerical Solutions

We illustrate some numerical results for our optimal control problem. For the numerical results shown in this section we use the functions in (3.4). For the results that we present in this chapter we use a Laplace kernel for k_1, k_2, and k_3. This kernel was chosen since it has fat tails which represents well the stratified dispersal of the populations of gypsy

moth:

$$k_i(x,y) = \frac{1}{2}\beta \exp\big(-\beta\,|x-y|\big) \text{ with } i = 1,2,3. \tag{3.60}$$

For the numerical approximations we use the following values for the parameters:

Table 3.1: Parameter values for the Integrodifference model

Parameter	γ	r	b	f	ρ	β
Values	6	0.008	0.03	0.3	1.5	10

Some of the parameters (γ, ρ, f) are taken from previous works [67, 24, 86], others (r, b) are adjusted to have the characteristic oscillator behavior of gypsy moth populations. The trapezoidal rule is used to numerically approximate the integrals. Accuracy results are in Appendix B.1.

We start by showing outcomes of our spatial model. Our first objective is to observe the effects of incorporating space in the model. We compare our spatial model with a non-spatial version that uses the same functions F and G in (3.4),

$$\begin{aligned} \widetilde{N}_{k+1} &= F\big(\widetilde{N}_k, \widetilde{Z}_k\big) \\ \widetilde{Z}_{k+1} &= G\big(\widetilde{N}_k, \widetilde{Z}_k\big). \end{aligned} \tag{3.61}$$

where $\widetilde{N}_k$ and $\widetilde{Z}_k$ are the densities of gypsy moth and the virus at time k, and the parameters are the same ones in our spatial model. In Figure 3.1(a), we have graphs of the discrete model with the cyclic oscillations, a characteristic of the populations of gypsy moth. Figure 3.1(b) shows the corresponding integrodifference model. On the top is the density of gypsy moth and on the bottom the density of the virus for a period of 50 years. The spatial model maintains the oscillations in time and the peaks occur at similar time in different locations that gives the spatial synchrony, characteristic of gypsy moth populations. Density of gypsy is scale by a factor of 10^{-1} and virus density by a factor of 10^{1}.

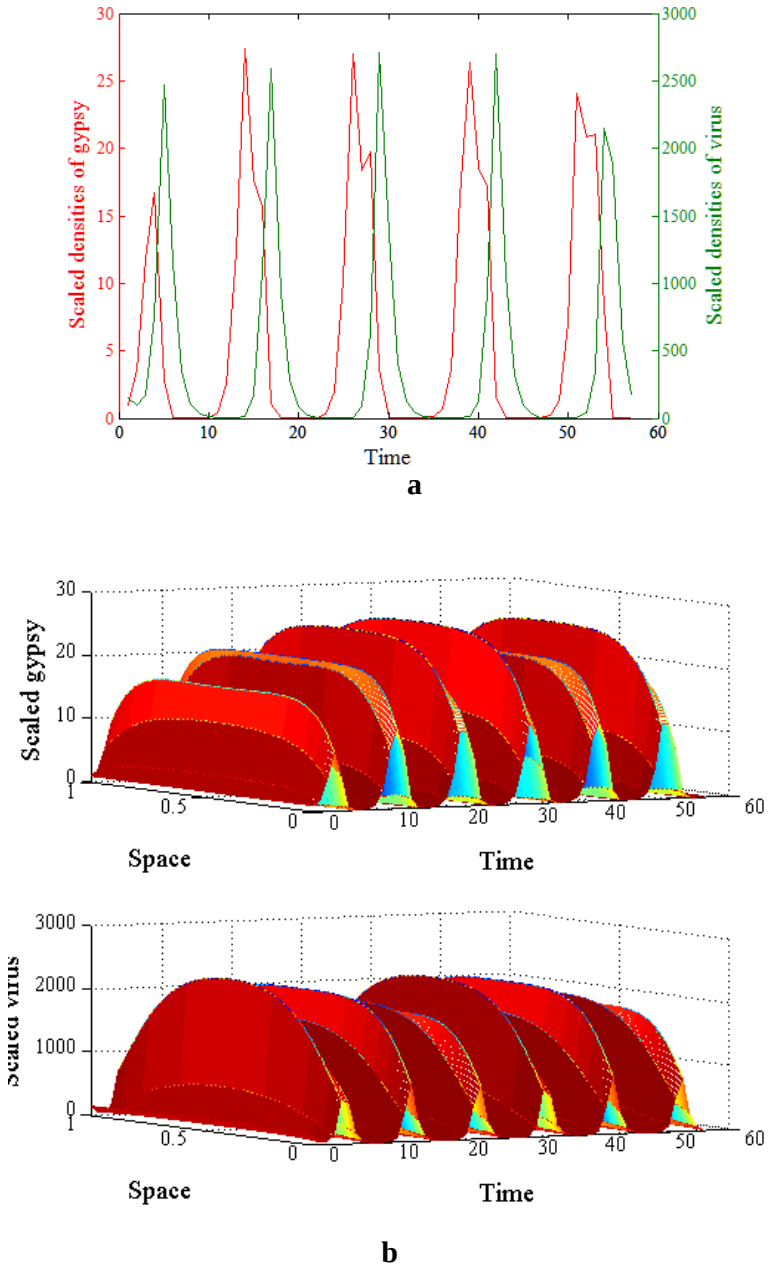

Figure 3.1: Population dynamics of gypsy moth and the virus. a. Non-spatial model. b. Integrodifference model. With parameters in Table 3.1

We use the Forward-Backward sweep numerical method to approximate optimal control solutions and corresponding state solutions. To find the optimal control we use an iterative process, using initial conditions for the states and final time conditions for the adjoints. Starting with the initial conditions of the state and a guess for the control, in our case half of the maximum control, we solve the state equations forward in time. Using these new values of the states, we solve the adjoint equations backwards. The adjoint values are used in the control characterization to calculate a new control value. The control is updated by taking a convex combination of the old value and the value calculated from the characterization. The new estimate of the states and the optimal control are compared with those from the previous iteration. We use a tolerance of 0.1% and when relative errors in the states and control are below the tolerance, the iteration stops [42]. The trapezoidal rule is used to get integral approximations. We found that our numerical simulations always converged in less than 30 iterations. We found no indications of any non-uniqueness in the optimal control calculations.

We will display the optimal control results in the following way. The left part (a) will present the results without control and the part right (b) the ones with control. For both (a) and (b), we present in the top the density of the control, followed by the density of gypsy moth and the density of the virus.

For the optimal control results, we start with constant initial conditions for both gypsy moth and the virus, with densities of 10 for both species. In Figure 3.2 we can observe two interesting results. First, the second peak of gypsy moth in Figure 3.2(b) is considerable smaller that the one in Figure 3.2(a). Second, our results suggest timing and intensity of the optimal control. In the top graph of Figure 3.2(b) we observe the control should be applied at the beginning. We also should have a peak of the control around year six, which is when both the virus and gypsy moth are at low densities. Controlling gypsy moth at those times, does not eliminate the outbreak but the densities at the outbreak are considerable lower.

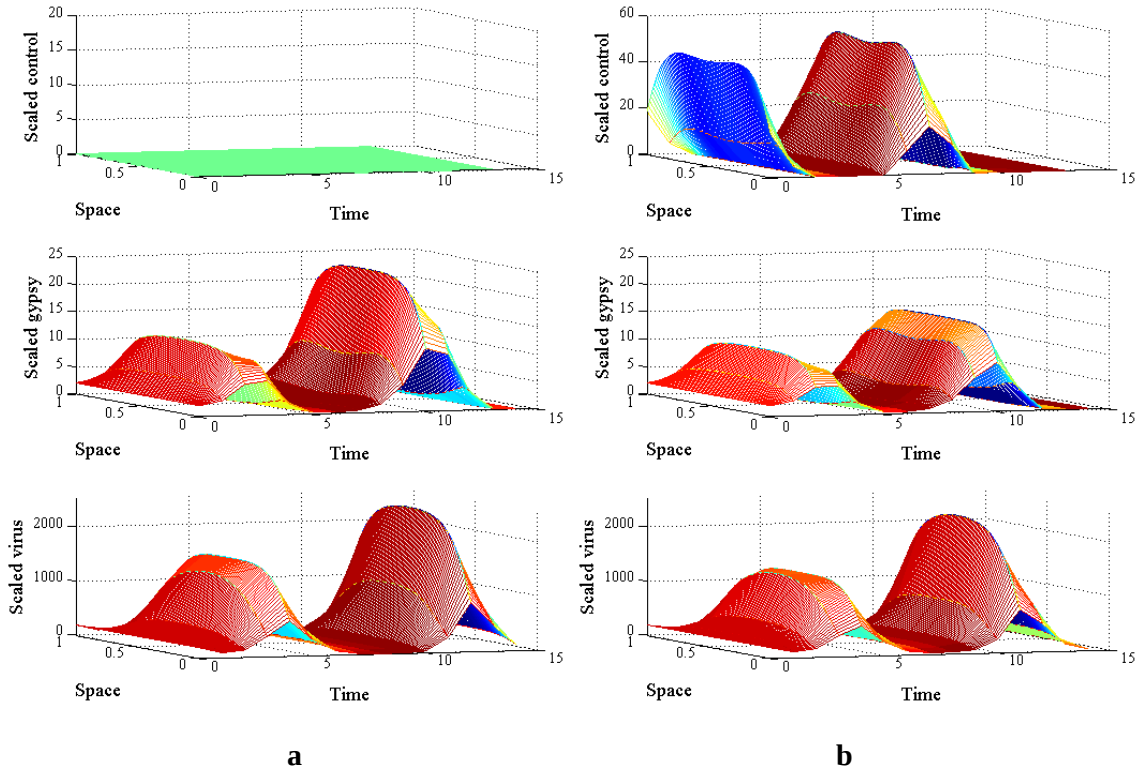

Figure 3.2: a. No control. b. With Control. $A = B = C = 1$, with other parameters in Table 3.1

We explore the effects of changing spatial initial conditions, on the optimal control and the states. Previously the initial conditions were constant over time. Here we explore different spatial arrangements for the initial conditions of both gypsy moth and the *Ld*MNPV virus. We investigate two types of initial conditions: aggregate ones (Figure 3.3) where gypsy moth and the *Ld*MNPV virus share the same space, and shifted conditions (Figure 3.4) where the two species are mostly in different locations. Most of the graphic output for different initial conditions is in the Appendix B.2

We start with the aggregate spatial conditions. Results for the three spatial initial conditions in Figure 3.3, are in Figure 3.5, Figure B.1, and Figure B.2. We present the results in the following way. In the left part (a) will present the results without control and part (b) the ones with control. For both (a) and (b), we present in the top the density of the control, then the density of gypsy moth and last the density of the virus. Finally part (c) is a rotation of the control graph presented in part(b).

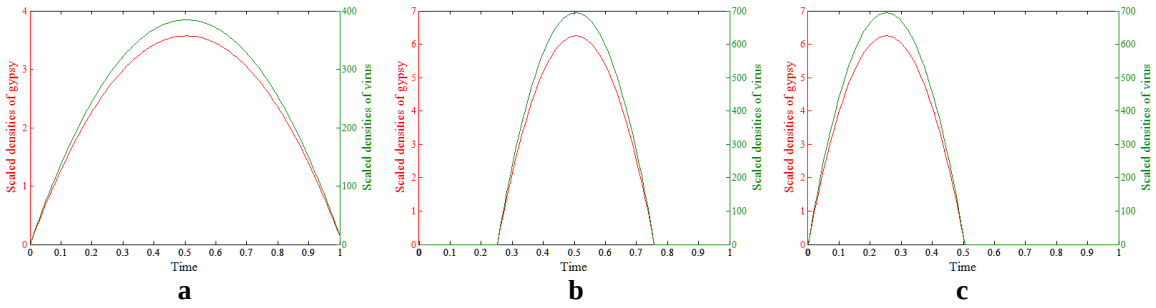

Figure 3.3: Aggregate spatial initial conditions

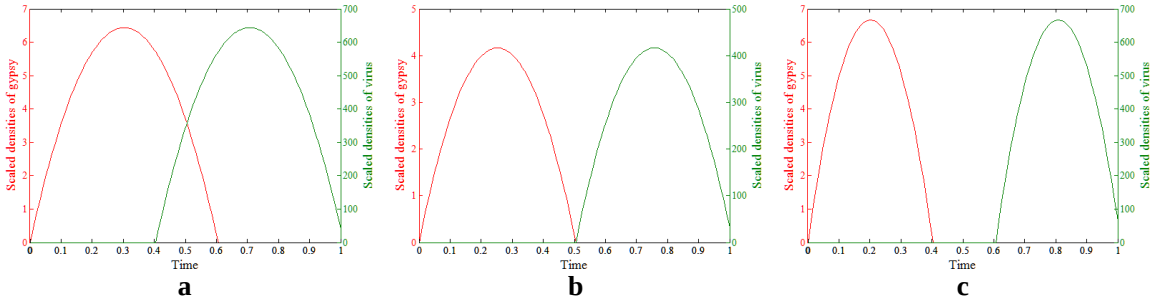

Figure 3.4: Shifted spatial initial conditions

First we investigate the dynamics of the system without control. As we can see in Figure 3.5(a), spatially varying initial conditions have an impact in the dynamics of the system. As expected where the density of the virus is higher, there will be a lower density of the gypsy moth. This creates the two peaks effect observed in the gypsy moth around year five in Figure 3.5(a).

When the initial conditions are aggregated in the center of the space, Figure 3.3(a) and (b), the effects of the initial conditions are transient and around year 10, the densities of gypsy moth and the virus become less heterogeneous through the space, and this can be observed in Figure 3.5(a) and Figure B.1(a). When the species are aggregated in the border of the space, as in Figure 3.3(c), the effects of the initial conditions last longer, Figure B.2(a), and one can still see some aggregation effect around year 14. Then we incorporate management into the population. In Figure 3.5(b), we observe that the spatially varying initial conditions cause the control to be larger in the region with less gypsy moth, which is consistent with our initial results with homogeneous initial conditions. As expected we also observe a decrease in the density of gypsy moth. These results are also shown in Figure B.1(b) and Figure B.2(b)

For the shifted spatial conditions, results for the three spatial initial conditions in Figure 3.4, are shown in Figure B.3, Figure B.4, and Figure B.5. The effects of shifted initial conditions on the dynamics without management are also transient. When initial conditions of the species do not share any space, Figure 3.4(b) and (c), around year 10 the densities are less heterogeneous through space, Figure B.4(a), Figure B.5(a). When species occupy partially the same space, Figure 3.4(a), the heterogeneity provide by the initial conditions lasts longer, as in Figure B.3(a). The optimal control for shifted initial conditions, also reflects the spatial arrangements of the corresponding initial conditions. We also need to apply more control where gypsy moth is at low densities. The managed density of gypsy moth is lower when compared to the non-management option; see Figure B.5(a), Figure B.3(a), and Figure B.4(a).

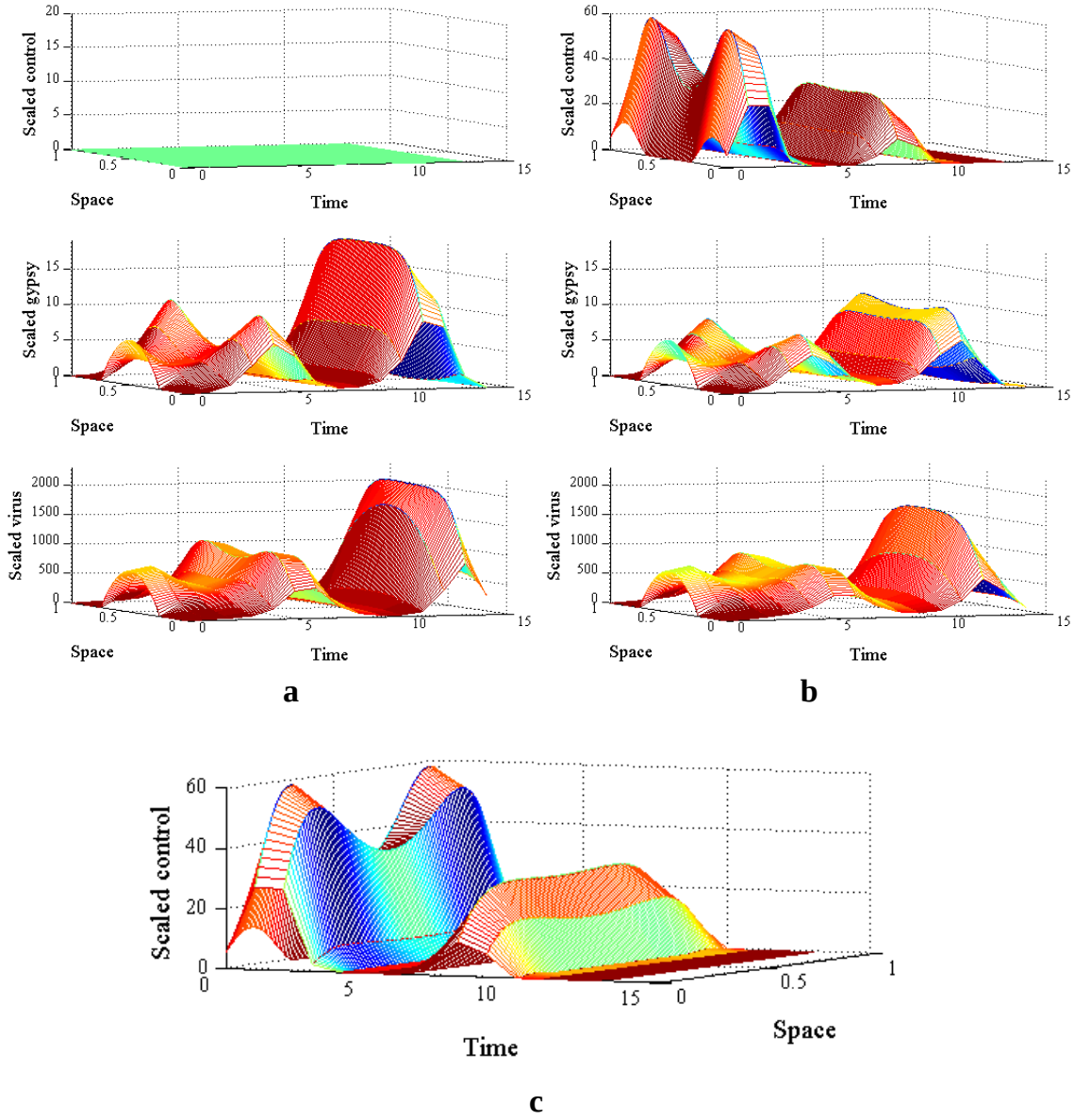

Figure 3.5: Effect of the optimal control over a period of 15 years with aggregate spatial initial conditions in Figure 3.3(b). a. Dynamics without control. b. Dynamics with control. c. Different view of the control display in b

3.7 Conclusions

Optimal control theory for integrodifference equations is a relatively new research area. Several applications of optimal control in a single species model have been developed. In this chapter, we present a new application of optimal control theory for a system of integrodifference equations. We formulated a two species coupled integrodifference system and its associated objective functional for the management of gypsy moth populations and its biological control agent. Using appropriate analysis and control techniques, we prove the existence of the optimal control for our system of integrodifference equations. We also developed the characterization of the optimal control and proved the existence of the sensitivity system and adjoint system. Finally we showed uniqueness of the optimal control, under a concavity assumption on the objective functional.

We apply the theory developed to the invasive pest gypsy moth. Our results suggest timing and intensity of the control. The optimal management strategy usually indicate applying the biocontrol agent when the gypsy moth densities are at a low level. Applying the control does not eliminate the outbreaks but reduces the density of gypsy moth at the outbreaks. This result is consistent over several different spatial initial conditions.

The theory developed in this chapter give important tools that can be easily extended to other integrodifference systems modeling a variety of populations. Other types of control actions can be incorporated.

Acknowledgments

This work was done in collaboration with Suzanne Lenhart, and K.A. Jane White (University of Bath, U.K).

Chapter 4

Conclusions and Future Extensions

This dissertation develops optimal control results to manage the invasive species gypsy moth. Using a host-pathogen model and a model that includes a generalist predator, we find that the optimal control should occur a year or two before the peaks of gypsy moth in the non-management scenario for both models. For the host-pathogen model, the control results hold for a variety of parameters. For the two models, the optimal control is highly sensitive to the initial conditions at the moment we start to implement the control. For the host-pathogen model, three general possible optimal control management options were presented based on the starting densities of gypsy moth. For the model with predation we illustrated two general control scenarios. For both models, when densities are high, control is required immediately. The optimal control for the model with predation needs fewer applications that in the host-pathogen model, which is expected since the predator helps to suppress the population of gypsy moth.

We also completed new work on optimal control for systems of integrodifference equations. We designed an objective functional to minimize the cost generated by the defoliation caused by the gypsy moth and the cost of controlling the population. Existence, characterization and uniqueness results for the optimal control and corresponding states have been developed. We used a forward-backward sweep numerical method, and our numerical results suggest spatial and temporal locations and intensity of optimal controls.

The models and theory developed in this dissertation could be extended in several ways, as discussed below.

4.1 Non-Spatial model

The discrete models used in Chapter 2 can be modified to incorporate other ecological features. A more realistic timing in the sources of mortality would be to use models that impose the mortality by the virus first and then allow predation [53, 32]. A second modification would be to change the functional response of the predator. Experimental studies show different results with respect to the intensity of predation when the density of gypsy moth increases [22, 65]. Therefore we can incorporate a different functional response, such as type III, that will allow for comparisons based on those responses. Another expansion would be a model that includes a simple discrete spatial structure, with two locations with gypsy moth populations. This would apply control to just one of the populations and allow emigration from the other one. Therefore the population not being controlled acts as a source for the other one, and creates a rescue effect.

Another avenue to investigate in future work is to add structured populations to the model. The structure could be given by stage (eggs, larva, pupae, adult) or by gender (male, female). The case of stage structure, is particularly important in the infection process, since the larval stage can have up to six instars, and each instar has a different susceptibility to the infection.

Currently we are investigating ways to change the model so that the gypsy moth population comes back at a somewhat higher level after the completion of control actions. This increase growth after management is indicated by field observations (Liebhold personal communication).

4.2 Spatial model

The theory developed in Chapter 3 can be used for implementing optimal control problems for many integrodifference systems. Although chapter 3 focus on two integrodifference equations, the theory is valid and easily extended for several equations.Chapter 3 results could assist in developing optimal control for integrodifference equations for a variety of applications ranging from dispersal of invasive species to dispersal of species as response to climate change.

In the particular case of the invasion of gypsy moth developed in Chapter 3, future work should include different functions for local dynamics, especially ones that include predation. One can modify the model to implement a different type of control, in particular pesticides like Bt. Finally in the spatial model, it may very important to include Allee effects and stochastic features, given that both affect low density founder populations.

Bibliography

[1] R.M. Anderson and R.M. May, *Regulation and stability of host-parasite population interactions: I. regulatory processes*, Journal of Animal Ecology **47** (1978), no. 1, 219 – 247. 4

[2] ———, *Infectious diseases and population cycles of forest insects*, Science **210** (1980), no. 4470, 658 – 661. 4

[3] ———, *The population dynamics of microparasites and their invertebrate hosts*, Philosophical Transactions of the Royal Society of London. Series B, Biological Sciences **291** (1981), no. 1054, 451 – 524. 4

[4] K. Barber, W. Kaupp, and S. Holmes, *Specificity testing of the nuclear polyhedrosis virus of the gypsy moth, lymantria dispar (l.)*, The Canadian Entomologist **125** (1993), 1055 – 1066. 54

[5] L. Berkovitz and N. Medhin, *Applied mathematics and nonlinear science : Nonlinear optimal control theory*, Chapman and Hall/CRC, Boca Raton, FL, USA, 2012. 5

[6] G. Bernon, J. Tardiff, R. Hansen, and J. Podgwaite, *Production of gypsy moth nuclear polyhedrosis virus (npv)*, Tech. Report General Technical Report NE-167, USDA-Forest Service, 1991. 54

[7] H. A . Bess, S. H. Spurr, and E.W. Littlefield, *Forest site conditions and the gypsy moth*, Harvard Forest Bulletin **22** (1947), 1 – 56. 41

[8] G. Blissard and G. Rohrmann, *Baculovirus diversity and molecular biology*, Annual Review of Entomology **35** (1990), 127 – 155. 14

[9] D.J. Borror, C.A. Triplehorn, and N.F. Johnson, *An introduction to the study of insects*, 6th edition ed., Saunders College Publishing, Fort Worth, TX, 1992. 15

[10] N.F. Britton, *Essential mathematical biology*, Springer-Verlag, 2003. 11, 53

[11] R. Campbell and J. Podgwaite, *The disease complex of the gypsy moth. i. major components*, Journal of Invertebrate Pathology **18** (1972), 101 – 107. 14

[12] R.W. Campbell and R.J. Sloan, *Natural regulation of innocuous gypsy moth populations.*, Environmental Entomology **6** (1977), 315 – 322. 41

[13] M.D. Canon, C.D. Cullum, and E. Polak, *Theory of optimal control and mathematical programming*, McGraw-Hill, New York, 1970. 104

[14] C. Doane, *Primary pathogens and their role in the development of an epizootic in the gypsy moth*, Journal of Invertebrate Pathology **15** (1970), 21 – 23. 14

[15] C. Doane and M. McManus, *The gypsy moth: Research toward integrated pest management*, Technical Bulletin 1584, Washington, DC: U.S. Department of Agriculture, 2007. 2, 14

[16] G. Dwyer, J. Dushoff, J. S Elkinton, and S.A Levin, *Pathogen-driven outbreaks in forest defoliators revisited: Building models from experimental data*, The American Naturalist **156** (2000), no. 2, 105 – 120. 4, 16, 19, 20, 29, 44

[17] G. Dwyer, J. Dushoff, and S. Yee, *The combined effects of pathogens and predators on insect outbreaks*, Nature **430** (2004), 341 – 345. 4, 16, 19, 20, 24, 29, 41, 42, 44, 46

[18] G. Dwyer and J.S. Elkinton, *Using simple models to predict virus epizootics in gypsy moth populations*, Journal of Animal Ecology **62** (1993), no. 1, 1 – 11. 4

[19] B.D. Elderd, J. Dushoff, and G. Dwyer, *Host-pathogen interactions, insect outbreaks, and natural selection for disease resistance*, American Naturalist **172** (2008), no. 6, 829 – 842. 4

[20] J. Elkinton and A. Liebhold, *Population dynamics of gypsy moth in north america*, Annual Review of Entomology **35** (1990), 571 – 596. 14, 41, 52

[21] J.S. Elkinton, W. M. Healy, J.P. Buonaccorsi, G. H. Boettner, A.M. Hazzard, H.R. Smith, and A. M Liebhold, *Interactions among gypsy moths, white-footed mice, and acorns*, Ecology **77** (1996), 2332 – 2342. 41

[22] J.S. Elkinton, A.M. Liebhold, and R. Muzika, *Effects of alternative prey on predation by small mammals on gypsy moth pupae*, Population Ecology **46** (2004), 171 – 178. 89

[23] W. Fleming and R. Rishel, *Deterministic and stochastic optimal control*, Springer-Verlag, New York, 1975. 5

[24] M. A. Foster, J. C Schultz, and M. D. Hunter, *Modelling gypsy moth–virus–leaf chemistry interactions: Implications of plant quality for pest and pathogen dynamics*, Journal of Animal Ecology **61** (1992), 509 – 520. 4, 80

[25] E. Fuller, B.D. Elderd, and G. Dwyer, *Pathogen persistence in the environment and insect-baculovirus interactions: disease-density thresholds, epidemic burnout, and insect outbreaks*, American Naturalist **179** (2012), no. 3, E70 – E96. 4

[26] H. Gaff, H. R. Joshi, and S. Lenhart, *Optimal harvesting during an invasion of a sublethal plant pathogen*, Environment and development economics **12** (2007), no. 5, 673 – 686. 11, 53

[27] G. Gale, J. Dececco, M. Marshall, W. Mcclain, and R. Cooper, *Effects of gypsy moth defoliation on forest birds: an assessment using breeding bird census data*, Journal of Field Ornithology **72** (2001), no. 2, 291 304. 2

[28] T. Glare, E. Newby, and T. Nelson, *Safety testing of a nuclear polyhedrosis virus for use against gypsy moth, lymantria dispar, in new zealand.*, Proceedings of the Forty-Eighth New Zealand Plant Protection Congress **August** (1995), 264 – 269. 54

[29] J.R. Gould, J.S. Elkinton, and W. E. Wallner, *Density-dependent suppression of experimentally created gypsy moth lymantria dispar (lepidoptera: Lymantriidae) populations by natural enemies*, Journal of Animal Ecology **50** (1990), 213 – 233. 41

[30] A. Hajek and P. Tobin, *Micro-managing arthropod invasions: eradication and control of invasive arthropods with microbes*, Biological Invasions **12** (2010), 2895 – 2912. 15

[31] A. Hastings, K. Cuddington, K.F. Davies, C.J. Dugaw, S. Elmendorf, A. Freestone, S. Harrison, M. Holland, J. Lambrinos, U. Malvadkar, B.A. Melbourne, K. Moore, C. Taylor, and D. Thomson, *The spatial spread of invasions: new developments in theory and evidence*, Ecology Letters **1** (2005), 91–101. 11, 53

[32] K. J. Haynes, A.M. Liebhold, and D.M. Johnson, *Elevational gradient in the cyclicity of a forest-defoliating insect*, Population Ecology **54** (2012), 239 – 250. 4, 89

[33] The MathWorks Inc, *Global optimization toolbox users guide*, revised for version 6.3 (release 2013a) ed., March 2013. 20, 21, 22, 23, 45, 46

[34] ———, *Optimization toolbox users guide*, revised for version 6.3 (release 2013a) ed., March 2013. x, 21, 22

[35] C.G. Jones, R.S. Ostfeld, M. P. Richard, E. M. Schauber, and J.O. Wolff, *Chain reactions linking acorns to gypsy moth outbreaks and lyme disease risk*, Science **279** (1998), 1023 – 1026. 41

[36] H. R. Joshi, S. Lenhart, and H. Gaff, *Optimal harvesting in an integrodifference population model*, Optimal Control Appl. Methods **27** (2006), no. 2, 61 – 75. 11, 53

[37] H. R. Joshi, S. Lenhart, H. Lou, and H. Gaff, *Harvesting control in an integrodifference population model with concave growth term*, Nonlinear Analysis: Hybrid Systems **1** (2007), no. 3, 417 – 429. 11, 53

[38] M. Kot, *Discrete-time traveling waves: Ecological examples*, Journal of Mathematical Biology **30** (1992), no. 4, 413–436. 11, 53

[39] M. Kot, M.A. Lewis, and P. van den Driessche, *Dispersal data and the spread of invading organisms*, Ecology **77** (1996), 2027–2042. 11, 53

[40] M. Kot and W.M. Schaffer, *Discrete time growth dispersal models*, Mathematical Biosciences **80** (1986), 109–136. 11, 53

[41] S. Lenhart, E.N. Bodine, P. Zhong, and H. Joshi, *Illustrating optimal control applications with discrete and continuous features*, In: Advances in Applied Mathematics, Modeling, and Computational Science (R. Melnik and I. Kotsireas, eds.), Springer, Vol. 66 of Fields Institute Communications, 2013, pp. 209–238. 11, 53

[42] S. Lenhart and J. T. Workman, *Optimal control of biological models*, Chapman and Hall/CRC, New York, 2007. 5, 82

[43] S. Lenhart and P. Zhong, *Investigating the order of events in optimal control of integrodifference equations*, Systems Theory: Modeling, Analysis and Control Proceedings Volume (2009), no. Presses Universitaires de Perpignan, France, 89–100. 11, 53

[44] D. Leonard, *Recent developments in ecology and control of the gypsy moth*, Annual Review of Entomology **19** (1974), 197 – 229. 15

[45] ———, *Bioecology of the gypsy moth.*, The Gypsy Moth: Research toward Integrated Pest Management (C. Doane and M. McManus, eds.), USDA Forest Service Technical Bulletinl 1584, Washington, DC: U.S. Department of Agriculture, 1981, pp. 9 – 29. 15

[46] A. Liebhold, J. Elkinton, D. Williams, and R.M Muzika, *What causes outbreaks of the gypsy moth in north america?*, Population ecology **42** (2000), 257 – 266. 41, 52

[47] A. Liebhold, J. Halverson, and G. Elmes, *Quantitative analysis of the invasion of gypsy moth in north america*, Journal of Biogeography **19** (1992), no. 5, 513 – 520. 52

[48] J.M. Morales, P.R. Moorcroft, J. Matthiopoulos, J.L Frair, J.G. Kie, R.A. Powell, E.H. Merrill, and D.T. Haydon, *Building the bridge between animal movement and population dynamics*, Philosophical Transactions of the Royal Society B **365** (2010), 2289–2301. 11, 53

[49] J.D. Murray, *Mathematical biology i: An introduction*, Springer-Verlag, 2002. 11, 53

[50] M.G. Neubert, M. Kot, and M.A. Lewis, *Invasion speeds in fluctuating environments*, Proceedings of the Royal Society Biological Sciences Series B **267** (2000), 1603–1610. 53

[51] A.J. Nicholson and V.A. Bailey, *The balance of animal populations*, Proceedings of the Zoological Society of London **105** (1935), 551 – 598. 4, 56

[52] A. Okubo and S. Levin, *Diffusion and ecological problems, modern perspectives*, Springer, Boca Raton, 2002. 11, 53

[53] Bjrnstad O.N., C. Robinet, and A.M. Liebhold, *Geographic variation in north-american gypsy moth population cycles: sub-harmonics, generalist predators and spatial coupling*, Ecology **91** (2010), 106 – 118. 4, 89

[54] J. Peacock, D.F. Schweitzer, J.L. Carter, and N. R. Dubois, *Laboratory assessment of the effects of bacillus thuringiensis on native lepidoptera*, Environmental Entomology **27** (1998), 450 – 457. 15, 54

[55] D. Pimentel, R. Zuniga, and D. Morrison, *Update on the environmental and economic costs associated with alien-invasive species in the united states*, Ecological Economics **52** (2005), no. 3, 273 – 288. 1

[56] J. Podgwaite, *Gypchek production in vivo*, Tech. Report General Technical Report NE-167, USDA-Forest Service, 1991. 54

[57] ———, *Gypchek - biological insecticide for the gypsy moth*, Journal of Forestry **97** (1999), 16 – 19. 54

[58] J. Podgwaite, K. Shields, R. Zerillo, and R. Bruen, *Environmental persistence of the nucleopolyhedrosis virus of the gypsy moth*, Environmental Entomology **8** (1979), 523 – 536. 15

[59] L. Pontryagin, V. Boltyanskii, R. Gamkrelize, and E. Mishchenko, *The mathematical theory of optimal processes*, The Macmillan Company, New York, 1964. 5, 19

[60] R. Reardon, N. Dubois, and W. McLane, *Bacillus thuringiensis for managing gypsy moth: A review*, Tech. Report Tech Transfer FHM-NC-01-94, USDA Forest Service, 1994. 15, 18

[61] R. Reardon, J. Podgwaite, and R. Zerillo, *Gypchek-the gypsy moth nucleopolyhedrosis virus product*, Tech. Report Tech Transfer FHTET-96-16, USDA Forest Service, 1996. 15, 19, 24, 54

[62] ———, *Gypchek - bioinsecticide for the gypsy moth*, Tech. Report FHTET-2009-01, USDA Forest Service, 2009. 54

[63] J. Reilly and A. Hajek, *Density-dependent resistance of the gypsy moth lymantria dispar to its nucleopolyhedrovirus, and the consequences for population dynamics*, Oecologia **154** (2008), 691 – 701. 15

[64] L.M. Rios and N.V. Sahinidis, *Derivative-free optimization: a review of algorithms and comparison of software implementations*, Journal of Global Optimization (2012), 1–47. 20

[65] E.M. Schauber, R.S. Ostfeld, and C.G. Jones, *Type 3 functional response of mice to gypsy moth pupae: is it stabilizing?*, Oikos **107** (2004), 592 – 531. 89

[66] E. Schnepf, N. Crickmore, J. Van Rie, D. Lereclus, J. Baum, J. Feitelson, D. Zeigler, and D. Dean, *Bacillus thuringiensis and its pesticidal crystal proteins*, Microbiology and Molecular Biology Reviews **62** (1998), 775 – 806. 15

[67] M. Shapiro, H.K. Preisler, and J.L. Robertson, *Enhancement of baculovirus activity on gypsy moth (lepidoptera: Lymantriidae) by chitinase*, Journal of Economic Entomology **80** (1987), 1113 – 1116. 80

[68] A. A. Sharov, D. Leonard, A. M. Liebhold, and N.S. Clemens, *Evaluation of preventive treatments in low-density gypsy moth populations using pheromone traps*, Journal of economic entomology **95** (2002), no. 6, 1205 – 1215. 1

[69] A. A. Sharov, D. Leonard, A. M. Liebhold, E. A. Roberts, and W. Dickerson, *"Slow the Spread": A national program to contain the gypsy moth*, Journal of forestry **100** (2002), no. 5, 30 – 35. 1, 2

[70] N. Shigesada and K. Kawasaki, *Biological invasions: Theory and practice*, Oxford University Press, 1997. 11, 53

[71] J.B. Skellam, *Random dispersal in theoretical populations*, Biometrika **38** (1951), 196–218. 11, 52

[72] H.R. Smith, *Wildlife and the gypsy moth*, Wildlife Society Bulletin **13** (1985), 166 – 174. 41

[73] L. Solter and A. Hajek, *Control of gypsy moth, lymantria dispar, in north america since 1878*, Use of microbes for control and eradication of invasive arthropods (A. Hajek, T. Glare, and M. OCallaghan, eds.), Springer, Dordrecht, The Netherlands, 2009, pp. 181 – 212. 15

[74] J. Strazanac and L. Butler, *Long-term evaluation of the effects of btk, gypchek, and entomophaga maimaiga on nontarget organisms in mixed broadleaf-pine forests in the central appalachians*, Tech. Report FHTET-2004-14., USDA-Forest Service, 2005. 54

[75] D. Thurber, W. Mcclain, and R. Whitmore, *Indirect effects of gypsy moth defoliation on nest predation*, Journal of Wildlife Management **58** (1994), no. 3, 493 500. 2

[76] P. Tobin, *Cost analysis and biological ramifications for implementing the gypsy moth slow the spread program*, Tech. Report NRS-37, USDA Forest Service, Northern Research Station, 2008. 19, 24

[77] P. Tobin and L. Blackburn, *Slow the spread: a national program to manage the gypsy moth*, Tech. Report NRS-6, USDA Forest Service, Northern Research Station, 2007. x, 1, 3, 14, 52

[78] P. Tobin and A. Liebhold, *Gypsy moth*, In: Encyclopedia of Biological Invasions (D. Simberloff and M. Rejmanek, eds.), University of California Press, 2011, pp. 298 – 304. 1, 2, 3, 14, 15, 18, 52

[79] Office of Technology Assessment U.S. Congress, *Harmful non-indigenous species in the united states*, Tech. Report OTA-F-565, U.S. Congress, Office of Technology Assessment, 1993. 1

[80] Forest Service. USDA, *Gypsy moth management in the united states: a cooperative approach. final environmental impact statement vol. 1-5*, Tech. Report NA-MR-01-08, USDA-Forest Service and Animal and Plant Health Inspection Service, 2008. 54

[81] R.W. VanKirk and M.A. Lewis, *Integrodifference models for persistence in fragmented habitats*, Bulletin of Mathematical Biology **59** (1997), no. 1, 107–137. 11, 53

[82] L. Volkman, *Nucleopolyhedrosis virus interactionswith their insect host*, Advances in Virus Research **48** (1997), 313 – 348. 14, 15

[83] D.L. Wagner, J.W. Peacock, J.L. Carter, and S.E. Talley, *Field assessment of bacillus thuringiensis on nontarget lepidoptera*, Environmental Entomology **25** (1996), 1444 – 1454. 15, 54

[84] M.H. Wang and M. Kot, *Speeds of invasion in a model with strong or weak allee effects*, Mathematical Biosciences **171** (2001), no. 1, 83–97. 53

[85] A. Whittle, *Gypsy Moth modelling with and application of Optimal Control Theory*, Ph.D. thesis, University of Bath, UK, May 2004. 5, 53

[86] A. Whittle, S. Lenhart, and K.A. White, *Optimal control of gypsy moth populations*, Bulletin of Mathematical Biology **70** (2008), no. 2, 398 – 411. 4, 5, 80

[87] M. Williamson, *Biological invasions*, Chapman and Hall, 1996. 1

[88] S. Woods and J. Elkinton, *Bimodal patterns of mortality from nuclear polyhedrosis virus in gypsy moth populations*, Journal of Invertebrate Pathology **50** (1987), 151 – 157. 15

[89] P. Zhong and S. Lenhart, *Optimal control of integrodifference equations with growth-harvesting-dispersal order*, Discrete and Continuous Dynamical Systems - Series B **17** (2012), 2281 – 2298. 11, 53

Appendices

Appendix A

A.1 Pontryagin's Maximum Principle approach

To make the expressions simpler we define $I_k = I\left(N_k\left(1-u_k\right), Z_k\right)$, $q = \frac{1}{C^2}$, and $a = \frac{\overline{v}}{\mu q}$. Therefore our system (2.1), is written as

$$\begin{aligned} 1 - I_k &= \left\{1 + a\left[N_k\left(1-u_k\right) I_k + \rho Z_k\right]\right\}^{-q} \\ N_{k+1} &= \gamma N_k\left(1-u_k\right)\left[1 - I_k\right] \\ Z_{k+1} &= f N_k\left(1-u_k\right) I_k. \end{aligned} \tag{A.1}$$

We form the Hamiltonian,

$$\begin{aligned} H_k =& e^{-\delta k}\left[A N_k + B\log(1-u_k)\right] \\ &+ \lambda_{N_{k+1}} \gamma N_k (1-u_k)(1-I_k) + \lambda_{Z_{k+1}} f N_k (1-u_k) I_k, \end{aligned} \tag{A.2}$$

with adjoint functions satisfying these backward difference equations:

$$\begin{aligned}
\lambda_{N_k} &= \frac{\partial H_k}{\partial N_k} \\
&= e^{-\delta k}A + \lambda_{N_{k+1}}\gamma(1-u_k)\left[1-\left(I_k + N_k I_k^{N'}\right)\right] + \lambda_{Z_{k+1}} f(1-u_k)\left(I_k + N_k I_k^{N'}\right) \\
\lambda_{Z_k} &= \frac{\partial H_k}{\partial Z_k} \\
&= -\lambda_{N_{k+1}}\gamma N_k(1-u_k)I_k^{Z'} + \lambda_{Z_{k+1}} f N_k(1-u_k)I_k^{Z'} \\
&= N_k(1-u_k)\left[-\lambda_{N_{k+1}}\gamma + \lambda_{Z_{k+1}} f\right] I_k^{Z'} \\
\lambda_{N_T} &= 0 \text{ and } \lambda_{Z_T} = 0
\end{aligned} \tag{A.3}$$

and

$$\begin{aligned}
I_k^{N'} &= \frac{\partial I_k}{\partial N_k} \\
&= \frac{qa(1-u_k)I_k\left\{1+a\left[N_k(1-u_k)I_k+\rho Z_k\right]\right\}^{-q-1}}{1-qa(1-u_k)N_k\left\{1+a\left[N_k(1-u_k)I_k+\rho Z_k\right]\right\}^{-q-1}} \\
I_k^{Z'} &= \frac{\partial I_k}{\partial Z_k} \\
&= \frac{qa\left\{1+a\left[N_k(1-u_k)I_k+\rho Z_k\right]\right\}^{-q-1}\rho}{1-qa\left\{1+a\left[N_k(1-u_k)I_k+\rho Z_k\right]\right\}^{-q-1}N_k(1-u_k)}.
\end{aligned} \tag{A.4}$$

The Hamiltonian differentiated with respect to the control gives

$$\begin{aligned}
\frac{\partial H_k}{\partial u_k} =& \frac{e^{-\delta k}B}{u_k - 1} + \lambda_{N_{k+1}}\gamma N_k\left[I_k - 1 - I_k^{u'}(1-u_k)\right] \\
&+ \lambda_{Z_{k+1}} f N_k\left[I_k^{u'}(1-u_k) - I_k\right]
\end{aligned} \tag{A.5}$$

where

$$\begin{aligned}
I_k^{u'} &= \frac{\partial I_k}{\partial u_k} \\
&= \frac{-qaN_k\left\{1+a\left[N_k(1-u_k)I_k+\rho Z_k\right]\right\}^{-q-1}I_k}{1-qaN_k\left\{1+a\left[N_k(1-u_k)I_k+\rho Z_k\right]\right\}^{-q-1}(1-u_k)}.
\end{aligned} \tag{A.6}$$

If we assume that our objective functional is minimized with respect u, on the interior of the control set, we set $\frac{\partial H_k}{\partial u_k} = 0$, and obtain

$$\begin{aligned} 0 =& \frac{e^{-\delta k}B}{u_k - 1} + \lambda_{N_{k+1}}\gamma N_k\Big[I_k - 1 - I_k^{u'}(1-u_k)\Big] \\ &+ \lambda_{Z_{k+1}} f N_k\Big[I_k^{u'}(1-u_k) - I_k\Big]. \end{aligned} \tag{A.7}$$

We can not solve explicitly for the control, but we can get the following implicit equation:

$$u_k = 1 - \frac{e^{-\delta k}B}{\lambda_{N_{k+1}}\gamma N_k\Big[I_k - 1 - I_k^{u'}(1-u_k)\Big] + \lambda_{Z_{k+1}} f N_k\Big[I_k^{u'}(1-u_k) - I_k\Big]}. \tag{A.8}$$

In order to utilize Pontryagin's Maximum Principle, the Hamiltonian must satisfy the concavity condition if we are to decide whether a control achieves the maximum or the minimum. Since we are doing a minimization problem we need:

$$\frac{\partial^2 H_k}{\partial u_k^2} \geq 0 \text{ at } u^* \tag{A.9}$$

for all time steps k [13]. If we calculate the second derivative of the Hamiltonian with respect to the control, we obtain

$$\begin{aligned} \frac{\partial^2 H_k}{\partial u_k^2} =& -\frac{e^{-\delta k}B}{(u_k-1)^2} + \lambda_{N_{k+1}}\gamma N_k\Big[I_k^{u'} - I_k^{u''} + I_k^{u''}u_k + I_k^{u'}\Big] \\ &+ \lambda_{Z_{k+1}} f N_k\Big[I_k^{u''} - I_k^{u''}u_k - I_k^{u'} - I_k^{u'}\Big] \\ =& \frac{-e^{-\delta k}B}{(u_k-1)^2} + \lambda_{N_{k+1}}\gamma N_k(-1)\Big[-2I_k^{u'} + I_k^{u''}(1-u_k)\Big] \\ &+ \lambda_{Z_{k+1}} f N_k\Big[I_k^{u''}(1-u_k) - 2I_k^{u'}\Big] \\ =& \frac{-e^{-\delta k}B}{(u_k-1)^2} + \lambda_{N_{k+1}}\gamma N_k(-1)\Big[I_k^{u''}(1-u_k) - 2I_k^{u'}\Big] \\ &+ \lambda_{Z_{k+1}} f N_k\Big[I_k^{u''}(1-u_k) - 2I_k^{u'}\Big] \\ =& \frac{-e^{-\delta k}B}{(u_k-1)^2} + N_k\Big[I_k^{u''}(1-u_k) - 2I_k^{u'}\Big]\Big[\lambda_{N_{k+1}}\gamma(-1) + \lambda_{Z_{k+1}} f\Big] \\ =& \frac{-e^{-\delta k}B}{(u_k-1)^2} + N_k\Big[I_k^{u''}(1-u_k) - 2I_k^{u'}\Big]\Big[\lambda_{Z_{k+1}} f - \lambda_{N_{k+1}}\gamma\Big] \end{aligned} \tag{A.10}$$

where

$$
\begin{aligned}
I_k^{u'} =& \frac{\partial I_k}{\partial u_k} \\
=& \frac{-qaN_k \left\{1 + a\left[N_k(1-u_k)I_k + \rho Z_k\right]\right\}^{-q-1} I_k}{1 - qaN_k \left\{1 + a\left[N_k(1-u_k)I_k + \rho Z_k\right]\right\}^{-q-1}(1-u_k)} \\
I_k^{u''} =& \frac{\partial^2 H_k}{\partial u_k^2} \\
=& \frac{qaN_k \Big\{1 + a\left[N_k(1-u_k)I_k + \rho Z_k\right]\Big\}^{-q-1}}{1 - qaN_k \Big\{1 + a\left[N_k(1-u_k)I_k + \rho Z_k\right]\Big\}^{-q-1}(1-u_k)} \\
& * \left\{(-q-1)\Big\{1 + a\left[N_k(1-u_k)I_k + \rho Z_k\right]\Big\}^{-1} aN_k \left[I_k^{u'}(1-u_k) - I_k\right]^2 - 2I_k^{u'}\right\}.
\end{aligned}
\tag{A.11}
$$

Since we can not guarantee that

$$
\frac{\partial^2 H_k}{\partial u_k^2} \geq 0 \tag{A.12}
$$

for all parameter sets, we will not utilize Pontryagin's Maximum Principle for this problem. Therefore we are going to use direct optimization methods to solve this particular optimal control problem.

A.2 Dynamics for the host-pathogen model

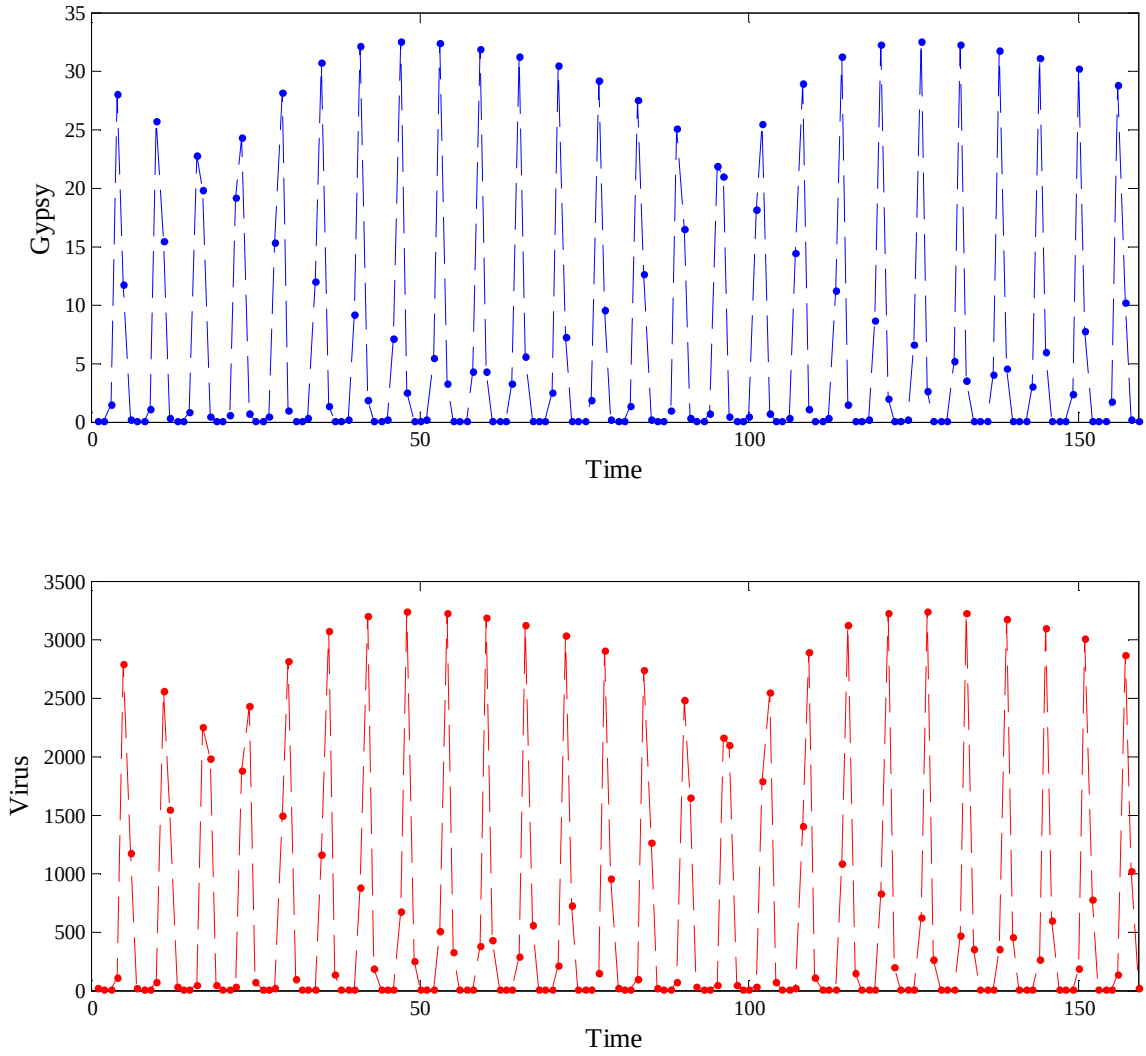

Figure A.1: Gypsy moth and virus population from host-pathogen model. With long-period, large-amplitude cycles in the densities.

A.3 Optimal control results for smaller times

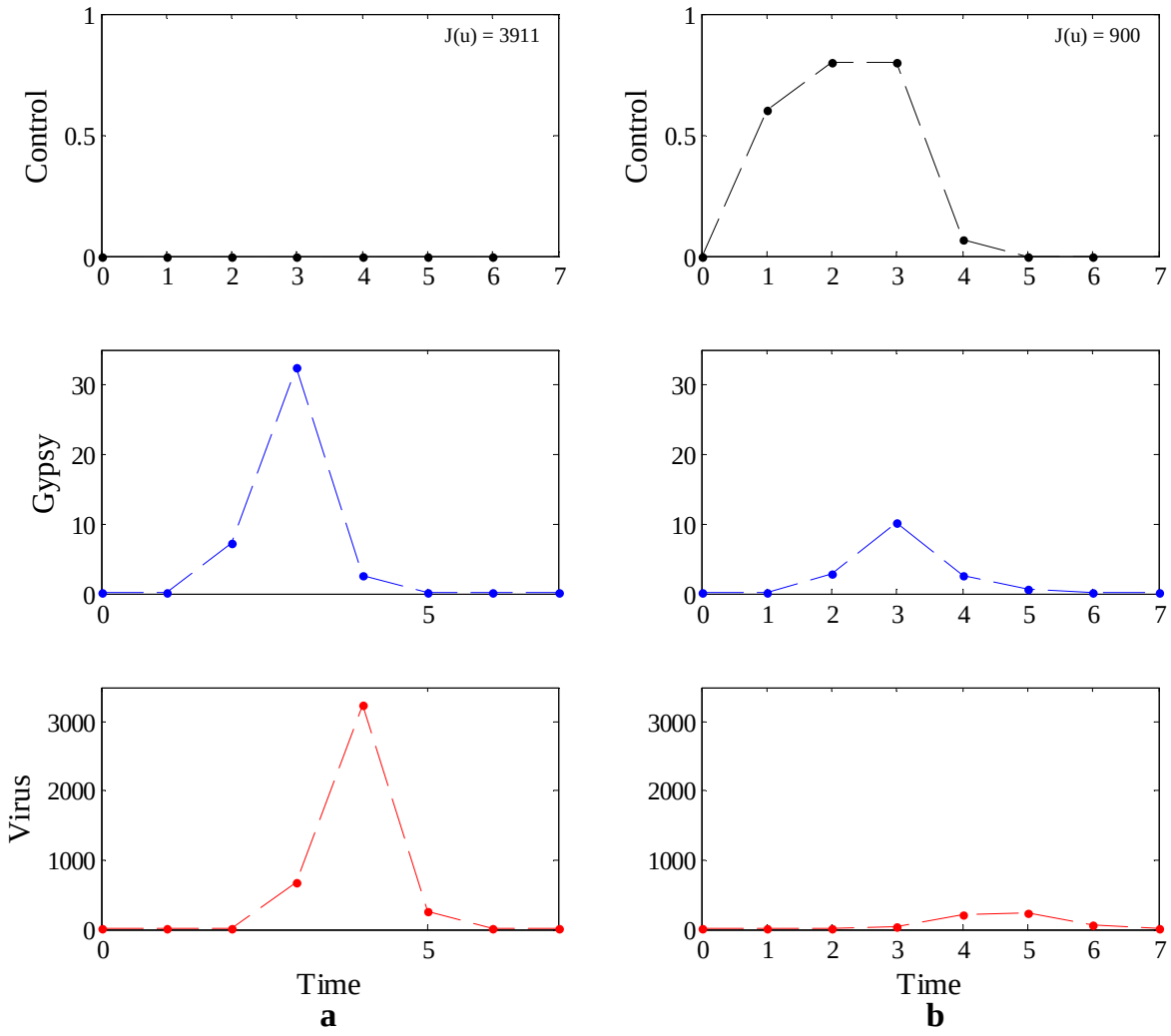

Figure A.2: Comparison of populations and objective functional values for a shorter time period of 7 years, without control(a) and with control(b), with parameters in Table 2.1

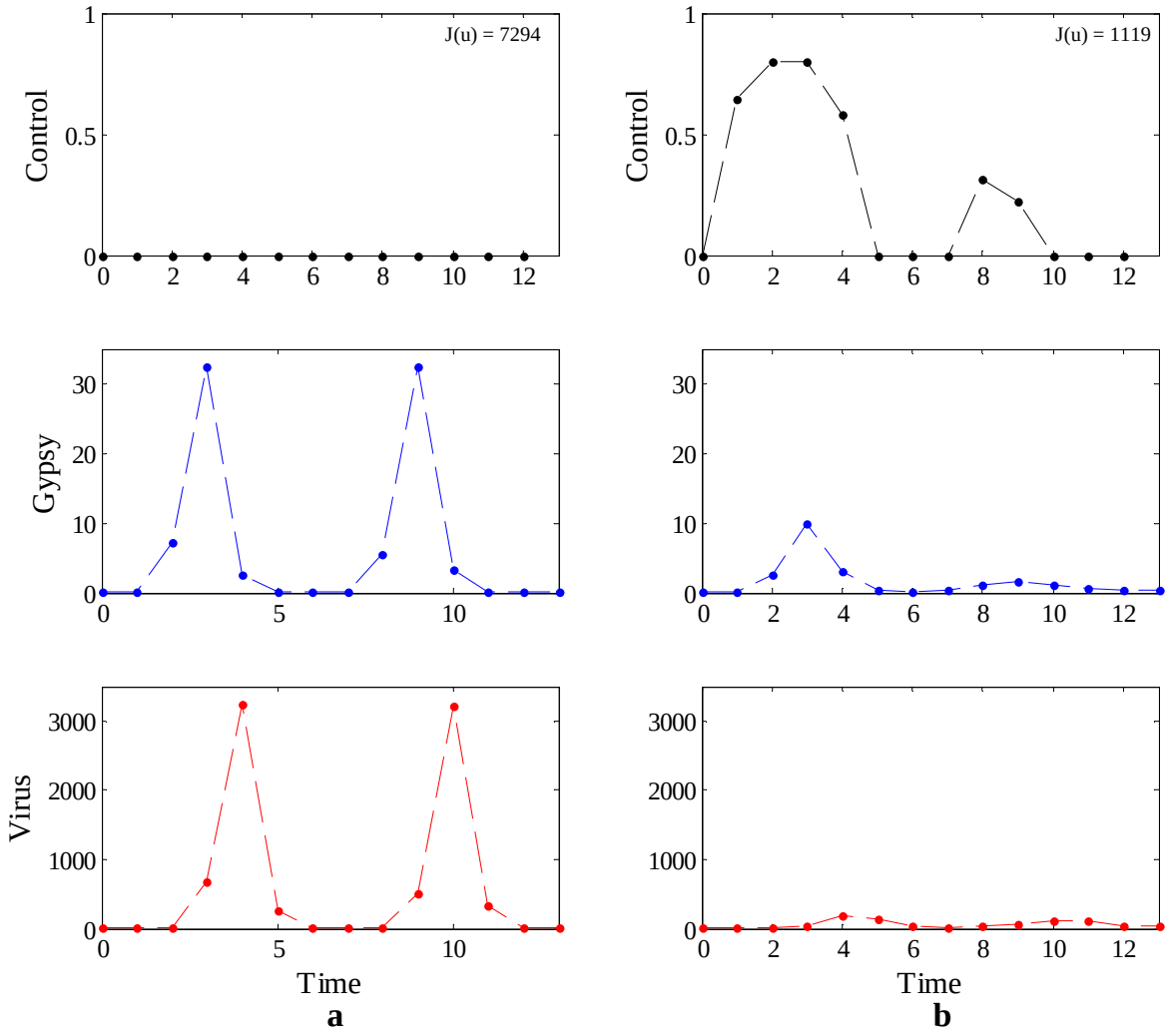

Figure A.3: Comparison of populations and objective functional values for a shorter time period of 13 years, without control(a) and with control(b), with parameters in Table 2.1

A.4 Variation of Parameters in the host-pathogen model

Table A.1: Effect of Variation of A on the optimal control. Empty space means a value of zero for the control, rows highlighted are in Figure 2.6(b).

A	Control																				OF
	1	2	3	4	5	6	7	8	9	10	11	12	13	14	15	16	17	18	19	20	
0.1																					10
0.5																					51
1			0.48	0.07																	102
3			0.8	0.71																	181
6		0.05	0.8	0.8					0.02												265
9		0.15	0.8	0.8					0.24												343
10		0.19	0.8	0.8					0.26	0.07											368
20		0.39	0.8	0.8					0.24	0.47											606
30		0.52	0.8	0.8	0.27				0.3	0.49											834
40		0.6	0.8	0.8	0.45				0.35	0.46											1055
50		0.64	0.8	0.8	0.54				0.38	0.45											1273
60		0.66	0.8	0.8	0.59				0.4	0.44											1489
70		0.68	0.8	0.8	0.62				0.41	0.43											1705
80		0.69	0.8	0.8	0.64				0.43	0.42	0.05							0.02	0.08		1919
90		0.7	0.8	0.8	0.65				0.45	0.42	0.1							0.19	0.25		2133
100		0.7	0.8	0.8	0.65				0.46	0.42	0.14							0.31	0.37		2345
200		0.73	0.8	0.8	0.68				0.54	0.44	0.26						0.39	0.77	0.8		4424
300		0.73	0.8	0.8	0.69				0.56	0.42	0.27					0.05	0.45	0.8	0.8		6478
400		0.74	0.8	0.8	0.7				0.58	0.43	0.27	0.05				0.07	0.47	0.8	0.8		8530
500		0.74	0.8	0.8	0.7				0.58	0.43	0.27	0.08				0.07	0.48	0.8	0.8		10581
600		0.74	0.8	0.8	0.7			0.01	0.59	0.43	0.28	0.1				0.08	0.49	0.8	0.8		12632
900		0.74	0.8	0.8	0.72			0.09	0.59	0.45	0.29	0.14				0.08	0.5	0.8	0.8		18782
1000		0.74	0.8	0.8	0.72			0.11	0.6	0.45	0.29	0.15				0.08	0.5	0.8	0.8		20832
3000		0.74	0.8	0.8	0.74			0.24	0.63	0.53	0.43	0.34	0.27	0.22	0.22	0.26	0.58	0.8	0.8		61779
6000		0.75	0.8	0.8	0.74			0.28	0.64	0.56	0.48	0.41	0.35	0.31	0.3	0.32	0.61	0.8	0.8		123154
9000		0.75	0.8	0.8	0.75			0.29	0.64	0.57	0.49	0.43	0.37	0.33	0.32	0.33	0.62	0.8	0.8		184520
10000		0.75	0.8	0.8	0.75			0.29	0.64	0.57	0.5	0.43	0.37	0.34	0.32	0.34	0.62	0.8	0.8		204975

Table A.2: Effect of Variation of δ on the optimal control. Empty space means a value of zero for the control, rows highlighted are in Figure 2.7(b).

Delta	Control																				OF
	1	2	3	4	5	6	7	8	9	10	11	12	13	14	15	16	17	18	19	20	
0.001		0.63	0.8	0.8	0.55				0.39	0.43											1447
0.002		0.63	0.8	0.8	0.54				0.39	0.43											1437
0.003		0.63	0.8	0.8	0.54				0.39	0.43											1427
0.01		0.64	0.8	0.8	0.54				0.38	0.44											1360
0.02		0.64	0.8	0.8	0.54				0.38	0.45											1273
0.03		0.64	0.8	0.8	0.54				0.37	0.46											1193
0.1		0.67	0.8	0.8	0.52				0.33	0.5											796
0.2		0.7	0.8	0.8	0.47				0.29	0.55	0.06										489
0.3		0.73	0.8	0.8	0.41				0.25	0.59	0.12										318

Table A.3: Effect of Variation of γ on the optimal control.. Empty space means a value of zero for the control, rows highlighted are in Figure 2.9(b).

Gamma	Control																				OF
	1	2	3	4	5	6	7	8	9	10	11	12	13	14	15	16	17	18	19	20	
5				0.56	0.8	0.65															224
10			0.38	0.8	0.8	0.51															305
15			0.4	0.8	0.8	0.66															372
20			0.5	0.8	0.8	0.66					0.25										450
25		0.35	0.8	0.8	0.66					0.33											530
30		0.53	0.8	0.8	0.64					0.4											613
35		0.58	0.8	0.8	0.62					0.45											690
40		0.56	0.8	0.8	0.61				0.1	0.46											764
45		0.61	0.8	0.8	0.6				0.18	0.46											843
50		0.58	0.8	0.8	0.6				0.24	0.45											915
55		0.6	0.8	0.8	0.59				0.28	0.45											991
60		0.56	0.8	0.8	0.57				0.31	0.45											1057
65		0.59	0.8	0.8	0.56				0.34	0.45											1133
70		0.6	0.8	0.8	0.55				0.36	0.45											1202
74.6		0.64	0.8	0.8	0.54				0.38	0.45											1273
75		0.65	0.8	0.8	0.54				0.38	0.45											1280
80		0.65	0.8	0.8	0.53				0.39	0.44											1342
85		0.67	0.8	0.8	0.52				0.4	0.44											1407
90		0.65	0.8	0.8	0.5				0.4	0.43											1453
95		0.19	0.8	0.8	0.48				0.38	0.41											1441
100		0.65	0.8	0.8	0.48				0.4	0.42											1557
105		0.71	0.8	0.8	0.47				0.41	0.42											1628
110		0.8	0.8	0.8	0.31				0.43	0.43											1751
115		0.8	0.8	0.8	0.01				0.43	0.42	0.01										1853
120			0.8	0.8	0.8				0.01	0.5	0.24										1878
125			0.8	0.8	0.8				0.33	0.41	0.03							0.03	0.1		1925
130			0.8	0.8	0.6				0.46	0.42	0.07							0.09	0.16		1957
135			0.8	0.8	0.58				0.48	0.42	0.09							0.14	0.21		2034
140			0.8	0.8	0.6				0.49	0.43	0.11							0.19	0.25		2114
145			0.8	0.8	0.58				0.5	0.43	0.13							0.23	0.3		2190
150			0.8	0.8	0.62				0.5	0.43	0.15							0.27	0.33		2272

Table A.4: Effect of Variation of ϕ on the optimal control. Empty space means a value of zero for the control, rows highlighted are in Figure 2.10.

Phi	Control																				OF
	1	2	3	4	5	6	7	8	9	10	11	12	13	14	15	16	17	18	19	20	
5																	0.46	0.8	0.8		7898
10																	0.44	0.8	0.8		4325
15			0.25	0.09													0.41	0.8	0.8		3017
20			0.52	0.38	0.2												0.4	0.8	0.8		2386
25			0.71	0.5	0.32	0.04											0.37	0.75	0.8		2072
30			0.79	0.6	0.41	0.15											0.29	0.69	0.78		1855
35			0.8	0.69	0.41	0.14											0.15	0.61	0.69		1690
40		0.16	0.8	0.76	0.41	0.13												0.53	0.57		1577
45		0.1	0.8	0.8	0.41	0.1												0.46	0.49		1480
50			0.8	0.8	0.44													0.35	0.4		1408
55			0.8	0.8	0.46													0.12	0.26		1349
60			0.8	0.8	0.44					0.1									0.17		1306
65			0.8	0.8	0.8	0.26					0.22										1283
70		0.67	0.8	0.8	0.42				0.1	0.21											1291
75		0.46	0.8	0.8	0.43				0.16	0.26											1249
80		0.43	0.8	0.8	0.44				0.21	0.3											1236
85		0.58	0.8	0.8	0.47				0.27	0.35											1261
90		0.58	0.8	0.8	0.49				0.31	0.39											1261
95		0.62	0.8	0.8	0.52				0.35	0.42											1270
100		0.64	0.8	0.8	0.54				0.38	0.45											1273
105		0.64	0.8	0.8	0.56				0.4	0.47											1270
110		0.65	0.8	0.8	0.59				0.42	0.49											1272
115		0.69	0.8	0.8	0.61				0.44	0.51											1280
120		0.64	0.8	0.8	0.63				0.45	0.52											1264
125		0.66	0.8	0.8	0.65				0.47	0.54											1268
130		0.61	0.8	0.8	0.66				0.48	0.55											1251
135		0.68	0.8	0.8	0.68				0.49	0.56											1268
140		0.69	0.8	0.8	0.7				0.5	0.57											1269
145		0.71	0.8	0.8	0.72				0.51	0.58											1271
150		0.72	0.8	0.8	0.73				0.52	0.59											1272
155		0.71	0.8	0.8	0.74				0.52	0.59											1269
160		0.63	0.8	0.8	0.75				0.52	0.6											1246
165		0.71	0.8	0.8	0.76				0.53	0.61											1268
170		0.75	0.8	0.8	0.77				0.54	0.62											1275
175		0.75	0.8	0.8	0.78				0.54	0.62											1273
180		0.73	0.8	0.8	0.79				0.55	0.63											1268
185		0.75	0.8	0.8	0.79				0.55	0.63											1273
190		0.79	0.8	0.8	0.8				0.56	0.64											1278
195		0.74	0.8	0.8	0.8				0.56	0.65											1270
200		0.72	0.8	0.8	0.8				0.56	0.66											1266

Table A.5: Effect of Variation of $\frac{1}{C^2}$ on the optimal control. Empty space means a value of zero for the control.

$\frac{1}{C^2}$	Control																				OF
	1	2	3	4	5	6	7	8	9	10	11	12	13	14	15	16	17	18	19	20	
0.8																0.24	0.45	0.73	0.72		1387
0.82																0.12	0.34	0.65	0.63		1255
0.84																	0.26	0.58	0.55		1139
0.86																	0.16	0.53	0.47		1039
0.88																		0.49	0.38		951
0.89																		0.46	0.34		911
0.9																		0.43	0.32		874
0.91																		0.4	0.3		839
0.92																		0.36	0.28		806
0.94																		0.29	0.23		746
0.95																		0.25	0.2		718
0.96																		0.21	0.16		692
0.97																		0.14	0.13		668
0.98																		0.1	0.1		642
0.99			0.14																		631
1			0.14	0.38																	625
1.01			0.54	0.5	0.11																666
1.02			0.76	0.62	0.36																734
1.03		0.34	0.8	0.77	0.29																835
1.04		0.47	0.8	0.8	0.35					0.18											956
1.05		0.58	0.8	0.8	0.44				0.21	0.35											1110
1.06		0.64	0.8	0.8	0.54				0.38	0.45											1273
1.07		0.7	0.8	0.8	0.64				0.49	0.52											1445
1.08		0.72	0.8	0.8	0.71				0.58	0.56											1612
1.09		0.75	0.8	0.8	0.76				0.65	0.59	0.14										1786
1.1		0.74	0.8	0.8	0.79				0.69	0.62	0.2										1939
1.12		0.64	0.8	0.8	0.8				0.76	0.68	0.35										2163
1.14		0.25	0.8	0.8	0.8				0.8	0.73	0.43										2258
1.15		0.14	0.8	0.8	0.8				0.8	0.77	0.46										2372
1.16			0.8	0.8	0.8				0.8	0.8	0.51										2508
1.18			0.8	0.8	0.8				0.8	0.8	0.72										2787
1.19			0.8	0.8	0.8				0.8	0.8	0.74										2969
1.2			0.8	0.8	0.8				0.8	0.8	0.8										3137
1.21			0.8	0.8	0.8				0.77	0.8	0.8	0.14				0.46					3376
1.22			0.8	0.8	0.8				0.8	0.8	0.8	0.18				0.58	0.08				3564
1.23			0.8	0.8	0.8				0.78	0.8	0.8	0.28				0.71	0.31				3794
1.24			0.8	0.8	0.8				0.8	0.8	0.8	0.19				0.77	0.41				3985
1.25		0.74	0.8		0.8				0.8	0.8	0.8	0.6				0.8	0.74				4475
1.26			0.8	0.8	0.8				0.8	0.8	0.8	0.66				0.8	0.63				4411
1.27			0.8	0.8	0.8				0.8	0.8	0.8	0.66				0.8	0.7				4600
1.28	0.31	0.8	0.8		0.8				0.8	0.8	0.8	0.75				0.8	0.8				4718
1.29		0.76	0.8		0.8				0.8	0.8	0.8	0.79				0.8	0.8				4760
1.3		0.76	0.8		0.8				0.8	0.8	0.8	0.8				0.8	0.8				4837
1.32		0.8	0.78		0.8				0.8	0.8	0.8	0.8				0.8	0.8				5013
1.33		0.8	0.75		0.8				0.8	0.8	0.8	0.8				0.8	0.8				5104
1.34	0.72	0.8			0.8				0.8	0.8	0.8	0.8				0.8	0.8				5200
1.35	0.71	0.8			0.8				0.8	0.8	0.8	0.8				0.8	0.8				5306
1.36	0.2	0.8					0.15	0.8	0.8			0.8				0.8	0.8	0.8			6598
1.37	0.37	0.8			0.8				0.56		0.8				0.48						6576
1.38	0.33	0.8			0.8				0.54		0.8				0.47						6533

Table A.6: Effect of Variation of the Initial conditions on the optimal control. Empty space means a value of zero for the control.

IC		Control																				OF
N_0	Z_0	1	2	3	4	5	6	7	8	9	10	11	12	13	14	15	16	17	18	19	20	
0.001	0.01		0.633	0.8	0.8	0.540				0.377	0.448											1271
0.001	0.1		0.629	0.8	0.8	0.539				0.377	0.447											1270
0.001	1		0.590	0.8	0.8	0.535				0.373	0.445											1259
0.001	10		0.612	0.8	0.8	0.538				0.375	0.446											1265
0.001	100		0.602	0.8	0.8	0.537				0.374	0.446											1263
0.001	1000		0.629	0.8	0.8	0.539				0.377	0.447											1270
0.001	10000		0.659	0.8	0.8	0.542				0.379	0.449											1278
0.01	0.01		0.625	0.8	0.8	0.539				0.376	0.447											1269
0.01	0.1		0.616	0.8	0.8	0.538				0.375	0.446											1266
0.01	1		0.584	0.8	0.8	0.535				0.372	0.444											1258
0.01	10		0.644	0.8	0.8	0.541				0.378	0.448											1274
0.01	100		0.618	0.8	0.8	0.538				0.375	0.447											1267
0.01	1000		0.619	0.8	0.8	0.538				0.376	0.447											1267
0.01	10000		0.629	0.8	0.8	0.539				0.376	0.447											1270
0.1	0.01		0.626	0.8	0.8	0.539				0.376	0.447											1269
0.1	0.1		0.614	0.8	0.8	0.538				0.375	0.446											1266
0.1	1		0.604	0.8	0.8	0.537				0.374	0.446											1263
0.1	10		0.621	0.8	0.8	0.538				0.376	0.447											1268
0.1	100		0.628	0.8	0.8	0.539				0.376	0.447											1269
0.1	1000		0.645	0.8	0.8	0.541				0.378	0.448											1274
0.1	10000		0.615	0.8	0.8	0.538				0.375	0.446											1266
1	0.01		0.646	0.8	0.8	0.541				0.378	0.448											1274
1	0.1		0.588	0.8	0.8	0.535				0.372	0.445											1259
1	1		0.590	0.8	0.8	0.535				0.373	0.445											1259
1	10		0.605	0.8	0.8	0.537				0.374	0.446											1263
1	100		0.588	0.8	0.8	0.535				0.372	0.445											1259
1	1000		0.618	0.8	0.8	0.538				0.375	0.447											1267
1	10000		0.629	0.8	0.8	0.539				0.377	0.447											1270
10	0.01		0.627	0.8	0.8	0.539				0.376	0.447											1269
10	0.1		0.632	0.8	0.8	0.540				0.377	0.448											1271
10	1		0.632	0.8	0.8	0.540				0.377	0.448											1271
10	10		0.641	0.8	0.8	0.540				0.378	0.448											1273
10	100		0.611	0.8	0.8	0.538				0.375	0.446											1265
10	1000		0.603	0.8	0.8	0.537				0.374	0.446											1263
10	10000		0.656	0.8	0.8	0.542				0.379	0.449											1277
100	0.01		0.612	0.8	0.8	0.538				0.375	0.446											1265
100	0.1		0.612	0.8	0.8	0.538				0.375	0.446											1265
100	1		0.615	0.8	0.8	0.538				0.375	0.446											1266
100	10		0.643	0.8	0.8	0.541				0.378	0.448											1273
100	100		0.645	0.8	0.8	0.541				0.378	0.448											1274
100	1000		0.627	0.8	0.8	0.539				0.376	0.447											1269
100	10000		0.638	0.8	0.8	0.540				0.377	0.448											1272
500	0.01		0.633	0.8	0.8	0.540				0.377	0.448											1271
500	0.1		0.633	0.8	0.8	0.540				0.377	0.448											1271
500	1		0.633	0.8	0.8	0.540				0.377	0.448											1271
500	10		0.637	0.8	0.8	0.540				0.377	0.448											1272
500	100		0.640	0.8	0.8	0.540				0.378	0.448											1273
500	1000		0.614	0.8	0.8	0.538				0.375	0.446											1266
500	10000		0.588	0.8	0.8	0.535				0.372	0.445											1259

A.5 Windows for the control

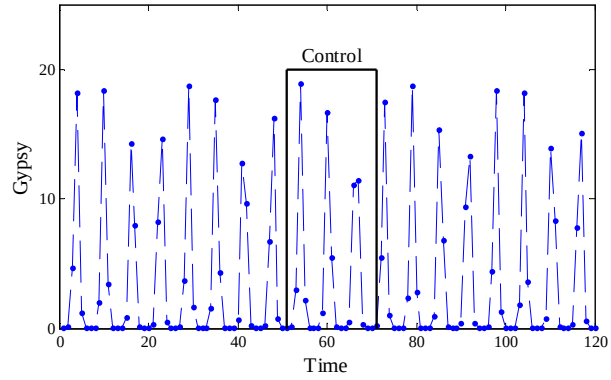

a

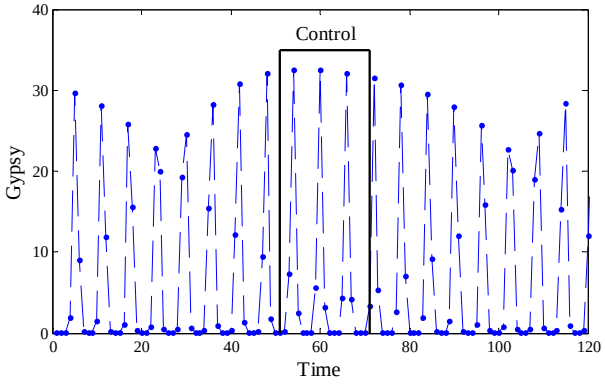

b

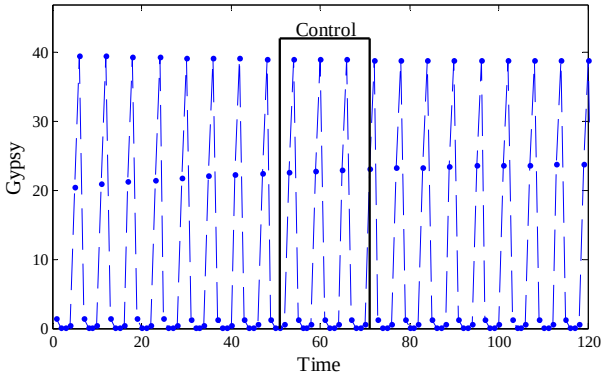

c

Figure A.4: Impact in the gypsy moth densities by variation in γ. a. $\gamma = 40$. b. $\gamma = 75$. c. $\gamma = 110$

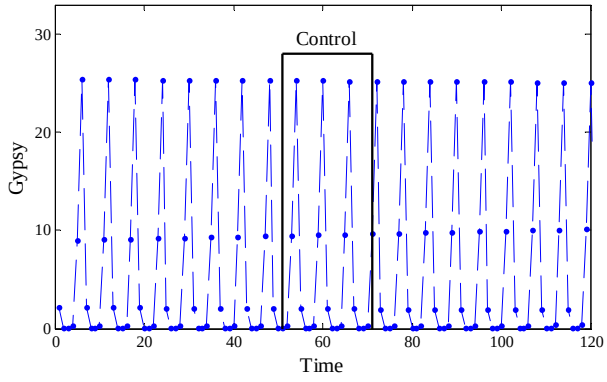

a

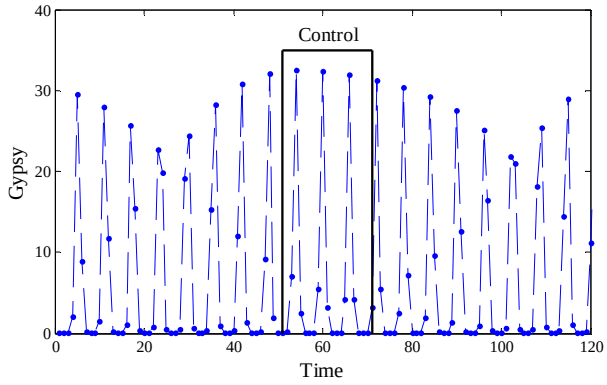

b

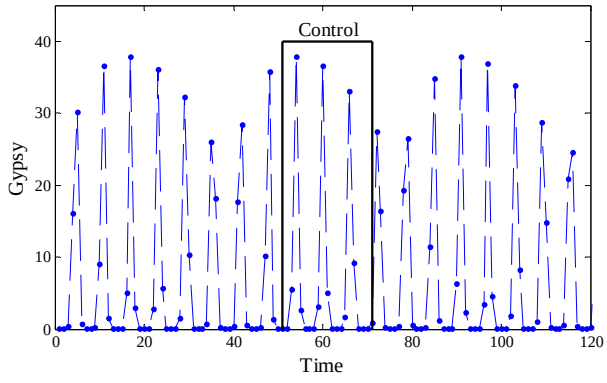

c

Figure A.5: Impact in the gypsy moth densities by variation in ϕ. a. $\phi = 70$. b. $\phi = 100$. c. $\phi = 140$

A.6 Statistical results for the factorial experiment

In this section we use $\frac{1}{C^2} = q$

Response Objective Functional

Summary of Fit

RSquare	0.974891
RSquare Adj	0.973232
Root Mean Square Error	167.1855
Mean of Response	1414.076
Observations (or Sum Wgts)	243

Analysis of Variance

Source	DF	Sum of Squares	Mean Square	F Ratio
Model	15	246352774	16423518	587.5824
Error	227	6344878	27951.002	Prob > F
C. Total	242	252697652		<.0001*

Sorted Parameter Estimates

Term	Estimate	Std Error	t Ratio	Prob>|t|
q	11924.931	218.9223	54.47	<.0001*
A	25.32528	0.525413	48.20	<.0001*
gamma	16.324163	0.352154	46.36	<.0001*
(q-1.06)*(A-50)	203.25504	10.72496	18.95	<.0001*
(A-50)*(gamma-74.6)	0.3177086	0.017252	18.42	<.0001*
(q-1.06)*(gamma-74.6)	121.15982	7.188309	16.86	<.0001*
phi	-3.028042	0.262707	-11.53	<.0001*
(q-1.06)*(phi-100)	55.691285	5.362478	10.39	<.0001*
delta	-9762.646	1313.534	-7.43	<.0001*
(gamma-74.6)*(phi-100)	-0.059286	0.008626	-6.87	<.0001*
(A-50)*(phi-100)	-0.06974	0.01287	-5.42	<.0001*
(A-50)*(delta-0.02)	-178.2597	64.34974	-2.77	0.0061*
(delta-0.02)*(gamma-74.6)	-111.1151	43.12985	-2.58	0.0106*
(q-1.06)*(delta-0.02)	-50112.38	26812.39	-1.87	0.0629
(delta-0.02)*(phi-100)	42.807711	32.17487	1.33	0.1847

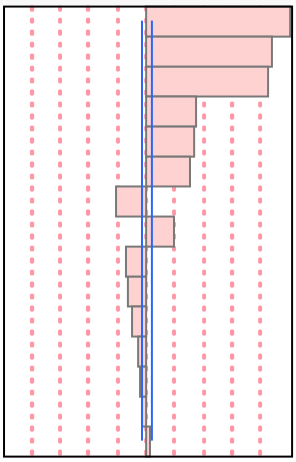

Figure A.6: Statistics for the factorial experiment with the objective functional as a response variable

Response sum

Summary of Fit

RSquare	0.925416
RSquare Adj	0.920488
Root Mean Square Error	0.467803
Mean of Response	2.9102
Observations (or Sum Wgts)	243

Analysis of Variance

Source	DF	Sum of Squares	Mean Square	F Ratio
Model	15	616.37339	41.0916	187.7700
Error	227	49.67665	0.2188	Prob > F
C. Total	242	666.05005		<.0001*

Sorted Parameter Estimates

Term	Estimate	Std Error	t Ratio	Prob>|t|
q	29.66928	0.612568	48.43	<.0001*
A	0.0205567	0.00147	13.98	<.0001*
gamma	0.0110584	0.000985	11.22	<.0001*
phi	0.0052707	0.000735	7.17	<.0001*
(A-50)*(phi-100)	-0.000203	0.000036	-5.63	<.0001*
(q-1.06)*(phi-100)	0.0836111	0.015005	5.57	<.0001*
(gamma-74.6)*(phi-100)	-0.000103	2.414e-5	-4.26	<.0001*
(A-50)*(gamma-74.6)	0.0001637	4.827e-5	3.39	0.0008*
(q-1.06)*(gamma-74.6)	-0.042265	0.020114	-2.10	0.0367*
(q-1.06)*(A-50)	-0.029572	0.03001	-0.99	0.3255
(A-50)*(delta-0.02)	0.0291111	0.180058	0.16	0.8717
(delta-0.02)*(gamma-74.6)	0.0194196	0.120682	0.16	0.8723
(q-1.06)*(delta-0.02)	8.5324074	75.02398	0.11	0.9096
(delta-0.02)*(phi-100)	-0.008259	0.090029	-0.09	0.9270
delta	-0.156481	3.675409	-0.04	0.9661

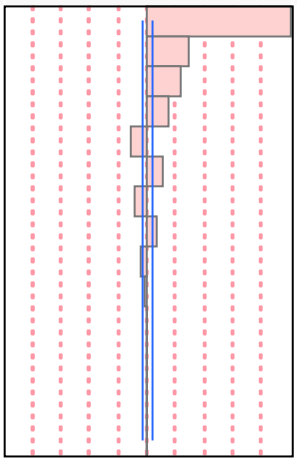

Figure A.7: Statistical analysis for the factorial experiment with the sum of controls over a period of 20 years as a response variable

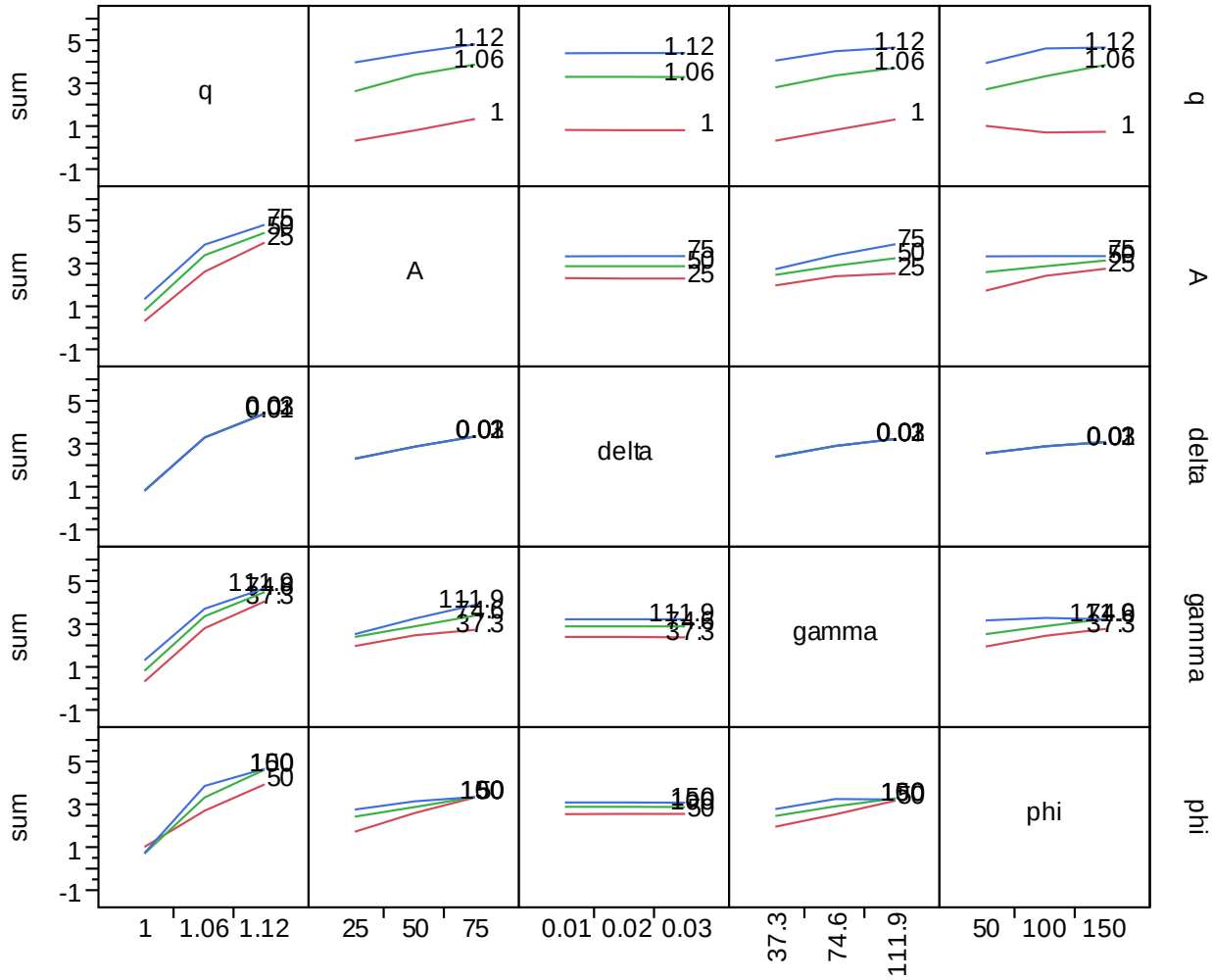

Figure A.8: Interaction plots for the five parameters of the host-pathogen model with sum of controls over a period of 20 years as a response variable

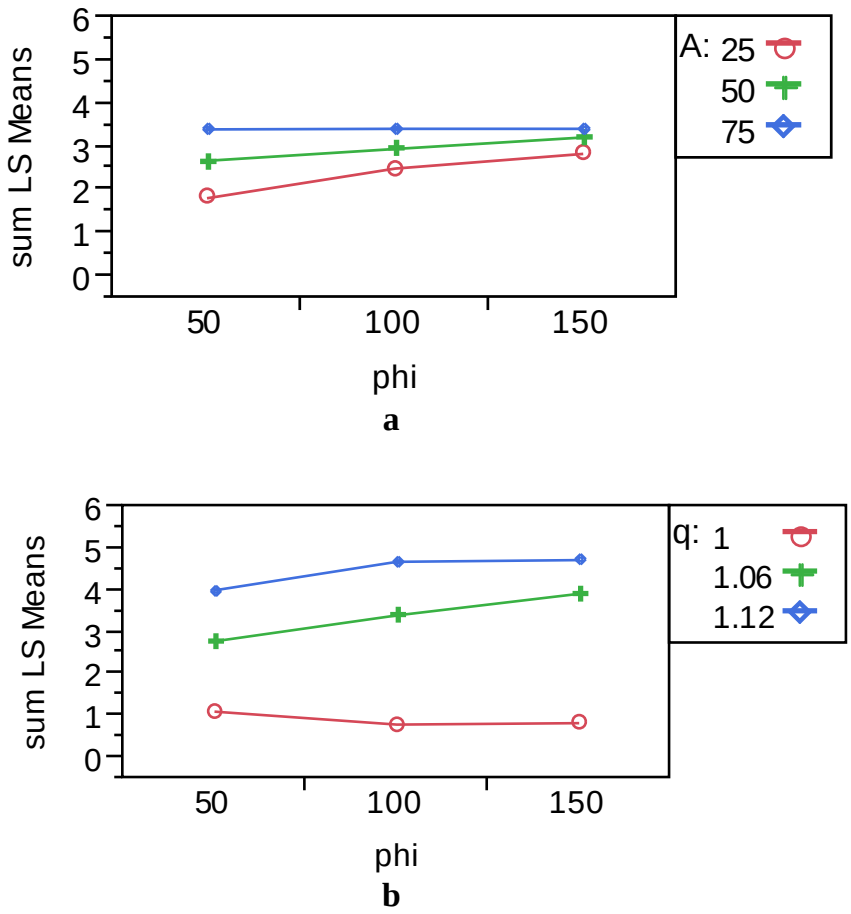

Figure A.9: Interaction plots in the host-pathogen model with sum of controls over a period of 20 years as a response variable. a $A\phi$. b. $q\phi$

A.7 Box plots for the host-pathogen model at different starting conditions

In the box plots the central mark is the median, the edges of the box are the 25th and 75th percentiles, the whiskers extend to the most extreme data points not considered outliers, and outliers are plotted individually. In some years, we have a box with edges at 0 and 0.8. This happened because in those years most of the data are 0 or 0.8, and therefore the 25th and 75th percentile are the same as the minimum and the maximum. If we analyze the median in Figure 2.13(a), we can observe that the median is at zero for years 0 and 1, and at 0.8 for years 2 and 3. From this pattern we deduce that we do not need to take immediate control action. In general the box plots provide the same patterns observed in Figure 2.13: for low densities we do not need to take immediate action, for high densities we need to take immediate action. Populations at medium densities have an average between the scenarios of low and high densities.

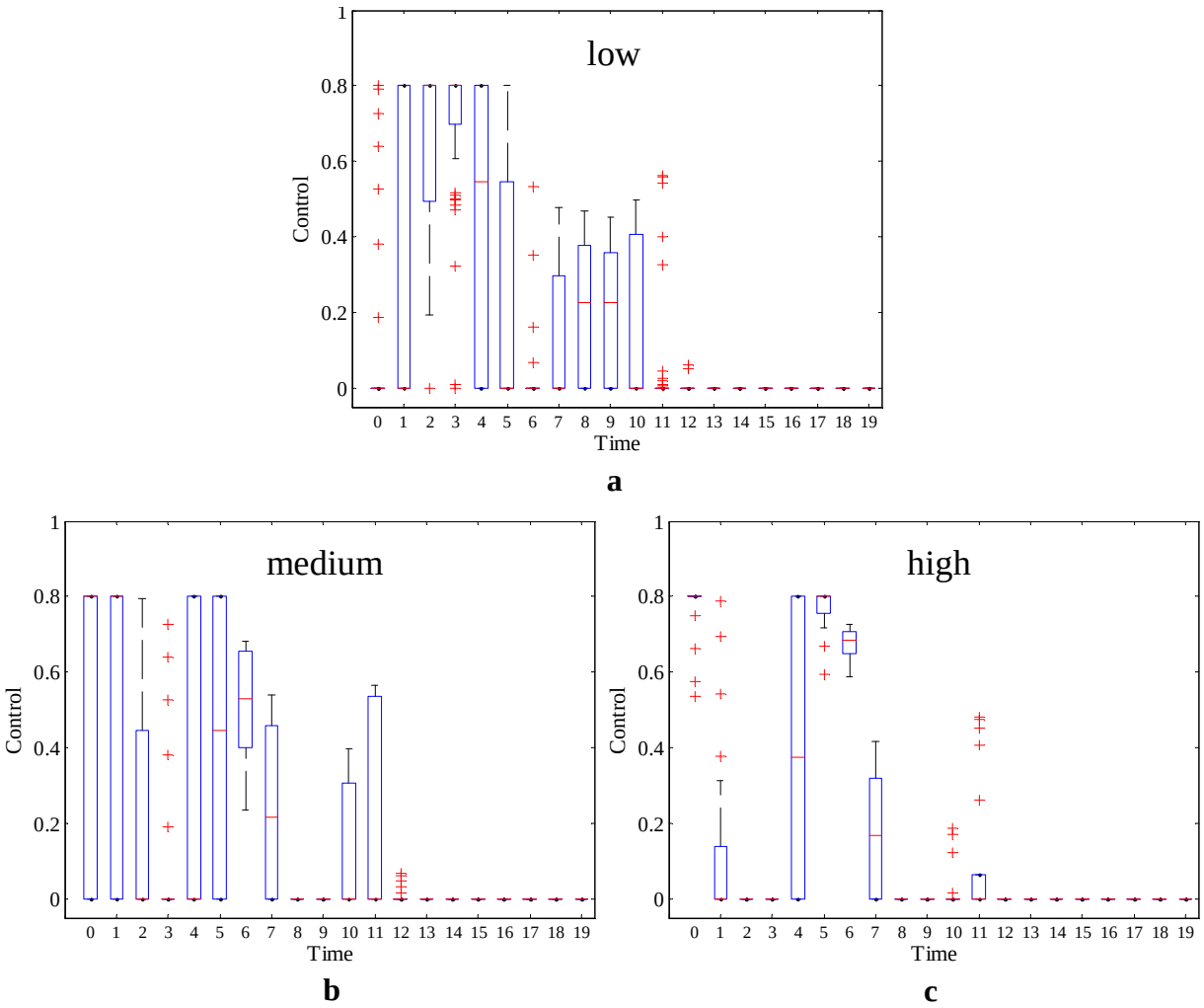

Figure A.10: Box plots for the optimal control for the host-pathogen model. a. Starting conditions for the control at low densities. b. Medium densities. c. High densities. With parameters in Table 2.1

A.8 Statistical results for host-pathogen model

Oneway Analysis of objective functional By density

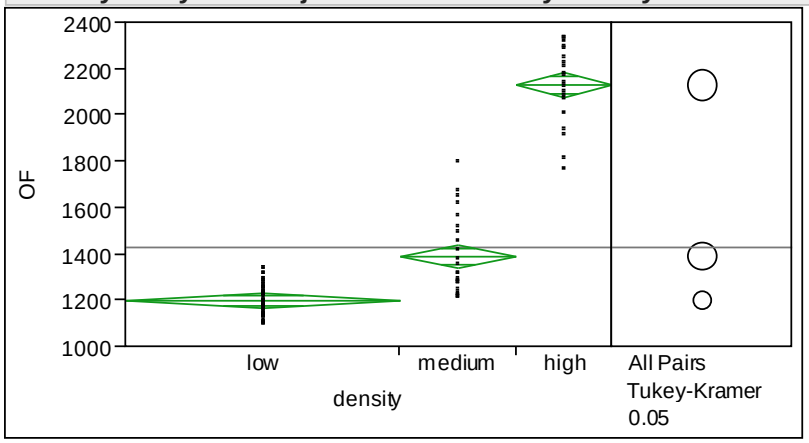

Oneway Anova

Summary of Fit

Rsquare	0.898375
Adj Rsquare	0.896301
Root Mean Square Error	122.0003
Mean of Response	1430.052
Observations (or Sum Wgts)	101

Analysis of Variance

Source	DF	Sum of Squares	Mean Square	F Ratio	Prob > F
density	2	12894499	6447249	433.1646	<.0001*
Error	98	1458638	14884		
C. Total	100	14353137			

Means Comparisons

Comparisons for all pairs using Tukey-Kramer HSD

Connecting Letters Report

Level		Mean
high	A	2131.8797
medium	B	1390.5915
low	C	1200.4113

Levels not connected by same letter are significantly different.

Ordered Differences Report

Level	- Level	Difference	Std Err Dif	Lower CL	Upper CL	p-Value
high	low	931.4684	31.70689	856.0102	1006.926	<.0001*
high	medium	741.2882	36.93741	653.3822	829.194	<.0001*
medium	low	190.1801	29.68658	119.5301	260.830	<.0001*

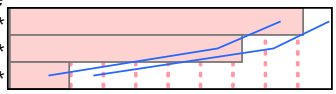

Figure A.11: Statistical analysis of the objective functional for different starting densities in the host-pathogen model

Oneway Analysis of Sum By density

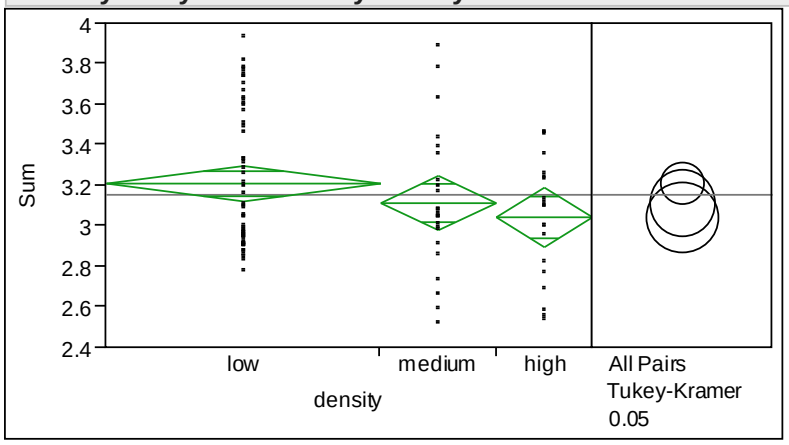

Oneway Anova

Summary of Fit

Rsquare	0.040989
Adj Rsquare	0.021417
Root Mean Square Error	0.331051
Mean of Response	3.155584
Observations (or Sum Wgts)	101

Analysis of Variance

Source	DF	Sum of Squares	Mean Square	F Ratio	Prob > F
density	2	0.459048	0.229524	2.0943	0.1286
Error	98	10.740308	0.109595		
C. Total	100	11.199356			

Means Comparisons

Comparisons for all pairs using Tukey-Kramer HSD

Connecting Letters Report

Level		Mean
low	A	3.2111860
medium	A	3.1156958
high	A	3.0449850

Levels not connected by same letter are significantly different.

Ordered Differences Report

Level	- Level	Difference	Std Err Dif	Lower CL	Upper CL	p-Value
low	high	0.1662010	0.0860376	-0.038557	0.3709588	0.1352
low	medium	0.0954901	0.0805554	-0.096221	0.2872011	0.4647
medium	high	0.0707108	0.1002308	-0.167825	0.3092465	0.7608

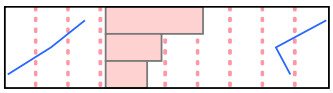

Figure A.12: Statistical analysis of the sum of the controls for different starting densities in the host-pathogen model

Oneway Analysis of 1st max By density

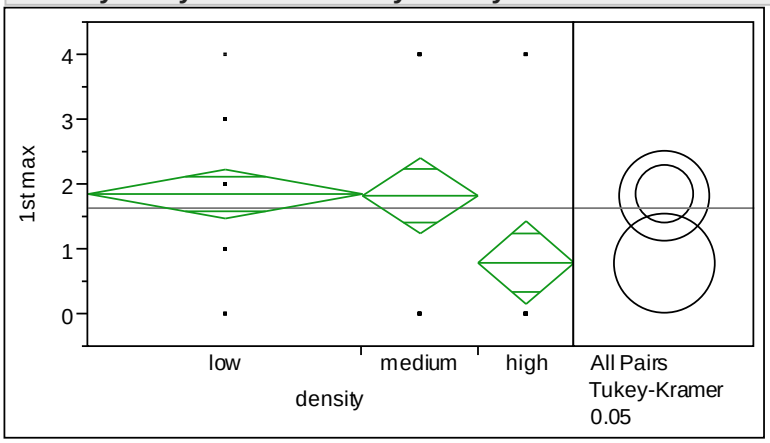

Oneway Anova

Summary of Fit

Rsquare	0.080291
Adj Rsquare	0.061521
Root Mean Square Error	1.4407
Mean of Response	1.643564
Observations (or Sum Wgts)	101

Analysis of Variance

Source	DF	Sum of Squares	Mean Square	F Ratio	Prob > F
density	2	17.75779	8.87890	4.2777	0.0166*
Error	98	203.41053	2.07562		
C. Total	100	221.16832			

Means Comparisons

Comparisons for all pairs using Tukey-Kramer HSD

Connecting Letters Report

Level		Mean
low	A	1.8596491
medium	A B	1.8333333
high	B	0.8000000

Levels not connected by same letter are significantly different.

Ordered Differences Report

Level	- Level	Difference	Std Err Dif	Lower CL	Upper CL	p-Value
low	high	1.059649	0.3744265	0.168565	1.950734	0.0155*
medium	high	1.033333	0.4361937	-0.004749	2.071415	0.0513
low	medium	0.026316	0.3505687	-0.807990	0.860622	0.9969

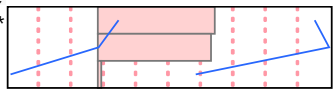

Figure A.13: Statistical analysis of the time of the maximum control for different starting densities in the host-pathogen model

A.9 Box plots for the model with predation at different starting conditions

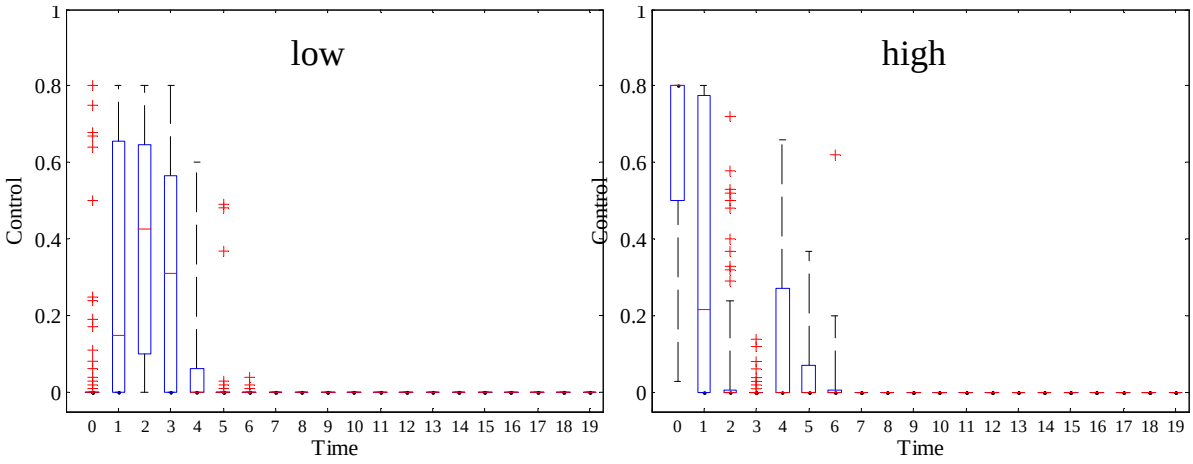

Figure A.14: Summary statistics for the optimal control for the model with predation. On each box, the central mark is the median, the edges of the box are the 25th and 75th percentiles, the whiskers extend to the most extreme data points not considered outliers, and outliers are plotted individually . a. With 100 different starting conditions. b. Starting conditions for the control at low densities. c. Medium densities. d. High densities. With parameters in Table 2.1

A.10 Statistical results for the model with predation

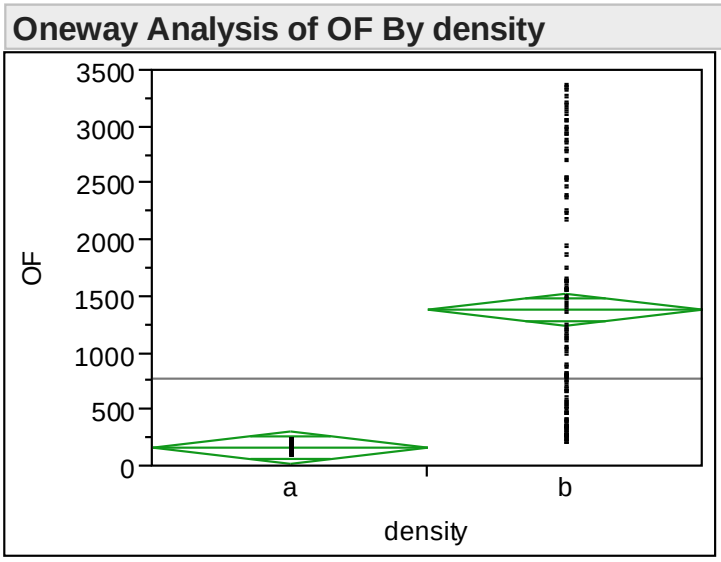

Oneway Anova

Summary of Fit

Rsquare	0.417463
Adj Rsquare	0.414521
Root Mean Square Error	723.5817
Mean of Response	778.7009
Observations (or Sum Wgts)	200

Analysis of Variance

Source	DF	Sum of Squares	Mean Square	F Ratio	Prob > F
density	1	74290797	74290797	141.8927	<.0001*
Error	198	103666944	523570.42		
C. Total	199	177957741			

Figure A.15: Statistical analysis of the objective functional for different starting densities in the model with predation

Oneway Analysis of Sum By density

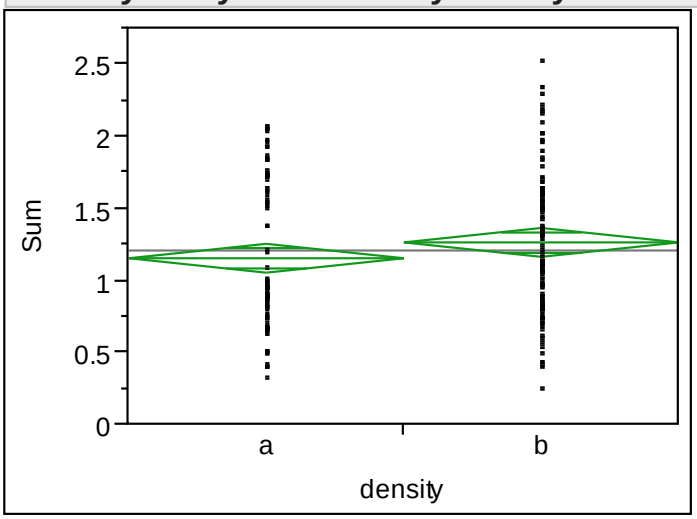

Oneway Anova

Summary of Fit

Rsquare	0.011487
Adj Rsquare	0.006495
Root Mean Square Error	0.508109
Mean of Response	1.2118
Observations (or Sum Wgts)	200

Analysis of Variance

Source	DF	Sum of Squares	Mean Square	F Ratio	Prob > F
density	1	0.594050	0.594050	2.3010	0.1309
Error	198	51.118702	0.258175		
C. Total	199	51.712752			

Figure A.16: Statistical analysis of the sum of the controls for different starting densities in the model with predation

Oneway Analysis of 1st max By density

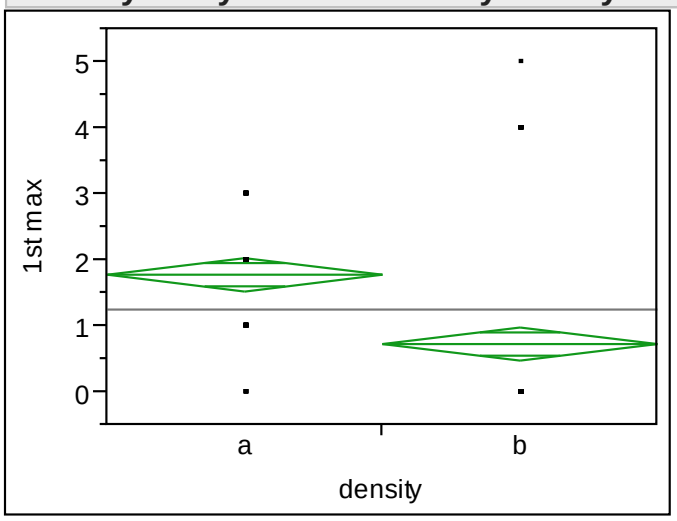

Oneway Anova

Summary of Fit

Rsquare	0.146611
Adj Rsquare	0.142301
Root Mean Square Error	1.27301
Mean of Response	1.255
Observations (or Sum Wgts)	200

Analysis of Variance

Source	DF	Sum of Squares	Mean Square	F Ratio	Prob > F
density	1	55.12500	55.1250	34.0161	<.0001*
Error	198	320.87000	1.6206		
C. Total	199	375.99500			

Figure A.17: Statistical analysis of the time of the maximum control for different starting densities in the model with predation

A.11 Optimal control results for model with predation

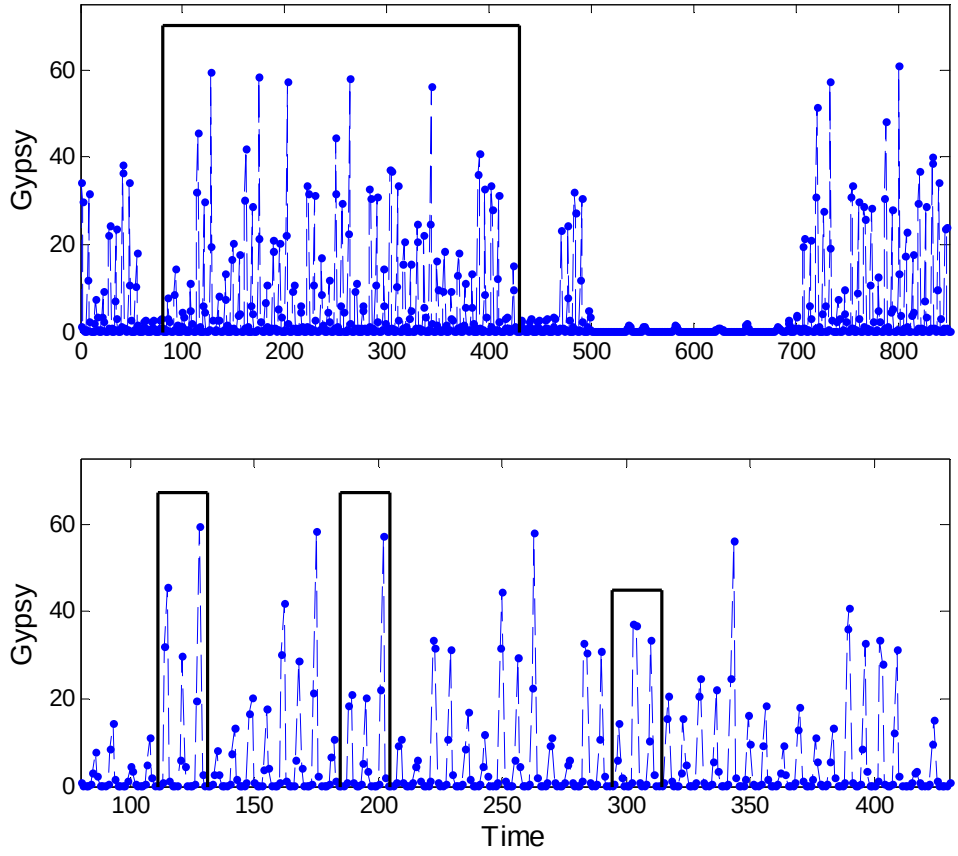

Figure A.18: Time intervals to control in the model with predation. The lower graphic presents the windows to control. Initial conditions are $N_0 = 10$ and $Z_0 = 1$, with other parameters in Table 2.3

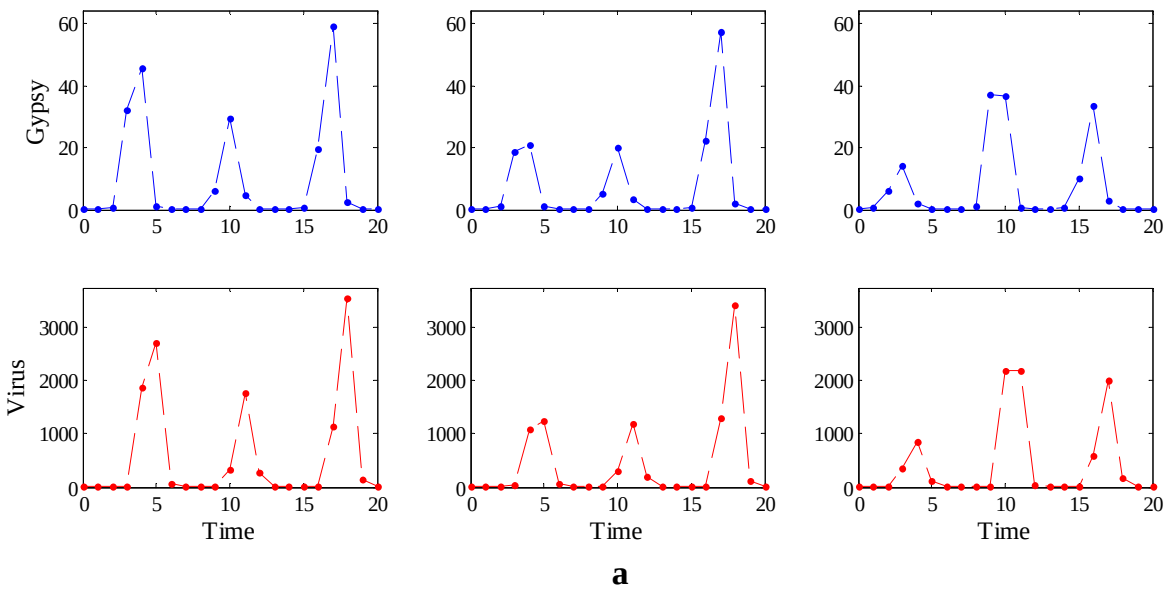

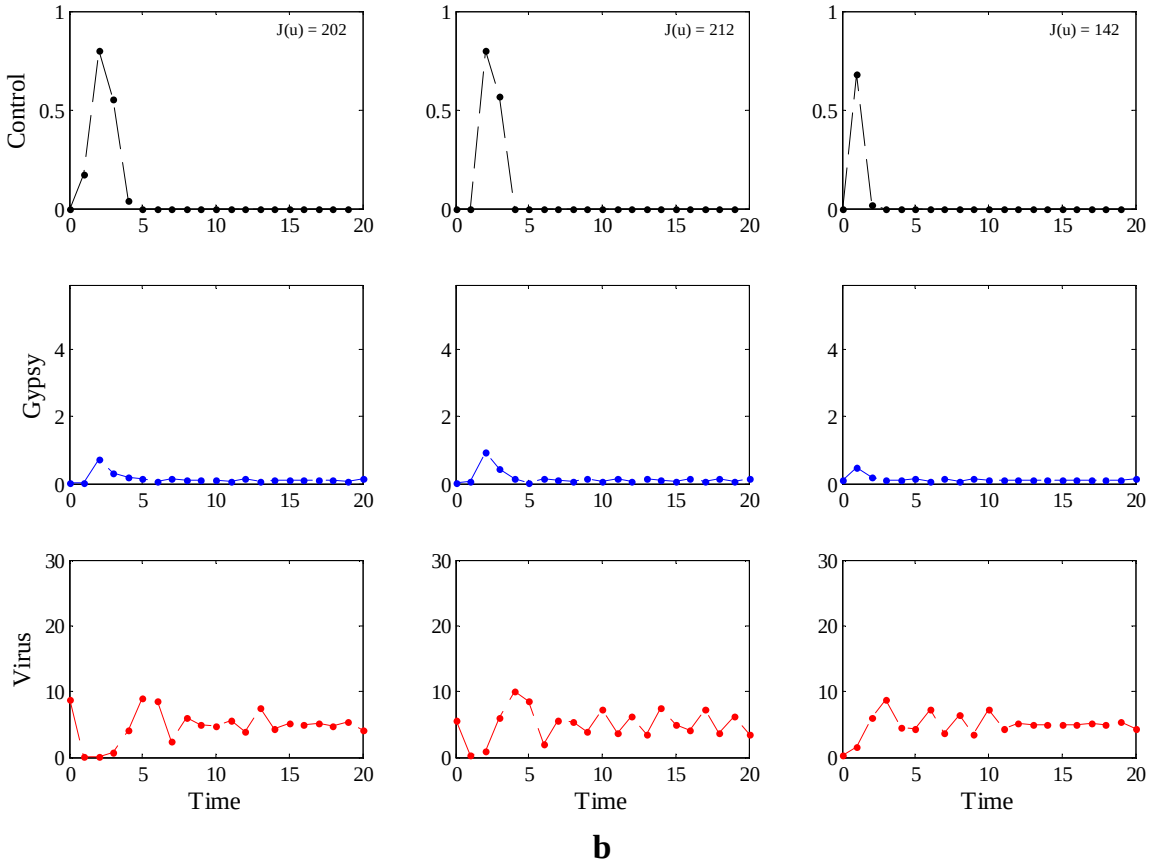

Figure A.19: Results for the model with predation. The three windows correspond to the time interval selection in the long term dynamics in Figure A.18. a. Dynamics without control. b. Dynamics with control. Initial conditions are $N_0 = 10$ and $Z_0 = 1$, with other parameters in Table 2.3

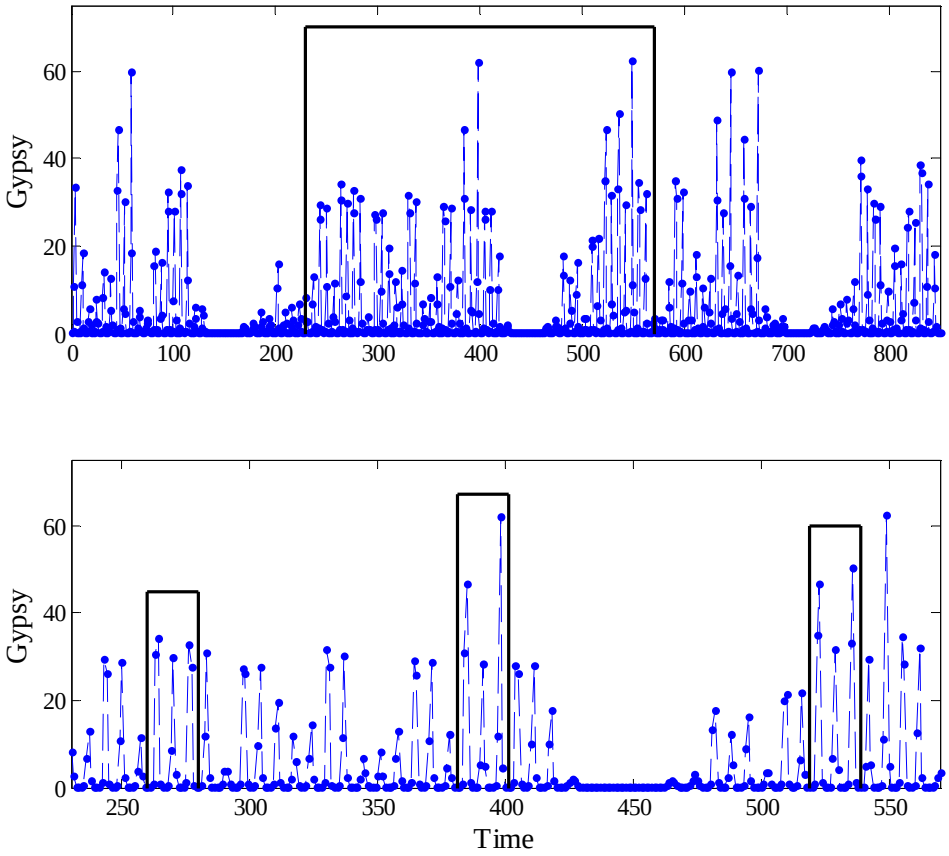

Figure A.20: Time intervals to control in the model with predation. The lower graphic presents the windows to control. Initial conditions are $N_0 = 1000$ and $Z_0 = 1$, with other parameters in Table 2.3

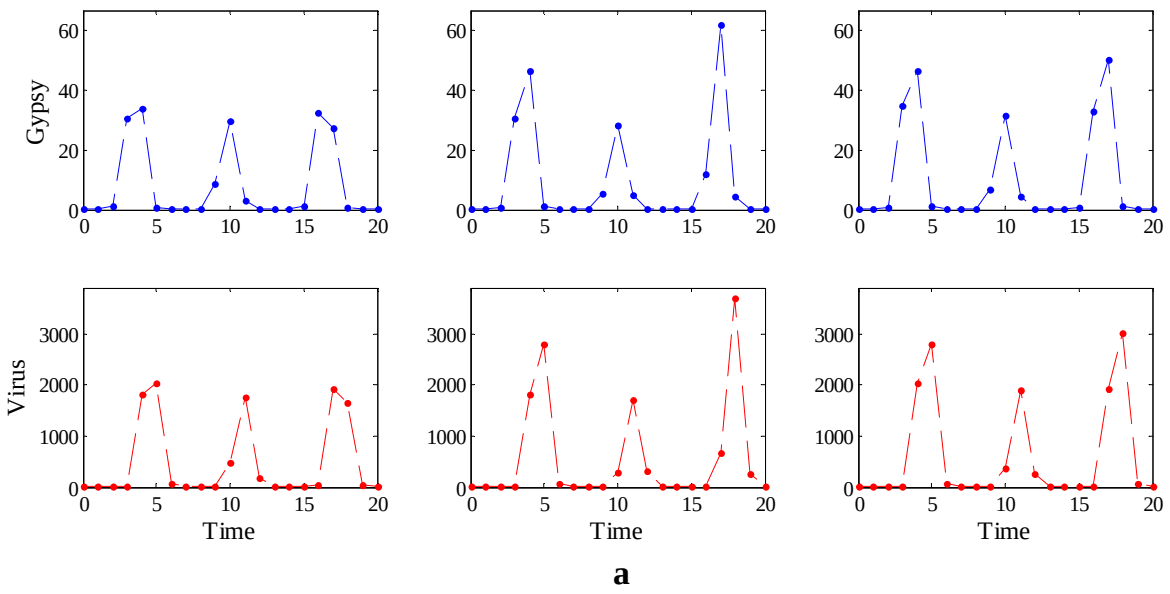

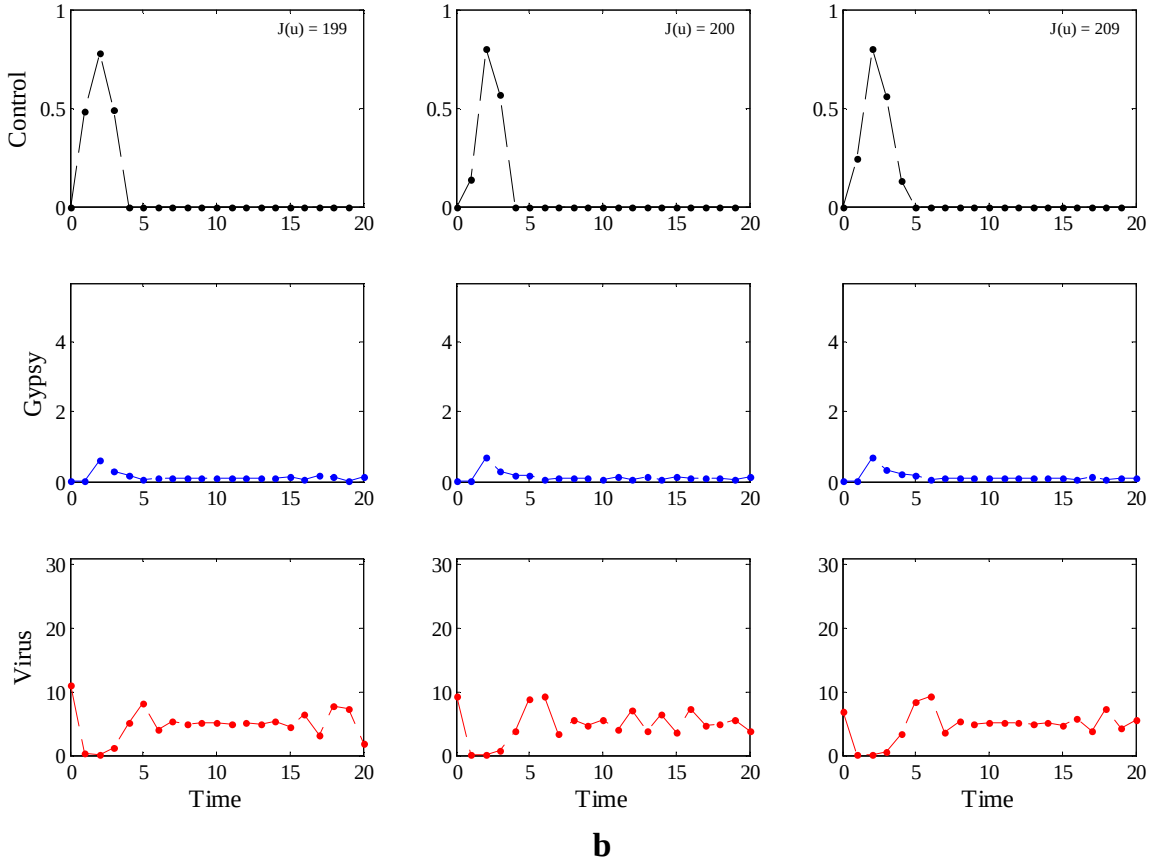

Figure A.21: Results for the model with predation. The three windows correspond to the time interval selection in the long term dynamics in Figure A.20. a. Dynamics without control. b. Dynamics with control. Initial conditions are $N_0 = 1000$ and $Z_0 = 1$, with other parameters in Table 2.3

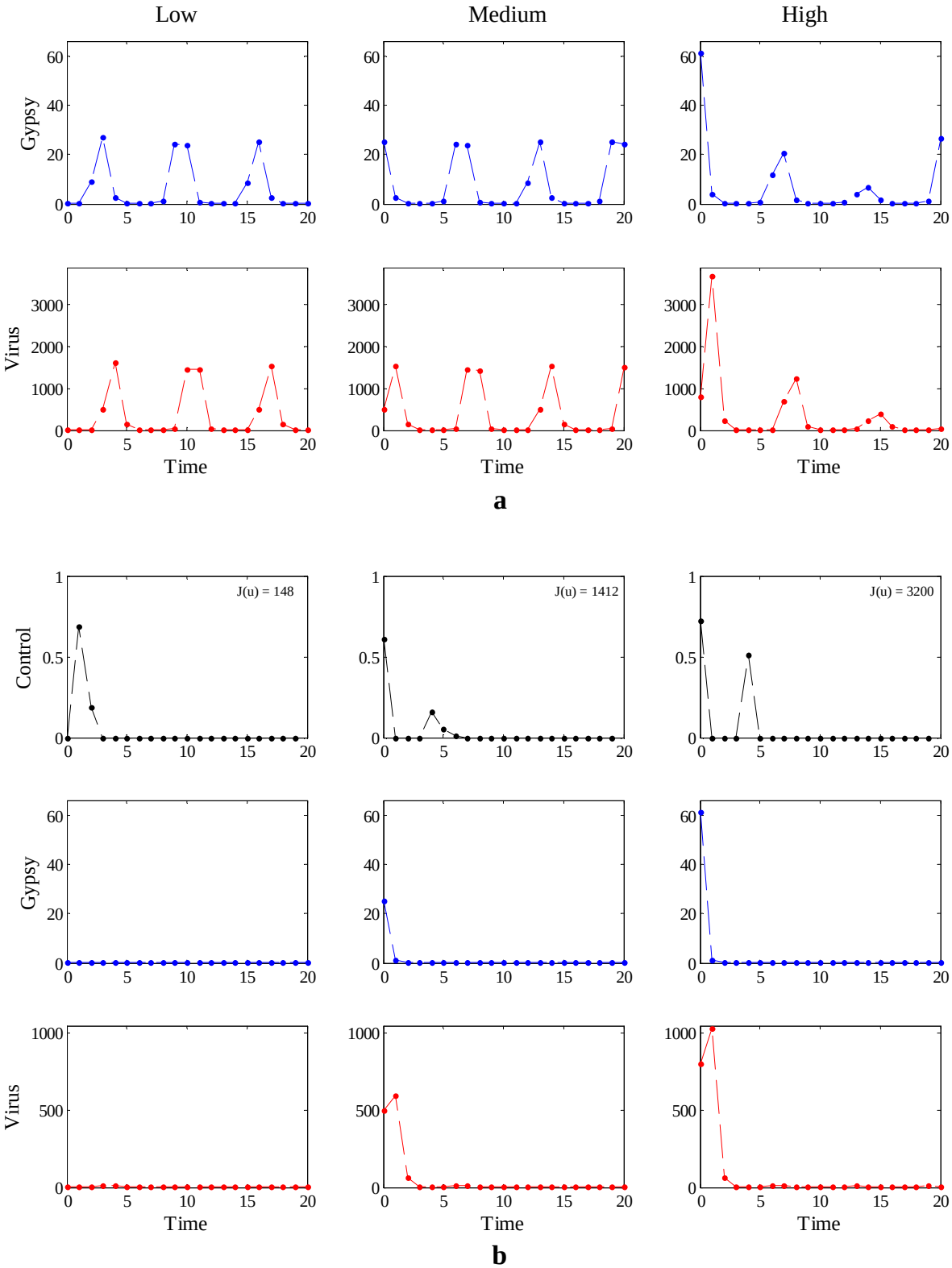

Figure A.22: Variation for starting point, low, medium and high densities of gypsy moth in the model with predation. a. Dynamics without control. b. Dynamics with control. With parameters in Table 2.3

Appendix B

B.1 Accuracy results for the trapezoidal rule

The error of the trapezoidal rules is the difference between the values of the integral and the numerical result:

$$error = \int_a^b f(x)dx - \frac{b-a}{n}\left[\frac{f(a)+f(b)}{2} + \sum_{k=1}^{n-1} f\left(a + k\frac{b-a}{n}\right)\right] \tag{B.1}$$

There exist a number ξ between a and b, such that:

$$error = -\frac{(b-a)^3}{12n^2} f''(\xi) \tag{B.2}$$

In our case the difference $a = 0$, $b = 1$ and $n = 100$, therefore

$$error = -\frac{1}{120000} f''(\xi) \tag{B.3}$$

$$= -0.000008333 f''(\xi) \tag{B.4}$$

B.2 Spatial initial conditions

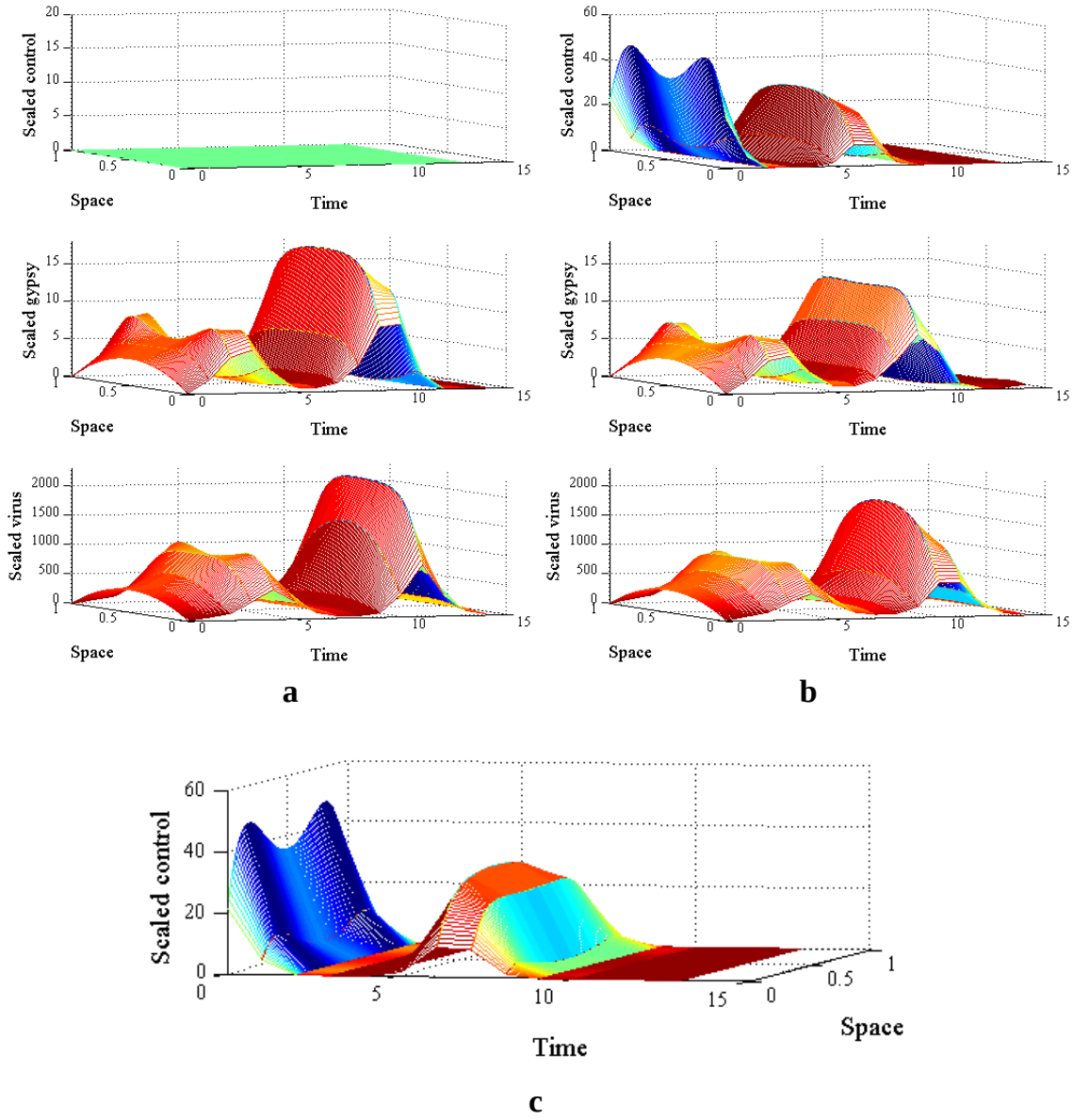

Figure B.1: Effect of the optimal control over a period of 15 years with aggregate spatial initial conditions in Figure 3.3(a). a. Dynamics without control. b. Dynamics with control. c. Different view of the control display in b

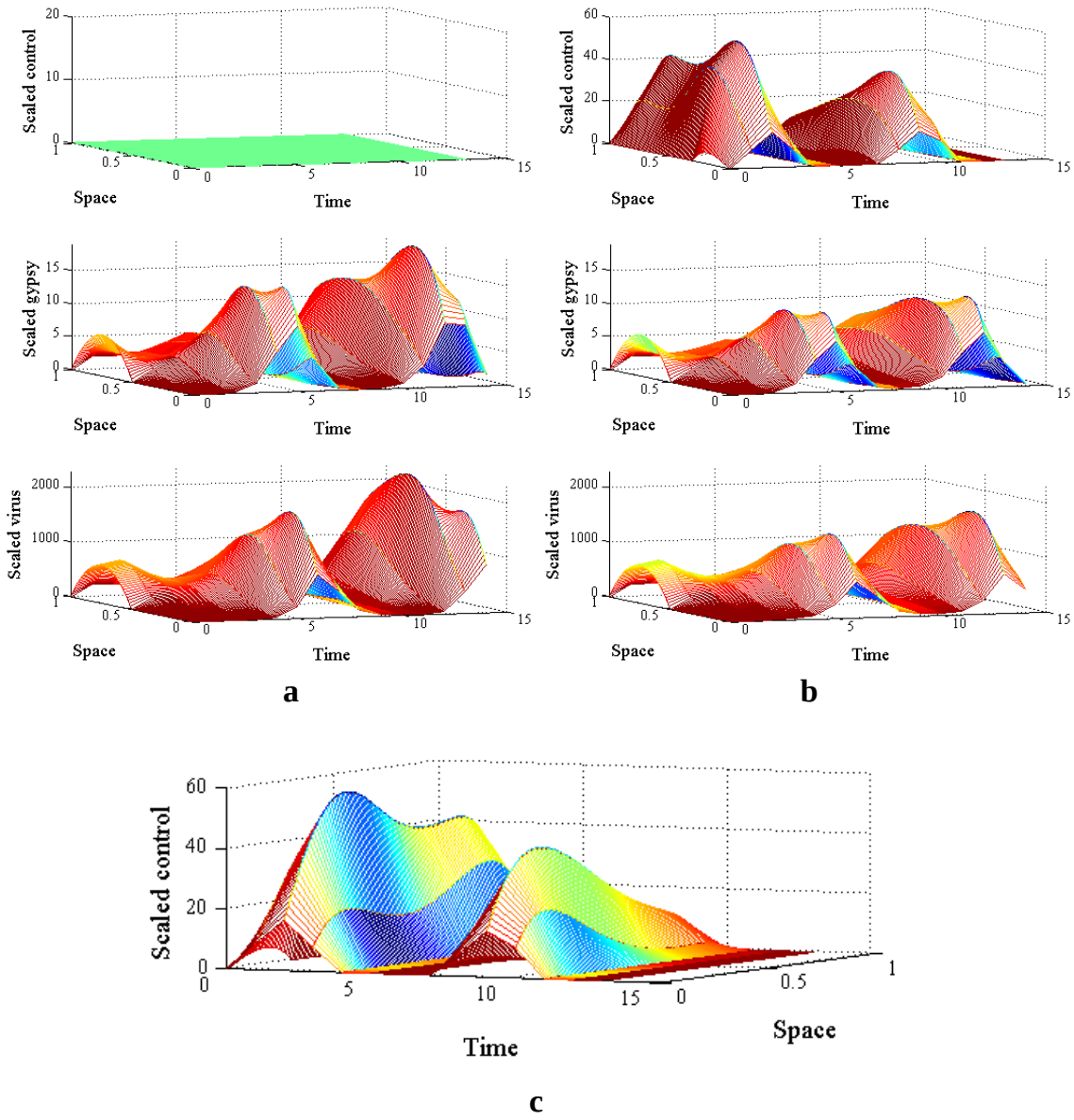

Figure B.2: Effect of the optimal control over a period of 15 years with aggregate spatial initial conditions in Figure 3.3(c). a. Dynamics without control. b. Dynamics with control. c. Different view of the control display in b

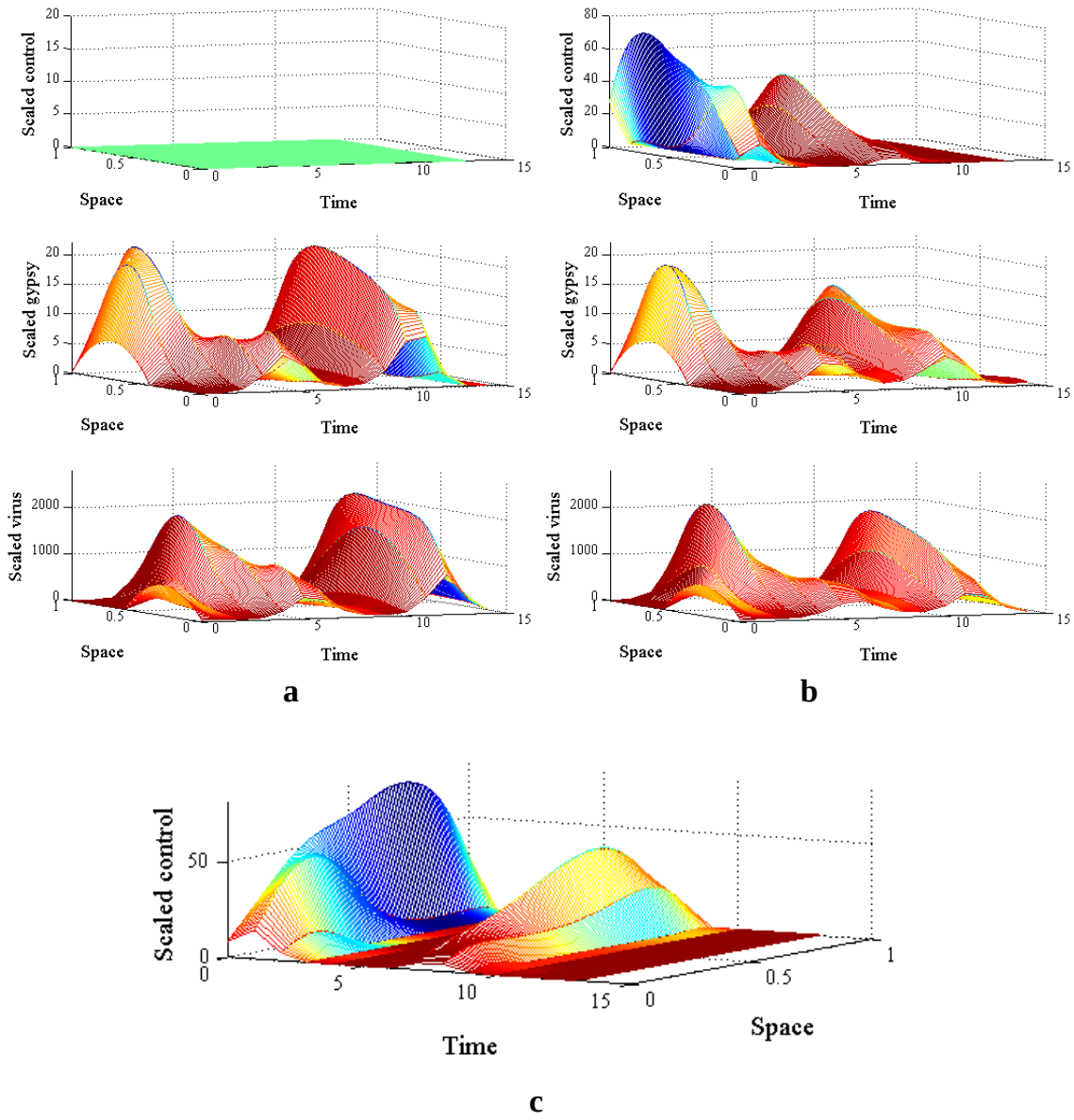

Figure B.3: Effect of the optimal control over a period of 15 years with shifted spatial initial conditions in Figure 3.4(a). a. Dynamics without control. b. Dynamics with control. c. Different view of the control display in b

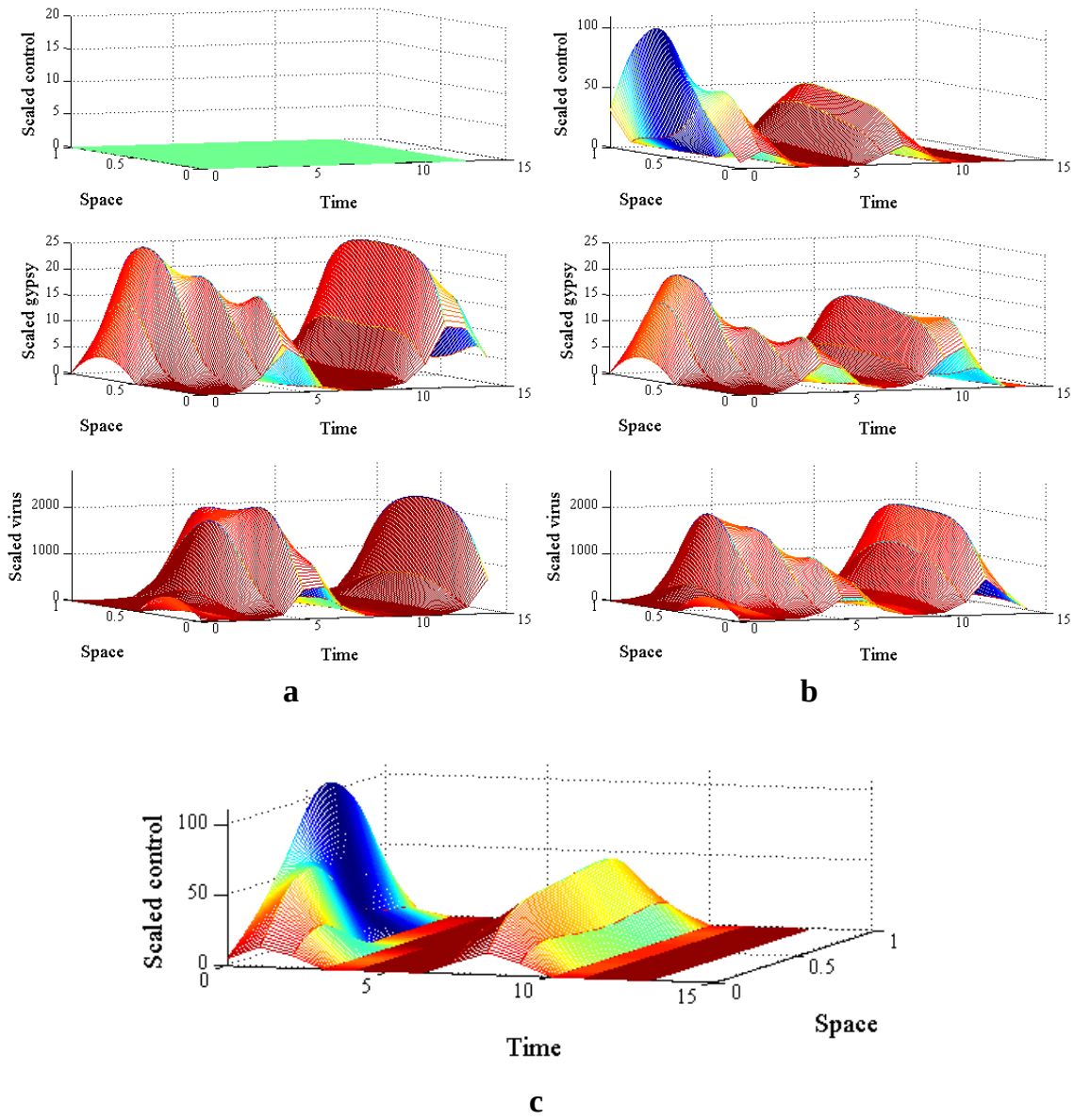

Figure B.4: Effect of the optimal control over a period of 15 years with shifted spatial initial conditions in Figure 3.4(b). a. Dynamics without control. b. Dynamics with control. c. Different view of the control display in b

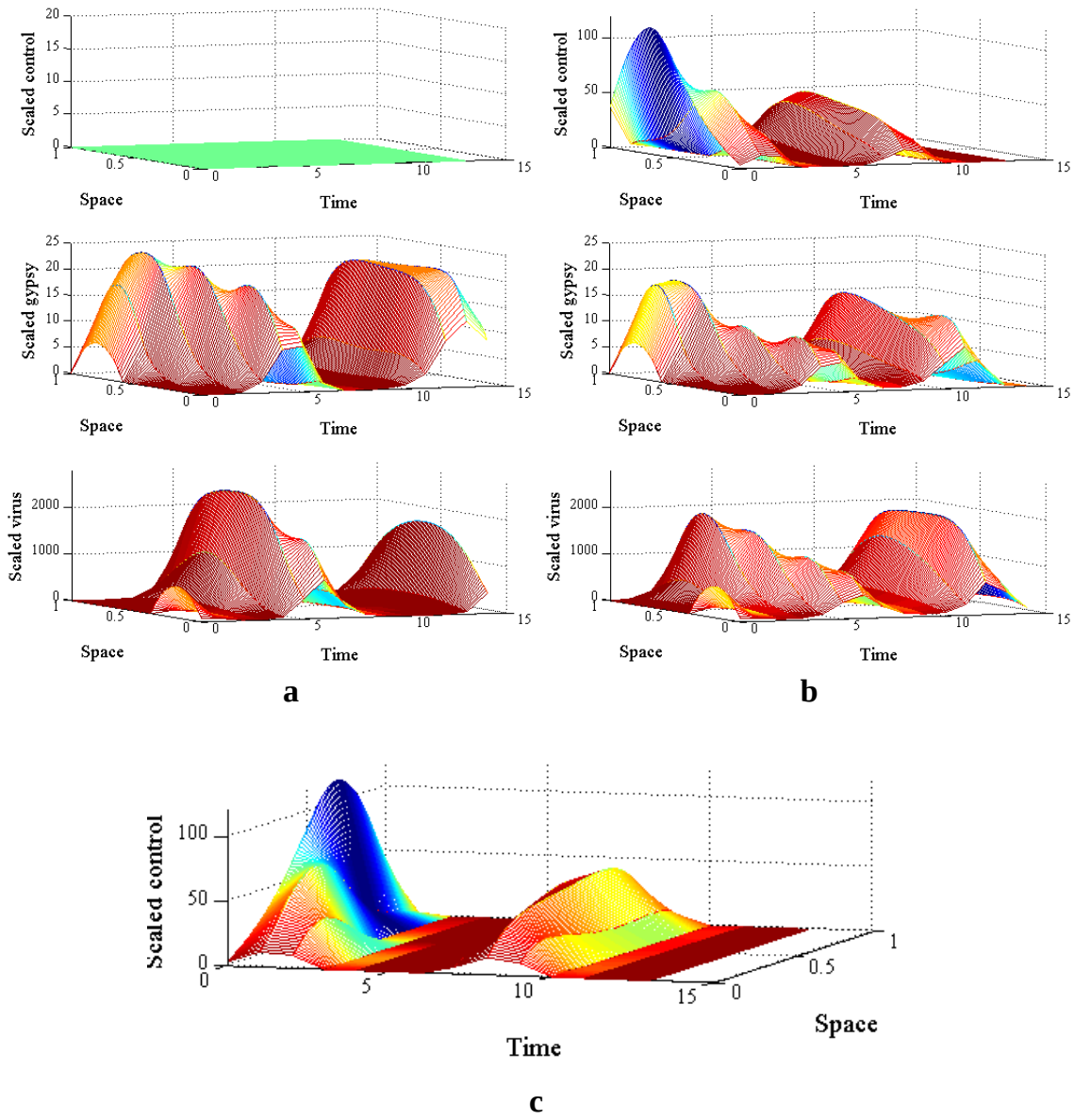

Figure B.5: Effect of the optimal control over a period of 15 years with shifted spatial initial conditions in Figure 3.4(c). a. Dynamics without control. b. Dynamics with control. c. Different view of the control display in b

Vita

Marco V. Martinez was born in Bogota, Colombia, on October 9, 1981. After graduating from Liceo de Cervantes El Retiro in 1998, he went to Pontificia Universidad Javeriana where he was a double major in Biology and Mathematics. From January of 2005 to July 2008, he was a lecturer in the departments of Mathematics and Biology in the Pontificia Universidad Javeriana. In August 2008, Marco began his graduate career in the Department of Mathematics at the University of Tennessee, Knoxville.

Marco graduated with a doctorate in Mathematics and masters in Statistics in August of 2013. He continues his work in mathematical ecology and in teaching Mathematics as an Assistant Professor at North Central College in Chicago, Illinois.